

Correlators on non-supersymmetric Wilson line in $\mathcal{N} = 4$ SYM and $\text{AdS}_2/\text{CFT}_1$

Matteo Beccaria,^a Simone Giombi^b and Arkady A. Tseytlin^{1c}

^a*Dipartimento di Matematica e Fisica Ennio De Giorgi,
Università del Salento & INFN, Via Arnesano, 73100 Lecce, Italy*

^b*Department of Physics, Princeton University, Princeton, NJ 08544, USA*

^c*Blackett Laboratory, Imperial College, London SW7 2AZ, U.K.*

E-mail: matteo.beccaria@le.infn.it, sgiombi@princeton.edu,
tseytlin@imperial.ac.uk

ABSTRACT: Correlators of local operators inserted on a straight or circular Wilson loop in a conformal gauge theory have the structure of a one-dimensional “defect” CFT. As was shown in arXiv:1706.00756, in the case of supersymmetric Wilson-Maldacena loop in $\mathcal{N} = 4$ SYM one can compute the leading strong-coupling contributions to 4-point correlators of the simplest “protected” operators by starting with the $\text{AdS}_5 \times S^5$ string action expanded near the AdS_2 minimal surface and evaluating the corresponding tree-level AdS_2 Witten diagrams. Here we perform the analogous computations in the non-supersymmetric case of the standard Wilson loop with no coupling to the scalars. The corresponding non-supersymmetric “defect” CFT_1 should have an unbroken $SO(6)$ global symmetry. The elementary bosonic operators (6 SYM scalars and 3 components of the SYM field strength) are dual respectively to the S^5 embedding coordinates and AdS_5 coordinates transverse to the minimal surface ending on the line at the boundary. The $SO(6)$ symmetry is preserved on the string side provided the 5-sphere coordinates satisfy Neumann boundary conditions (as opposed to Dirichlet in the supersymmetric case); this implies that one should integrate over the S^5 expansion point. The massless S^5 fluctuations then have logarithmic propagator, corresponding to the boundary scalar operator having dimension $\Delta = \frac{5}{\sqrt{\lambda}} + \dots$ at strong coupling. The resulting functions of 1d cross-ratio appearing in the 4-point functions turn out to have a more complicated structure than in the supersymmetric case, involving polylog (Li_3 and Li_2) functions. We also discuss consistency with the operator product expansion which allows extracting the leading strong coupling corrections to the anomalous dimensions of the operators appearing in the intermediate channels.

¹Also at Lebedev Institute and ITMP, Moscow State University.

Contents

1	Introduction	2
2	Correlators on supersymmetric Wilson line at strong coupling	7
2.1	AdS ₅ × S ⁵ string action in static gauge as AdS ₂ bulk theory action	7
2.2	Conformal invariance and crossing constraints on 4-point functions in CFT ₁	8
2.3	Strong-coupling expansion of the SO(5) scalar 4-point function	9
2.4	Analytic continuation to the “chaos configuration”	11
3	Non-supersymmetric Wilson line case: SO(6) invariant correlators	12
4	Two-point function $\langle Y^A Y^B \rangle$	14
4.1	Leading logarithmic correction	14
4.2	Subleading corrections	15
5	Mixed four-point function $\langle x^i x^j Y^A Y^B \rangle$	19
6	Four-point function $\langle Y^A Y^B Y^C Y^D \rangle$	23
6.1	Leading-order contributions	23
6.2	Order $\frac{1}{(\sqrt{\lambda})^3}$ contributions: Dirichlet/Neumann relations	25
6.3	Contact diagram contribution and $G_{S,T,A}$ functions at order $\frac{1}{(\sqrt{\lambda})^3}$	29
6.4	OPE and anomalous dimensions	33
A	Four-point correlators of generalized free fields	35
B	Anomalous dimensions from OPE in supersymmetric case	36
C	AdS contact integrals	36
D	Green’s functions for 2d massless scalar	37
E	Equivalence of different parametrizations of S⁵	39
F	Neumann/Dirichlet relations for bulk integrals	40
G	“Reducible” contributions to G_S at order $\frac{1}{(\sqrt{\lambda})^3}$	41
H	Direct computation of G_T and G_A functions at order $\frac{1}{(\sqrt{\lambda})^3}$	44
I	3-point function $\langle Y Y [Y Y] \rangle$	46

1 Introduction

Wilson loops are important observables in gauge theories. In addition to the standard Wilson loop (WL), in the $\mathcal{N} = 4$ super Yang-Mills theory one can define also a special Wilson-Maldacena loop (WML) which is locally-supersymmetric due to an extra coupling to SYM scalars. In the case of a straight line or circular loop that we shall consider below, the WML is also globally supersymmetric (BPS).

Both WL and WML are natural objects to study [1, 2]. For smooth contours their expectation values do not have logarithmic divergences and thus are consistent with conformal covariance. For straight line or circular contour they preserve a $SL(2, \mathbb{R})$ subgroup of the 4d conformal group, and hence they may be viewed as examples of one-dimensional conformal defects of the 4d gauge theory. In fact, the WL and WML may be interpreted respectively as the UV and IR fixed points of a 1d RG flow of the scalar coupling constant in the Wilson line exponent [2] (see also [3]). In the large N limit, their expectation values in the strong coupling ($\lambda \gg 1$) expansion are given by the $AdS_5 \times S^5$ string path integral over the world surfaces ending on an infinite line (or circle) at the boundary of AdS_5 and with the S^5 scalars subject to the Dirichlet (in the WML case) or the Neumann (in the WL case) boundary conditions [1, 2].

In addition to the WL expectation value it is interesting also to study correlation functions of local operators inserted along the loop (see, e.g., [4, 5, 1, 6–8]).¹ These correlators are constrained by the $SL(2, \mathbb{R})$ 1d conformal symmetry, and define an effective defect 1d CFT [5, 6, 9].² In the supersymmetric WML case this CFT₁ was studied in [9, 11] (see also [12–23] for some recent discussions of the 1d defect CFT approach to Wilson loop computations in $\mathcal{N} = 4$ SYM). In [11] it was shown how to compute some correlation functions on the supersymmetric WML at strong coupling using string theory, i.e. AdS/CFT. Our aim below will be to perform analogous computations in the case of the standard WL which should correspond to a different, non-supersymmetric defect CFT.

Let us first review the supersymmetric WML case, i.e. $W = \text{Tr} \mathcal{P} e^{\int dt (i\dot{x}^\mu A_\mu + |\dot{x}| \theta^A \Phi_A)}$, where Φ_A are the SYM scalars ($A = 1, \dots, 6$). For an infinite straight line (or circle) and θ^A being a constant vector this operator preserves 16 of the 32 supercharges of the $\mathcal{N} = 4$ superconformal group $PSU(2, 2|4)$. Choosing the defining line as the Euclidean time $x^0 = t \in (-\infty, \infty)$ and θ^A pointing in the 6-th direction we get $W = \text{Tr} \mathcal{P} e^{\int dt (iA_t + \Phi_6)}$. The correlators of the gauge-theory operators $O(x)$ inserted along the line (we suppress exponential factors appearing between the operators)

$$\langle\langle \mathcal{O}(t_1) \cdots \mathcal{O}(t_n) \rangle\rangle \equiv \langle \text{Tr} \mathcal{P} [O(x(t_1)) \cdots O(x(t_n)) e^{\int dt (iA_t + \Phi_6)}] \rangle \quad (1.1)$$

can be interpreted as correlators of the corresponding conformal operators $\mathcal{O}(t)$ in an effective defect CFT₁. We shall use the notation $\langle\langle \cdots \rangle\rangle$ for correlators of operators inserted on the Wilson line. We shall sometimes not distinguish between $O(x(t))$ and $\mathcal{O}(t)$ like in eq.(1.2) below.

This CFT has $d = 1$, $\mathcal{N} = 8$ superconformal symmetry $OSp(4^*|4) \subset PSU(2, 2|4)$ which contains: (i) $SO(5)$ subgroup of the $SO(6)$ rotating 5 scalars Φ_a ($a = 1, \dots, 5$) not coupled directly to the loop; (ii) $SO(3) \times SO(2, 1)$ subgroup of the 4d conformal group $SO(2, 4)$ ($SO(3)$ rotations around the line and dilatations, translation and special conformal transformation along the line); (iii) 16 supercharges preserved by the WML. The operators O on the line belong to representations of $OSp(4^*|4)$ (i.e. are

¹The operator insertions are equivalent to deformations of the Wilson line [5, 9], so that the knowledge of all of the correlators should, in principle, allow one to compute the expectation value of a general Wilson loop which is a deformation of a line or circle.

²More generally, the data of a defect CFT include additional observables, such as “bulk-defect” correlators, that describe the coupling between operators on the defect and “bulk” operators inserted away from the defect. See e.g. [10].

labelled by the 1d scaling dimension Δ and representation of “internal” $SO(3) \times SO(5)$. The simplest multiplet contains 8+8 operators corresponding to a short representation of $OSP(4^*|4)$ with protected dimensions; the bosonic ones are the 5 scalars Φ_a (with $\Delta = 1$) and the 3 “displacement” operators in the directions ($i = 1, 2, 3$) transverse to the line $\mathbb{F}_{ti} \equiv iF_{ti} + D_i\Phi_6$ (with $\Delta = 2$). Their 2-point functions in the planar SYM theory then have the exact form

$$\langle\langle \Phi_a(t_1)\Phi_b(t_2) \rangle\rangle = \delta_{ab} \frac{C_\Phi}{(t_{12})^2}, \quad (1.2)$$

where $C_\Phi(\lambda) = 2B(\lambda) = \frac{\lambda}{8\pi^2} - \frac{\lambda^2}{192\pi^2} + \dots$ is twice the Bremsstrahlung function $B(\lambda) = \frac{\sqrt{\lambda} I_2(\sqrt{\lambda})}{4\pi^2 I_1(\sqrt{\lambda})}$ [7, 8]. Similarly, one finds $\langle\langle \mathbb{F}_{ti}(t_1)\mathbb{F}_{ti}(t_2) \rangle\rangle = \delta_{ij} \frac{C_{\mathbb{F}}(\lambda)}{(t_{12})^4}$, where $C_{\mathbb{F}} = 12B(\lambda)$. The three-point functions of these elementary operators $O = (\Phi_a, \mathbb{F}_{ti})$ vanish by the $SO(3) \times SO(5)$ symmetry while their four-point correlators are non-trivial functions of the 1d conformal cross-ratio χ and the ’t Hooft coupling. For example, for 4 operators of the same dimension

$$\langle\langle \mathcal{O}_\Delta(t_1) \mathcal{O}_\Delta(t_2) \mathcal{O}_\Delta(t_3) \mathcal{O}_\Delta(t_4) \rangle\rangle = \frac{1}{(t_{12} t_{34})^{2\Delta}} G(\chi; \lambda), \quad \chi = \frac{t_{12} t_{34}}{t_{13} t_{24}}. \quad (1.3)$$

Ref. [11] computed these correlators at strong coupling using the dual string theory in $AdS_5 \times S^5$. At large string tension $T = \frac{\sqrt{\lambda}}{2\pi}$ the minimal surface corresponding to the $\frac{1}{2}$ BPS Wilson line is represented by AdS_2 space embedded into AdS_5 and fixed at a point in the S^5 . The 1d conformal group $SO(2, 1)$ is then the isometry of AdS_2 , i.e. one gets a novel example of the AdS_2/CFT_1 duality. This CFT_1 , which is “induced” from the 4d CFT on the 1d defect, is not expected to have a description based on a local 1d Lagrangian (for example, representing the Wilson loop path ordered exponential in terms of a 1d auxiliary fermionic path integral [24–29] and integrating out the 4d fields would lead to a non-local 1d fermion action).

The AdS_2 multiplet of string fluctuations transverse to the string surface includes [30]: (i) 5 massless scalars y^a (S^5 fluctuations near the fixed vacuum point); (ii) 3 massive ($m^2 = 2$) scalars x^i (AdS_5 fluctuations), and (iii) 8 fermions with $m^2 = 1$. These AdS_2 fields are then naturally identified with the 8+8 basic CFT_1 operators [6, 31, 32]. The standard relation $\Delta(\Delta - d) = m^2$ between the AdS_{d+1} scalar mass and the corresponding CFT_d operator dimension implies that the massless y^a fields should be dual to the scalars Φ^a with $\Delta = 1$ inserted on the line and subject to the standard (Dirichlet) boundary conditions, while the AdS_5 fluctuations x^i with $m^2 = 2$ should be dual to \mathbb{F}_{ti} with $\Delta = 2$.

As was explained in [11], using the quartic vertices between the y_a and x_i fields appearing in the expansion of the string action around the AdS_2 minimal surface one is able to compute the corresponding tree-level Witten diagrams in AdS_2 and extract the strong coupling predictions for the four-point functions of the protected operators on the WML

$$\langle\langle \mathcal{O}(t_1) \cdots \mathcal{O}(t_n) \rangle\rangle = \langle X(t_1) \cdots X(t_n) \rangle_{AdS_2}. \quad (1.4)$$

Here $\langle \cdots \rangle_{AdS_2}$ is the expectation value in the 2d world-sheet theory with the bulk-to-boundary propagators attached to the points t_1, \dots, t_n at the boundary, $X \sim y^a$ corresponds to $\mathcal{O} \sim \Phi^a$ and $X \sim x^i$ corresponds to $\mathcal{O} \sim \mathbb{F}_{ti}$. The expansion parameter for the AdS_2 Witten diagrams is the inverse string tension $T^{-1} = \frac{2\pi}{\sqrt{\lambda}}$.³

³As the 2d theory defined by the fundamental superstring action is to be UV finite, the duality with the boundary 1d CFT should hold for any value of λ , including world-sheet loop corrections.

Applying the OPE to (1.3) one can extract the leading corrections to the scaling dimensions of the “two-particle” operators built out of products of two of the protected insertions ($y_a \partial_t^n y_a$, etc.). In particular, for the lowest-dimension unprotected operator $y_a y_a$ at strong coupling one finds [11, 3]

$$\Delta = 2 - \frac{5}{\sqrt{\lambda}} + \mathcal{O}\left(\frac{1}{(\sqrt{\lambda})^2}\right). \quad (1.5)$$

The $y_a y_a$ operator may be identified with Φ_6 for which at weak coupling one finds [1]

$$\langle\langle \Phi_6(t_1) \Phi_6(t_2) \rangle\rangle = \frac{C_{\Phi_6}}{(t_{12})^{2\Delta}}, \quad C_{\Phi_6} = \frac{\lambda}{8\pi^2} + \dots, \quad \Delta = 1 + \frac{\lambda}{4\pi^2} + \dots, \quad (1.6)$$

so that (1.5) is consistent with a smooth growth of Δ from weak to strong coupling.

Let us now turn to our present case of interest – correlators on the standard (non-supersymmetric) Wilson line. Since here $W = \text{Tr } \mathcal{P} e^{i \int dt \dot{x}^\mu A_\mu}$ has no coupling to scalars, the full $SO(6)$ global symmetry should be preserved, i.e. the correlators of operators inserted on the line should correspond to a non-supersymmetric CFT_1 with the $SO(2,1)$ conformal and $SO(3) \times SO(6)$ “internal” symmetry. Since there is no supersymmetry, the dimension of the scalars will no longer be protected. In particular, instead of (1.2) (and (1.6)) we should get

$$\langle\langle \Phi_A(t_1) \Phi_B(t_2) \rangle\rangle = \delta_{AB} \frac{C'_\Phi}{(t_{12})^{2\Delta}}, \quad C'_\Phi = \frac{\lambda}{8\pi^2} + \dots, \quad \Delta = 1 - \frac{\lambda}{8\pi^2} + \dots. \quad (1.7)$$

The leading weak-coupling term in C'_Φ is the same as in (1.2) or (1.6), as it is determined just by the normalization of the free scalar propagator. In general, however, the 2-point function normalization factor like C'_Φ is scheme dependent and hence arbitrary, since the operator gets renormalized and has non-trivial scaling dimension.⁴ The leading correction to Δ in (1.7) was computed in [1].⁵

Our aim will be to explore these CFT_1 correlators at strong coupling using similar AdS_2/CFT_1 set-up as in [11]. The minimal surface in AdS_5 corresponding to the straight-line WL at the boundary has the same AdS_2 geometry and thus the spectrum of string fluctuations will again contain 5 massless S^5 scalars y^a , 3 AdS_5 scalars x^i with $m^2 = 2$ and 8 fermions with $m^2 = 1$. The boundary conditions for the scalar x^i do not change, and this should be dual to the usual field strength operator F_{ti} . The latter, being the displacement operator in the defect CFT_1 , should have protected dimension, i.e. $\Delta_F = 2$ for all λ .

In the supersymmetric WML case, where the expansion is around a particular point in S^5 , one may use an explicit parametrization of S^5 like ($Y_A Y_A = 1$)

$$Y_a = \frac{y_a}{1 + \frac{1}{4}y^2}, \quad Y_6 = \sqrt{1 - Y_a Y_a} = \frac{1 - \frac{1}{4}y^2}{1 + \frac{1}{4}y^2}, \quad ds_{S^5}^2 = dY_A dY_A = \frac{dy_a dy_a}{(1 + \frac{1}{4}y^2)^2}. \quad (1.8)$$

⁴ The reason why the normalization constant C_Φ in (1.2) in the supersymmetric WML case is meaningful is that Φ^a has protected dimension and is in the same multiplet as the displacement operator $\mathbb{F}_{ti} = iF_{ti} + D_t \Phi_6$; this has a natural normalization due to its relation to translations in the directions orthogonal to the defect. Hence the normalization constant in its 2-point function defines a meaningful observable, somewhat analogous to the “central charge” coefficient C_T in the correlator of two stress tensors. In the non-supersymmetric WL case the displacement operator dual to x^i will be simply proportional to the field strength component $F_{ti} = iF_{ti}$ [8] and the coefficient in the corresponding 2-point function (5.1) will also be a meaningful function of λ . However, the scalar operator normalization $C'_\Phi = C_Y$ will be scheme-dependent and we shall fix it in a particular way (see (4.3)).

⁵ Recently, it was rederived as a consequence of integrability of a certain $SO(6)$ invariant spin chain [16]. This provides a weak-coupling indication that correlators on the standard WL may be described by an integrable theory. Since the $AdS_5 \times S^5$ superstring action is an integrable 2d theory, the approach of [11] suggests that the same may be expected also at strong coupling (both in the supersymmetric and non-supersymmetric cases).

Then the expansion in $\frac{1}{\sqrt{\lambda}}$ is equivalent to expansion in powers of y_a subject to Dirichlet b.c. and one is left with $SO(5)$ as manifest symmetry of their correlators [11].⁶

The key difference with the supersymmetric WML case is that now the S^5 scalars should be subject to the Neumann (or “alternative” [34]) boundary conditions which break supersymmetry [1–3]. This leads, in particular, to an additional integration over a point in S^5 restoring the full $SO(6)$ symmetry in the corresponding correlators.⁷ We will assume that the counterparts of the SYM scalars Φ_A on the string side should be the S^5 embedding coordinates Y_A ($Y_A Y_A = 1$) on which $SO(6)$ acts linearly. For a massless AdS_2 scalar one has $\Delta(\Delta - 1) = 0$ which gives $\Delta = 0$ for the Neumann (N) boundary conditions. The first non-vanishing strong-coupling correction to Δ in this case was argued to be [1]

$$\Delta = \frac{5}{\sqrt{\lambda}} + \mathcal{O}\left(\frac{1}{(\sqrt{\lambda})^2}\right). \quad (1.9)$$

The same result was found also in [3], following [2].⁸ We will reproduce (1.9) directly by computing the 2-point function (1.7) interpreted as the scalar correlator $\langle Y_A(t_1) Y_B(t_2) \rangle_{AdS_2}$ below.

In the case of Neumann boundary conditions on y_a in (1.8) one is to integrate over their zero mode or position of the expansion point on S^5 . This is equivalent to integrating over the embedding coordinates Y_A without breaking $SO(6)$. Then we should have the following analog of (1.4),(1.7)

$$\langle\langle \Phi_{A_1}(t_1) \cdots \Phi_{A_n}(t_n) \rangle\rangle = \langle Y_{A_1}(t_1) \cdots Y_{A_n}(t_n) \rangle_{AdS_2}. \quad (1.10)$$

The computation of (1.10) can be implemented in a manifestly $SO(6)$ covariant way by setting $Y_A = n_A + \zeta_A(\sigma) + \dots$ ($n_A \zeta_A = 0$) and integrating over the fluctuations ζ_A and the constant direction n_A . In practice, it is sufficient to consider the $SO(6)$ singlets like $\langle Y_A(t_1) Y_A(t_2) Y_B(t_3) Y_B(t_4) \rangle$ which will not depend on the position of the expansion point n_A and thus averaging over n_A will not be required. Such $SO(6)$ singlets will also be IR finite in the quantum theory [37–39].

The rest of the paper is organized as follows. In section 2 we shall first review the computation of 4-point correlators on the supersymmetric Wilson line at strong coupling, following [11]. The starting point is the bosonic part of the $AdS_5 \times S^5$ string action expanded near the AdS_2 minimal surface that defines the corresponding quartic vertices between the x^i and y^a fields. After summarizing some general relations for 4-point functions in CFT_1 we will present the expressions for the leading-order strong-coupling terms in the $G(\chi)$ functions in the scalar 4-point correlators in (2.34) and (2.38). In section 2.4 we make some comments on the analytic continuation to the out of time order correlators relevant for chaos [40], which appear to display a maximal Lyapunov exponent.

In section 3 we will turn to the non-supersymmetric Wilson line case and describe the general $SO(6)$ invariant computational scheme, based on using the Neumann propagator for the fluctuations of the Y^A fields and averaging over the S^5 expansion point n^A . In section 4 we shall use it to compute the 2-point function (1.7) at strong coupling or $\langle Y_A(t_1) Y_B(t_2) \rangle$ for $SO(6)$ scalars in AdS_2 (see (4.1),(4.2)). We shall reproduce the leading term in the dimension Δ in (1.9) and also demonstrate

⁶ Let us note also that in the present case of UV finite $AdS_5 \times S^5$ superstring model there will be no automatic restoration of $SO(6)$ symmetry (either in flat 2d space or AdS_2 , cf. [33]).

⁷ The contribution of the S^5 zero modes implies also that in contrast to the large λ asymptotics $\langle W \rangle \sim (\sqrt{\lambda})^{-3/2} e^{\sqrt{\lambda}}$ of the WML [35], for the standard WL one gets $\langle W \rangle \sim \sqrt{\lambda} e^{\sqrt{\lambda}}$ [3]. Let us note also that integration over sphere 0-modes is important also in the context of ratio of BPS Wilson loops in [36].

⁸ As $Y_6 = 1 - \frac{1}{2} y_a y_a + \dots$ (see (1.8)) at strong coupling Φ_6 may be identified with $y_a y_a$ and thus should have the dimension $2 - \frac{5}{\sqrt{\lambda}} + \dots$ as in (1.5). Since in the WL case all 6 scalars have the same dimension, (1.5) and (1.9) are then consistent [3] with the fact that the dimensions of scalars with the standard (D) and alternative (N) boundary conditions in AdS_2 should sum up to 2.

(in section 4.2) that the subleading $\frac{1}{(\sqrt{\lambda})^2} \log^2$ corrections “exponentiate”, i.e. have the right coefficient to be consistent with the 1d conformally invariant form of the 2-point function in (4.1). The subleading $\frac{1}{(\sqrt{\lambda})^2} \log$ correction in (4.1) corresponding next to leading coefficient d_2 in $\Delta = \frac{5}{\sqrt{\lambda}} + \frac{d_2}{(\sqrt{\lambda})^2} + \dots$ should receive contributions from the fermionic 1-loop graphs (cf. Fig. 3) and we will not attempt to compute it here.

In section 5 we will compute the mixed correlator $\langle\langle F_t^i(t_1) F_t^i(t_2) \Phi_A(t_3) \Phi_B(t_4) \rangle\rangle$ at strong coupling or the leading contribution to the $G(\chi)$ function in $\langle x^i(t_1) x^j(t_2) Y_A(t_3) Y_B(t_4) \rangle$ in (5.2) coming from the diagrams in Figs. 6 and 7. The resulting connected contribution to G is given by (5.16), (5.18) and happens to be simply proportional to the expression in the supersymmetric case in (2.37), (2.38). The reason for this relation is explained in section 6.2.

Section 6 is devoted to the computation of the Y -scalar 4-point function (6.1), (6.2). We shall first determine the leading order $\frac{1}{(\sqrt{\lambda})^2}$ contribution to the singlet function $G_S(\chi)$ (6.10), (6.11) coming from tree-level graphs in Fig. 8 and graphs with 1-loop propagator corrections like in Fig. 9. The corresponding functions in the traceless symmetric G_T and antisymmetric G_A parts of the correlator are given in (6.12), (6.13). We shall then turn to the order $\frac{1}{(\sqrt{\lambda})^3}$ contribution coming from the tree-level graph with contact bulk vertex in Fig. 11.

In section 6.2 we will explain how one can by-pass the complication of directly computing the AdS_2 bulk integrals of the products of four logarithmic Neumann propagators by first differentiating the correlator over the boundary points, then relating it to correlators in the theory with standard Dirichlet propagators and finally integrating back. In addition to the contact diagram contribution there is also the order $\frac{1}{(\sqrt{\lambda})^3}$ contribution coming from “reducible” tree diagrams in Fig. 12 and similar diagrams with 1-loop “dressed” propagators which are computed in Appendix G (see (G.11), (G.17)). It is only the sum of all $\frac{1}{(\sqrt{\lambda})^3}$ corrections that is conformally invariant with the resulting singlet function given in (6.59). Similar expressions are found for G_T and G_A functions. Compared to the supersymmetric case expressions in (2.34) they are more complicated containing polylog (Li_3 and Li_2) functions of χ . In section 5 and section 6.4 we also comment on the consistency of the results for the G -functions with the OPE in (2.11) extracting the leading-order strong-coupling corrections to the dimensions of composite operators appearing in the intermediate channels (cf. Appendix B). We also include several other Appendices reviewing some general relations and discussing technical points.

There are a number of interesting directions to explore in the future. One is how the classical integrability of the $\text{AdS}_5 \times S^5$ string theory is reflected in the correlation functions like (1.10). Some connection to integrability is expected since, on the one hand, the knowledge of tree-level correlators is related to the value of string action on world sheets ending on more general wavy contours, while, on the other hand, the classical string integrability allows one to find more general Wilson-line type solutions (cf., e.g., [41] and [42]). It would be important to identify more direct correspondence at the level of particular correlators (and the associated AdS_2 Witten diagrams) possibly analogous to constraints on flat-space S-matrix in integrable 2d models. Another is an extension of the computations in [11] and the present paper to AdS_2 world-sheet loop level including also the Green-Schwarz fermions. Finally, it would be interesting to establish a connection between the strong-coupling results for the correlators found in this paper and general results obtained in the framework of 1d bootstrap (generalizing the analysis of [17] in the supersymmetric case).

2 Correlators on supersymmetric Wilson line at strong coupling

Before turning to the non-supersymmetric WL case let us start with a review of the computation of 4-point correlators on the supersymmetric Wilson line at strong coupling following [11].

2.1 AdS₅ × S⁵ string action in static gauge as AdS₂ bulk theory action

The bosonic part of the superstring action on AdS₅ × S⁵ may be written as

$$S_B = \frac{1}{2}T \int d^2\sigma \sqrt{h} h^{\mu\nu} \left[\frac{1}{z^2} (\partial_\mu x^0 \partial_\nu x^0 + \partial_\mu x^i \partial_\nu x^i + \partial_\mu z \partial_\nu z) + \frac{\partial_\mu y^a \partial_\nu y^a}{(1 + \frac{1}{4}y^2)^2} \right], \quad T = \frac{\sqrt{\lambda}}{2\pi}, \quad (2.1)$$

where $\sigma^\mu = (t, s)$ are Euclidean world-sheet coordinates, $r = (0, i) = (0, 1, 2, 3)$ label 4-boundary coordinates and $a = 1, \dots, 5$ – the S⁵ coordinates. The minimal surface ending on the straight line $x^0 = t$ at the boundary is

$$z = s, \quad x^0 = t, \quad x^i = 0, \quad y^a = 0, \quad (2.2)$$

with the induced metric being the AdS₂ metric

$$g_{\mu\nu} d\sigma^\mu d\sigma^\nu = \frac{1}{s^2} (dt^2 + ds^2), \quad g_{\mu\nu} = \frac{1}{s^2} \delta_{\mu\nu}. \quad (2.3)$$

The embedding of AdS₂ into AdS₅ can be made explicit using the coordinates (here $x^2 = x^i x^i$, $i = 1, 2, 3$)

$$ds_{\text{AdS}_5}^2 = \frac{(1 + \frac{1}{4}x^2)^2}{(1 - \frac{1}{4}x^2)^2} ds_2^2 + \frac{dx^i dx^i}{(1 - \frac{1}{4}x^2)^2}, \quad ds_2^2 = \frac{1}{z^2} (dx_0^2 + dz^2). \quad (2.4)$$

Then perturbation theory near the above minimal surface can be described by the string action in the Nambu form taken in the static gauge $z = s$, $x^0 = t$

$$S_B = T \int d^2\sigma \sqrt{\det \left[\frac{(1 + \frac{1}{4}x^2)^2}{(1 - \frac{1}{4}x^2)^2} g_{\mu\nu}(\sigma) + \frac{\partial_\mu x^i \partial_\nu x^i}{(1 - \frac{1}{4}x^2)^2} + \frac{\partial_\mu y^a \partial_\nu y^a}{(1 + \frac{1}{4}y^2)^2} \right]} = T \int d^2\sigma \sqrt{g} L_B, \quad (2.5)$$

where $g_{\mu\nu}$ is the background AdS₂ metric (2.3). This action representing a straight fundamental string in AdS₅ × S⁵ stretched along z may be interpreted as a 2d field theory of 3+5 scalars (x^i, y^a) propagating in AdS₂ geometry. It has manifest (linearly-realised) symmetry $SO(2, 1) \times SO(3) \times SO(5)$.

Expanding (2.5) in powers of x^i and y^a we get an interacting theory for 3 massive ($m^2 = 2$) scalars x^i and 5 massless scalars y^a propagating in AdS₂ described by $L_B = L_2 + L_{4x} + L_{2x,2y} + L_{4y} + \dots$:

$$L_2 = \frac{1}{2} g^{\mu\nu} \partial_\mu x^i \partial_\nu x^i + x^i x^i + \frac{1}{2} g^{\mu\nu} \partial_\mu y^a \partial_\nu y^a, \quad (2.6)$$

$$L_{4x} = \frac{1}{8} (g^{\mu\nu} \partial_\mu x^i \partial_\nu x^i)^2 - \frac{1}{4} (g^{\mu\nu} \partial_\mu x^i \partial_\nu x^j) (g^{\rho\kappa} \partial_\rho x^i \partial_\kappa x^j) + \frac{1}{4} x^i x^i (g^{\mu\nu} \partial_\mu x^j \partial_\nu x^j) + \frac{1}{2} x^i x^i x^j x^j, \quad (2.7)$$

$$L_{2x,2y} = \frac{1}{4} (g^{\mu\nu} \partial_\mu x^i \partial_\nu x^i) (g^{\rho\kappa} \partial_\rho y^a \partial_\kappa y^a) - \frac{1}{2} (g^{\mu\nu} \partial_\mu x^i \partial_\nu y^a) (g^{\rho\kappa} \partial_\rho x^i \partial_\kappa y^a), \quad (2.8)$$

$$L_{4y} = -\frac{1}{4} (y^b y^b) (g^{\mu\nu} \partial_\mu y^a \partial_\nu y^a) + \frac{1}{8} (g^{\mu\nu} \partial_\mu y^a \partial_\nu y^a)^2 - \frac{1}{4} (g^{\mu\nu} \partial_\mu y^a \partial_\nu y^b) (g^{\rho\kappa} \partial_\rho y^a \partial_\kappa y^b). \quad (2.9)$$

Assuming that both scalars are subject to the standard (Dirichlet) boundary conditions at $z = s = 0$ and applying the standard AdS/CFT relation ($\Delta(\Delta - 1) = m^2$) we conclude that x^i and y^a should be dual, respectively, to the $\Delta = 2$ and $\Delta = 1$ operators at the 1d boundary $x^0 = t$. There are also 8 fermionic fields transforming in the (2, 4) representation of $SU(2) \times Sp(4) \simeq SO(3) \times SO(5)$.

Starting with the 2d bulk theory (2.5) and computing Witten diagrams with bulk-to-boundary propagators attached to the points $\{t_n\}$ on the boundary will give us correlators in the boundary CFT_1 and thus the strong-coupling expansion of the SYM correlators of the corresponding gauge-theory operators ($x_i \leftrightarrow \mathbb{F}_{ti}$, $y_a \leftrightarrow \Phi_a$) inserted along the WML (see (1.1),(1.4)). As the Lagrangian L_B has no cubic terms, the first non-trivial contribution to the simplest 4-point correlation functions of x^i and y^a is given just by the contact 4-point vertices in (2.7)–(2.9).

2.2 Conformal invariance and crossing constraints on 4-point functions in CFT_1

The 4-point function of primary operators \mathcal{O} with the same dimension Δ is constrained by the $SO(2,1)$ conformal invariance to take the form

$$\langle\langle \mathcal{O}_\Delta(t_1) \mathcal{O}_\Delta(t_2) \mathcal{O}_\Delta(t_3) \mathcal{O}_\Delta(t_4) \rangle\rangle = \frac{1}{(t_{12} t_{34})^{2\Delta}} G(\chi), \quad \chi = \frac{t_{12} t_{34}}{t_{13} t_{24}}. \quad (2.10)$$

The function $G(\chi)$ in (2.10) admits the OPE (see, e.g., [43])

$$G(\chi) = \sum_h c_{\Delta,\Delta;h} \chi^h F_h(\chi), \quad F_h \equiv {}_2F_1(h, h, 2h, \chi), \quad (2.11)$$

associated with the s-channel exchange of fields with conformal dimension h . The OPE coefficients in (2.11) may be expressed in terms of the coefficients in the 2-point and 3-point functions as $c_{\Delta,\Delta;h} = \frac{(C_{\Delta,\Delta,h})^2}{(C_{\Delta,\Delta})^2 (C_{h,h})^2}$. For the 4-point function with two pairwise equal dimensions, one has

$$\langle\langle \mathcal{O}_{\Delta_1}(t_1) \mathcal{O}_{\Delta_2}(t_2) \mathcal{O}_{\Delta_1}(t_3) \mathcal{O}_{\Delta_2}(t_4) \rangle\rangle = \frac{1}{(t_{12} t_{34})^{\Delta_1 + \Delta_2}} \left| \frac{t_{24}}{t_{13}} \right|^{\Delta_{12}} G(\chi), \quad (2.12)$$

$$G(\chi) = \sum_h c_{\Delta_1, \Delta_2; h} \chi^h {}_2F_1(h + \Delta_{12}, h - \Delta_{12}, 2h, \chi), \quad \Delta_{12} = \Delta_1 - \Delta_2, \quad (2.13)$$

The expressions for the $G(\chi)$ functions in (2.10),(2.12) in the case of the (generalized) free field theory are summarized in Appendix A.

Together with the conformal invariance, we should also take into account the crossing invariance of the 4-point function. Having in mind applications to the cases of $SO(5)$ or $SO(6)$ invariant scalar correlators in defect CFT_1 's associated with the WML or WL, let us discuss crossing for the general $SO(N)$ flavour symmetry. Let us consider a primary operator \mathcal{O}_A with dimension Δ and vector index $A = 1, \dots, N$ of $SO(N)$. Then the analog of the correlator (2.10) will be

$$\langle\langle \mathcal{O}^A(t_1) \mathcal{O}^B(t_2) \mathcal{O}^C(t_3) \mathcal{O}^D(t_4) \rangle\rangle = \frac{[C_\Delta(\lambda)]^2}{t_{12}^{\Delta} t_{34}^{\Delta}} G^{ABCD}(\chi). \quad (2.14)$$

where we separated the factor related to the normalization factor C_Δ in the 2-point function. G^{ABCD} can be decomposed into singlet, symmetric traceless tensor and antisymmetric tensor parts as

$$G^{ABCD} = G_S(\chi) \delta^{AB} \delta^{CD} + G_T(\chi) \left[\delta^{AC} \delta^{BD} + \delta^{BC} \delta^{AD} - \frac{2}{N} \delta^{AB} \delta^{CD} \right] + G_A(\chi) \left[\delta^{AC} \delta^{BD} - \delta^{BC} \delta^{AD} \right], \quad (2.15)$$

so that

$$\begin{aligned} G^{AABB} &= N^2 G_S, & G^{ABAB} &= N G_S + (N+2)(N-1) G_T + N(N-1) G_A, \\ G^{ABBA} &= N G_S + (N+2)(N-1) G_T - N(N-1) G_A. \end{aligned} \quad (2.16)$$

Thus G_S, G_T, G_A can be found as combinations of invariant contractions

$$G_S = \frac{1}{N^2} G^{AABB}, \quad G_T = \frac{1}{2(N+2)(N-1)} \left[G^{ABAB} + G^{ABBA} - \frac{2}{N} G^{AABB} \right], \quad (2.17)$$

$$G_A = \frac{1}{2N(N-1)} \left[G^{ABAB} - G^{ABBA} \right]. \quad (2.18)$$

Crossing transformations are generated by the leg exchanges $3 \leftrightarrow 4$ and $1 \leftrightarrow 3$ in (2.14) which, in addition to exchanging the corresponding flavour indices, amount to $t_3 \leftrightarrow t_4$ and $t_1 \leftrightarrow t_3$ or, equivalently,

$$\chi \xrightarrow{3 \leftrightarrow 4} \frac{\chi}{\chi-1}, \quad \chi \xrightarrow{1 \leftrightarrow 3} 1 - \chi. \quad (2.19)$$

From (2.17) one finds that under $3 \leftrightarrow 4$

$$G_S(\chi) = G_S\left(\frac{\chi}{\chi-1}\right), \quad G_T(\chi) = G_T\left(\frac{\chi}{\chi-1}\right), \quad G_A(\chi) = -G_A\left(\frac{\chi}{\chi-1}\right). \quad (2.20)$$

The $1 \leftrightarrow 3$ exchange leaves invariant G^{ABAB} and swaps $G^{AABB} \leftrightarrow G^{ABBA}$. Taking into account the transformation of the prefactor $\frac{1}{t_{12}^{2\Delta} t_{34}^{2\Delta}}$ in (2.14), this gives

$$G^{AABB}(\chi) = \left(\frac{\chi}{\chi-1}\right)^{2\Delta} G^{ABBA}(1-\chi), \quad G^{ABAB}(\chi) = \left(\frac{\chi}{\chi-1}\right)^{2\Delta} G^{ABAB}(1-\chi). \quad (2.21)$$

Using (2.20) and (2.21) we observe that instead of three functions in (2.15) we have only one independent, i.e. we can express the G_T and G_A in terms of G_S . Explicitly, we have

$$G^{ABAB}(\chi) = \chi^{2\Delta} G^{AABB}\left(\frac{1}{1-\chi}\right), \quad G^{ABBA}(\chi) = \left(\frac{\chi}{\chi-1}\right)^{2\Delta} G^{AABB}(1-\chi), \quad (2.22)$$

and therefore

$$G_T(\chi) = -\frac{N}{(N+2)(N-1)} G_S(\chi) + \frac{N^2}{2(N+2)(N-1)} \left[\chi^{2\Delta} G_S\left(\frac{1}{1-\chi}\right) + \left(\frac{\chi}{\chi-1}\right)^{2\Delta} G_S(1-\chi) \right], \quad (2.23)$$

$$G_A(\chi) = \frac{N}{2(N-1)} \left[\chi^{2\Delta} G_S\left(\frac{1}{1-\chi}\right) - \left(\frac{\chi}{\chi-1}\right)^{2\Delta} G_S(1-\chi) \right]. \quad (2.24)$$

2.3 Strong-coupling expansion of the $SO(5)$ scalar 4-point function

Let us now review the result of [11] for the tree-level 4-point correlator of the S^5 fluctuations y^a dual to the 5 SYM scalars Φ^a , $a = 1, \dots, 5$ not coupled to the Wilson-Maldacena loop in (1.1). Since the dimensions of the operators Φ^a are protected by supersymmetry, we should have⁹

$$\langle\langle \Phi^a(t_1) \Phi^b(t_2) \rangle\rangle = \langle y^a(t_1) y^b(t_2) \rangle = \delta^{ab} \frac{C_\Phi}{(t_{12})^2}, \quad (2.25)$$

$$\langle\langle \Phi^a(t_1) \Phi^b(t_2) \Phi^c(t_3) \Phi^d(t_4) \rangle\rangle = \langle y^a(t_1) y^b(t_2) y^c(t_3) y^d(t_4) \rangle = \frac{C_\Phi^2}{(t_{12} t_{34})^2} G^{abcd}(\chi). \quad (2.26)$$

With the normalization coefficient $[C_\Phi(\lambda)]^2$ extracted we will have $G^{a_1 a_2 a_3 a_4}(\chi) = \delta^{a_1 a_2} \delta^{a_3 a_4} + \mathcal{O}(\chi)$. The tensor $G^{a_1 a_2 a_3 a_4}$ can be split into the S, T, A parts according to (2.15) with $N = 5$. Expanding at strong coupling (i.e. small $\frac{1}{\sqrt{\lambda}}$) we will have

$$G_c(\lambda) = G_c^{(0)} + \frac{1}{\sqrt{\lambda}} G_c^{(1)} + \dots, \quad c = S, T, A. \quad (2.27)$$

The leading order contributions $G^{(0)}$ comes from with disconnected diagrams like in Fig. 1. Here and below for simplicity we draw the 1d boundary as a circle rather than a line. It is thus given by the

⁹In what follows we shall for simplicity omit the label AdS_2 in the corresponding correlators, i.e. $\langle y^a(t_1) y^b(t_2) \rangle_{\text{AdS}_2} \equiv \langle y^a(t_1) y^b(t_2) \rangle$, etc.

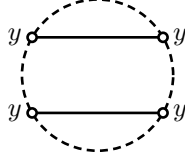


Figure 1. Leading order disconnected contribution $G^{(0)}$ with other similar diagrams obtained by crossing.

free-field contribution (cf. (A.2))

$$\begin{aligned} \langle\langle \Phi^a(t_1)\Phi^b(t_2)\Phi^c(t_3)\dots\Phi^d(t_4) \rangle\rangle_{\text{disc.}} &= C_\Phi^2 \left[\frac{\delta^{ab}\delta^{cd}}{t_{12}^2 t_{34}^2} + \frac{\delta^{ac}\delta^{bd}}{t_{13}^2 t_{24}^2} + \frac{\delta^{ad}\delta^{bc}}{t_{14}^2 t_{23}^2} \right] \\ &= \frac{C_\Phi^2}{(t_{12}t_{34})^2} \left[\delta^{ab}\delta^{cd} + \chi^2 \delta^{ac}\delta^{bd} + \frac{\chi^2}{(1-\chi)^2} \delta^{ad}\delta^{bc} \right]. \end{aligned} \quad (2.28)$$

Comparing with (2.15) gives

$$G_S^{(0)}(\chi) = 1 + \frac{2}{5} G_T^{(0)}(\chi), \quad G_T^{(0)}(\chi) = \frac{1}{2} \left[\chi^2 + \frac{\chi^2}{(1-\chi)^2} \right], \quad G_A^{(0)}(\chi) = \frac{1}{2} \left[\chi^2 - \frac{\chi^2}{(1-\chi)^2} \right]. \quad (2.29)$$

The first subleading correction comes from the contact diagram in Fig. 2 where the 4-point vertex

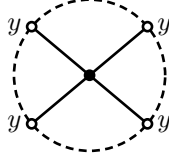


Figure 2. Contact diagram contributing to first subleading strong-coupling correction $G^{(1)}$.

comes from (2.9). The bulk-to-boundary propagator corresponding to a massive scalar in AdS_{d+1} is $(\Delta(\Delta - d) = m^2)$

$$K_\Delta(z, x; x') = \mathcal{C}_\Delta K_\Delta(z, x; x'), \quad K_\Delta(z, x; x') \equiv \left[\frac{z}{z^2 + (x - x')^2} \right]^\Delta, \quad (2.30)$$

$$\langle\langle \mathcal{O}_\Delta(x)\mathcal{O}_\Delta(x') \rangle\rangle = \frac{\mathcal{C}_\Delta}{|x - x'|^{2\Delta}}, \quad \mathcal{C}_\Delta = \frac{\Gamma(\Delta)}{2\pi^{d/2} \Gamma(\Delta + 1 - \frac{d}{2})}, \quad (2.31)$$

where we have assumed a particular normalization of the 2-point function of the associated boundary field.¹⁰ For $d = 1$ and $\Delta = 1$ this gives

$$d = 1, \Delta = 1: \quad K_1(z, t; t') = \frac{1}{\pi} K_1, \quad K_1 = \frac{z}{z^2 + (t - t')^2}, \quad \mathcal{C}_1 = \frac{1}{\pi}. \quad (2.32)$$

The contribution of the connected diagram corresponding to the vertex in (2.9) is then

$$\langle\langle \Phi^a(t_1)\Phi^b(t_2)\Phi^c(t_3)\Phi^d(t_4) \rangle\rangle_{\text{conn}} = \langle y^a(t_1)y^b(t_2)y^c(t_3)y^d(t_4) \rangle_{\text{conn}}$$

¹⁰Explicitly, in this normalization $C_\Phi(\lambda) = \mathcal{C}_1(1 - \frac{3}{2\sqrt{\lambda}} + \dots) = \frac{4\pi}{\sqrt{\lambda}} B(\lambda)$, with \mathcal{C}_1 given in (2.32). The higher order corrections in λ are determined by the Bremsstrahlung function $B(\lambda)$ and should be reproduced by computing loop corrections to the boundary-to-boundary propagators in Figure 1.

$$= \frac{(\mathcal{C}_1)^2}{(t_{12} t_{34})^2} \frac{1}{\sqrt{\lambda}} (G^{(1)})^{abcd}, \quad (2.33)$$

where the corresponding functions in (2.15) are then

$$\begin{aligned} G_S^{(1)}(\chi) &= -2 \frac{\chi^4 - 4\chi^3 + 9\chi^2 - 10\chi + 5}{5(\chi-1)^2} + \frac{(2\chi^4 - 11\chi^3 + 21\chi^2 - 20\chi + 10)\chi^2}{5(\chi-1)^3} \log \chi - \frac{(2\chi^4 - 5\chi^3 - 5\chi + 10)}{5\chi} \log(1-\chi), \\ G_T^{(1)}(\chi) &= -\frac{(2\chi^2 - 3\chi + 3)\chi^2}{2(\chi-1)^2} + \frac{(\chi^2 - 3\chi + 3)\chi^4}{(\chi-1)^3} \log \chi - \chi^3 \log(1-\chi), \\ G_A^{(1)}(\chi) &= -\frac{(\chi-2)(2\chi^2 - \chi + 1)\chi}{2(\chi-1)^2} + \frac{(\chi-2)(\chi^2 - 2\chi + 2)\chi^3}{(\chi-1)^3} \log \chi - (\chi^3 - \chi^2 - 1) \log(1-\chi). \end{aligned} \quad (2.34)$$

These expressions are found by computing AdS₂ integrals as discussed in Appendix C. Here and in what follows we assume as in [11] that $\log \chi \equiv \log |\chi|$, $\log(1-\chi) \equiv \log |1-\chi|$ so that the resulting expressions are defined as real on the whole line $\chi \in (-\infty, \infty)$.

The leading order terms (2.29) in $G_{S,T,A}(\chi)$ are given by the free-field expressions associated with the exchange of 2-particle states $\Phi^a \partial_t^k \Phi^b$ that can be decomposed as

$$[\Phi\Phi]_{2n}^S \sim \Phi^a \partial_t^{2n} \Phi^a, \quad [\Phi\Phi]_{2n}^T \sim \Phi^{(a} \partial_t^{2n} \Phi^{b)}, \quad [\Phi\Phi]_{2n+1}^A \sim \Phi^{[a} \partial_t^{2n+1} \Phi^{b]}. \quad (2.35)$$

The connected contributions (2.34) provide the $\frac{1}{\sqrt{\lambda}}$ corrections to the OPE coefficients and scaling dimensions $h_n = 2 + 2n + \frac{1}{\sqrt{\lambda}} \gamma^{(1)} + \dots$ of these operators. In general, there is a mixing between $[\Phi\Phi]_{2n}^S$ (with $n > 0$) and $\mathbb{F}\mathbb{F}$ and 2-fermion operators, while $[\Phi\Phi]_{2n+1}^A$ mixes with 2-fermion states in the $(\mathbf{1}, \mathbf{10})$ of $SU(2) \times Sp(4) \simeq SO(3) \times SO(5)$. The mixing is absent for $[\Phi\Phi]_0^S$ or $[\Phi\Phi]_{2n}^T$ and for these operators one finds (see Appendix B)

$$h_n = 2 + 2n + \frac{1}{\sqrt{\lambda}} \gamma^{(1)} + \dots, \quad \gamma_{[\Phi\Phi]_{2n}^T}^{(1)} = -3n - 2n^2, \quad \gamma_{[\Phi\Phi]_0^S}^{(1)} = -5. \quad (2.36)$$

Assuming that one can identify the scalar Φ_6 coupled to the WML with the singlet composite field $y^a y^a \sim [\Phi\Phi]_{n=0}^S$ one finds that strong coupling expansion of its dimension should be given by (1.5).

Finally, let us mention that one can similarly compute the strong-coupling expansion of the correlation functions involving AdS₅ coordinates x^i dual to the dimension $\Delta = 2$ operator \mathbb{F}_{it} inserted on the Wilson line. In particular, one finds for the connected part of the mixed correlator of two AdS and two sphere fluctuations [11]

$$\langle \langle \mathbb{F}_{it}^i(t_1) \mathbb{F}_{it}^j(t_2) \Phi^a(t_3) \Phi^b(t_4) \rangle \rangle_{\text{conn}} = \langle x^i(t_1) x^j(t_2) y^a(t_3) y^b(t_4) \rangle_{\text{conn}} = \delta^{ij} \delta^{ab} \frac{G_{\text{conn}}(\chi)}{t_{12}^4 t_{34}^2}, \quad (2.37)$$

$$G_{\text{conn}}(\chi) = \frac{1}{\sqrt{\lambda}} \mathcal{C}_1 \mathcal{C}_2 G^{(1)}(\chi) = \frac{1}{\sqrt{\lambda}} \frac{2}{3\pi^2} G^{(1)}(\chi), \quad G^{(1)} = -4 \left[1 - \left(\frac{1}{2} - \frac{1}{\chi} \right) \ln(1-\chi) \right]. \quad (2.38)$$

The explicit expression for the 4-point correlator of $x^i \sim \mathbb{F}_{it}^i$ can also be found in [11].

2.4 Analytic continuation to the ‘‘chaos configuration’’

It is interesting to consider the analytic continuation of the above results to the out of time order correlator relevant to chaos [40, 44]. Let us focus on the $SO(5)$ singlet part of the 4-point function of sphere coordinates, which is given by the contracted correlation function $\langle y^a(t_1) y^a(t_2) y^b(t_3) y^c(t_4) \rangle$. Following [44], in order to obtain the relevant thermal out of time order configuration $y^a(t) y^b(0) y^a(t) y^b(0)$, one can map the line to the thermal circle by $t_i = \tan(\pi\tau_i/\beta)$, $i = 1, \dots, 4$, and then continue to real time.¹¹ A convenient configuration considered in [40] is given by taking the four operators to be equally spaced along the thermal circle. This configuration can be obtained by setting

¹¹Equivalently, one should also be able to obtain the result by computing the 4-point functions directly in AdS Rindler coordinates $ds^2 = -(r^2/r_h^2 - 1)dt^2 + \frac{dr^2}{r^2/r_h^2 - 1}$.

$\tau_1 = it, \tau_2 = it + \beta/2, \tau_3 = \beta/4, \tau_4 = -\beta/4$, which corresponds to a value of the cross ratio

$$\chi = \frac{2}{1 - i \sinh(\frac{2\pi t}{\beta})}. \quad (2.39)$$

In order to reach this configuration, one has to start from the expression for $G_S(\chi)$ valid in the region $\chi > 1$, which can be simply obtained from (2.34) by letting $\log(1 - \chi) \rightarrow \log(\chi - 1)$. Then, one may take a large t limit (corresponding to the formal small χ limit of the $\chi > 1$ expression) to probe the chaotic behavior. Applying this procedure to the result for $G_S(\chi)$ given in (2.34), we find for the out of time order correlator

$$\frac{\langle y^a(t)y^b(0)y^a(t)y^b(0) \rangle}{\langle y^a y^a \rangle \langle y^b y^b \rangle} \simeq 1 - \frac{\pi}{2\sqrt{\lambda}} e^{\frac{2\pi t}{\beta}}, \quad (2.40)$$

where we have normalized by the product of 2-point functions (omitting the explicit positions along the thermal circle). The behavior (2.40) corresponds to a maximal Lyapunov exponent $\frac{2\pi}{\beta}$. The same behavior can be seen to arise from the $\langle xxyy \rangle$ correlator in (2.38) and the $\langle xxxx \rangle$ correlator that can be found in [11]. This maximally chaotic behavior for correlators on the string worldsheet was also found previously in [45, 46].

In our static gauge approach, this result can be seen to be essentially due to the 4-derivative vertices in the Nambu-Goto action: these lead to terms in the 4-point functions of the form $\simeq \chi^{-1} \log(1 - \chi)$, which are responsible for (2.40). We will see below that the same behavior persists for the correlators on the non-supersymmetric Wilson line, indicating that it is not sensitive to the boundary conditions. This should be due to the fact that the limit relevant to chaos is captured by the near horizon region, which is essentially flat space.¹² The chaotic behavior (2.40) should then also be related to the “gravitational-type” phase shift found in [47] for the S-matrix on a long string in flat space. It would be interesting to further clarify the relation of our calculations to the exact flat space S-matrix of [47].

3 Non-supersymmetric Wilson line case: $SO(6)$ invariant correlators

Let us now turn to the case of strong-coupling description of correlators on non-supersymmetric WL. As discussed in the introduction, the corresponding non-supersymmetric CFT_1 should be dual to the AdS_2 theory defined by the same string action (2.5)–(2.9) but now with Neumann boundary conditions for the S^5 fluctuations [1–3]: $\partial_s y^a|_{s=0} = 0$ (cf. (2.2), (2.3)). Then the $SO(6)$ symmetry of scalar correlators will be restored due to the remaining integration over the unfixed “zero mode” part of y^a .

This may be implemented systematically using the embedding coordinates Y_A (without choosing explicitly a particular parametrization or solution of $Y_A Y_A = 1$ as in (1.8)). Ignoring the dependence on the transverse AdS_5 fluctuations x_i in the string action (2.5) the bosonic Lagrangian in the static gauge will take the form

$$L_B = \sqrt{\det(g_{\mu\nu} + \partial_\mu Y_A \partial_\nu Y_A)} = \sqrt{g} (1 + L_2 + L_4 + \dots), \quad (3.1)$$

$$L_2 = \frac{1}{2} \partial^\mu Y_A \partial_\mu Y_A, \quad L_4 = \frac{1}{8} (\partial^\mu Y_A \partial_\mu Y_A)^2 - \frac{1}{4} (\partial^\mu Y_A \partial_\mu Y_B)^2, \quad (3.2)$$

so that the path integral over S^5 will be ($Y^2 \equiv Y_A Y_A, T = \frac{\sqrt{\lambda}}{2\pi}$)

$$Z = \int \mathcal{D}Y \delta(Y^2 - 1) \exp\left(-T \int d^2\sigma \sqrt{g} [L_2(Y) + L_4(Y) + \dots]\right). \quad (3.3)$$

¹²We thank Juan Maldacena for discussions on these points.

Let us separate the constant part n^A of Y^A that selects a particular point on S^5 as

$$Y^A = n^A + \tilde{y}^A(\sigma), \quad n^2 = 1. \quad (3.4)$$

Then (3.3) takes the form

$$Z = \int [dn] \int \mathcal{D}\tilde{y} \delta(n_A \tilde{y}_A + \frac{1}{2} \tilde{y}_A \tilde{y}_A) \exp\left(-T \int d^2\sigma \sqrt{g} [L_2(\tilde{y}) + L_4(\tilde{y}) + \dots]\right), \quad (3.5)$$

where $\int [dn] \dots \equiv \int d^6n \delta(n^2 - 1) \dots$ is the integral over S^5 . The δ -function constraint on \tilde{y}^A can be solved perturbatively in powers of an independent fluctuation y^A orthogonal to n^A as¹³

$$\tilde{y}^A = f(y^2) n^A + h(y^2) y^A, \quad n_A y^A = 0, \quad (3.6)$$

$$f = -\frac{1}{2} y^2 - (a + \frac{1}{8}) (y^2)^2 + \dots, \quad h = 1 + a y^2 + \dots, \quad y^2 = y_A y^A, \quad (3.7)$$

where a is an arbitrary coefficient. We can always choose $a=0$ or redefine¹⁴ $h(y^2) y^A \rightarrow \zeta^A$. This is equivalent to defining ζ^A as the part of Y^A orthogonal to n^A . This is what we shall do below, i.e. set

$$Y^A = \sqrt{1 - \zeta^2} n^A + \zeta^A = [1 - \frac{1}{2} \zeta^2 - \frac{1}{8} (\zeta^2)^2 + \dots] n^A + \zeta^A, \quad n^A \zeta^A = 0. \quad (3.8)$$

Then the path integral (3.3) or (3.5) takes the form

$$Z = \int [dn] \int \mathcal{D}\zeta \delta(n_A \zeta^A) \exp\left(-T \int d^2\sigma \sqrt{g} [L_2(\zeta) + L_4(\zeta) + \dots]\right), \quad (3.9)$$

$$L_2 = \frac{1}{2} \partial^\mu \zeta^A \partial_\mu \zeta^A, \quad L_4 = \frac{1}{2} \zeta^A \zeta^B \partial^\mu \zeta^A \partial_\mu \zeta^B + \frac{1}{8} (\partial^\mu \zeta^A \partial_\mu \zeta^A)^2 - \frac{1}{4} (\partial^\mu \zeta^A \partial_\mu \zeta^B)^2, \quad (3.10)$$

where we have substituted (3.8) into (3.2) keeping only terms up to quartic order in ζ^A .

The propagator for the massless scalar field ζ^A (with 5 independent components for fixed n^A) is then given by

$$\langle \zeta^A(\sigma) \zeta^B(\sigma') \rangle = P^{AB}(n) G_N(\sigma, \sigma'), \quad P^{AB} = \delta^{AB} - n^A n^B, \quad (3.11)$$

where P^{AB} is the projector orthogonal to n^A and G_N is the bulk Green's function in AdS_2 (2.3) corresponding to the Neumann boundary conditions (see Appendix D)

$$G_N(\sigma, \sigma') = -\frac{1}{4\pi} \left(\log[(t-t')^2 + (z-z')^2] + \log[(t-t')^2 + (z+z')^2] \right). \quad (3.12)$$

The corresponding bulk-to-boundary propagator will be also denoted as G_N :

$$G_N(t, z; t') \equiv G_N(t, z; t', 0) = -\frac{1}{2\pi} \log[(t-t')^2 + z^2]. \quad (3.13)$$

We will also use boundary-to-boundary propagator

$$G_N(t_1, t_2) \equiv G_N(t_1, 0; t_2, 0) = -\frac{1}{2\pi} N_{12}, \quad N_{12} \equiv \log(t_{12}^2). \quad (3.14)$$

As in the static gauge (used in (2.5),(3.3)) which is adapted to the expansion near the WL minimal surface the target-space AdS coordinate z is identified with the world-sheet coordinate s (see (2.2)) we shall often use $\sigma^\mu = (t, z)$ as the coordinates in the AdS_2 bulk theory. The propagator (3.12) is the standard Neumann one on a half-plane ($z \geq 0$) with a conformally-flat metric (the dependence on

¹³In the special case of the y^a parametrization in (1.8),(2.5) we had $n^A = (0, 0, 0, 0, 0, 1)$ and $\zeta^6 = 0$, $y^a = y^a$.

¹⁴Such local field redefinitions should preserve the ‘‘on-shell’’ correlators in AdS_2 , see Appendix E.

conformal factor drops out due to the conformal invariance of the massless scalar kinetic term in (3.9). The conformal factor re-enters via a covariant UV cutoff, e.g., after the replacement $(t-t')^2+(z-z')^2 \rightarrow [\frac{(t-t')^2+(z-z')^2}{zz'} + \varepsilon^2] z z'$ (see Appendix D).

In what follows we shall use this $SO(6)$ covariant set-up (3.9)–(3.12) to compute correlation functions of the S^5 embedding coordinates that should give as in (1.10) the corresponding scalar correlators in the boundary CFT_1 . The expectation value $\langle Y_{A_1}(t_1) \cdots Y_{A_n}(t_n) \rangle_{\text{AdS}_2}$ will be computed according to (3.8), (3.9), (3.10), i.e. will include integrating over ζ^A as well as averaging over the S^5 direction n^A . From now on we shall denote the AdS_2 expectation value simply by $\langle \cdots \rangle$.

The averaging over S^5 can be done using

$$\langle n^A n^B \rangle = \frac{1}{6} \delta^{AB}, \quad \langle n^A n^B n^C n^D \rangle = \frac{1}{48} (\delta^{AB} \delta^{CD} + \delta^{AC} \delta^{BD} + \delta^{AD} \delta^{BC}), \quad (3.15)$$

$$\langle P^{AB} \rangle = \frac{5}{6} \delta^{AB}, \quad \langle P^{AB} P^{CD} \rangle = \frac{33}{48} \delta^{AB} \delta^{CD} + \frac{1}{48} (\delta^{AC} \delta^{BD} + \delta^{AD} \delta^{BC}), \quad \text{etc.} \quad (3.16)$$

This averaging restores $SO(6)$ symmetry and implies that all correlators with odd number of Y_A should vanish, i.e. non-vanishing ones should be $\langle YY \rangle, \langle xxYY \rangle, \langle YYYYY \rangle$, etc.

4 Two-point function $\langle Y^A Y^B \rangle$

The 2-point boundary-to-boundary correlator of Y_A is supposed to reproduce the strong-coupling expansion of the 2-point function of the $SO(6)$ scalars (1.7). Its structure is fixed by 1d conformal invariance to be $(Y^A(t) \equiv Y^A(t, z = 0))$

$$\langle Y^A(t_1) Y^B(t_2) \rangle = \delta^{AB} \frac{C_Y}{|t_{12}|^{2\Delta}} = \delta^{AB} C_Y \left[1 - \left(\frac{d_1}{\sqrt{\lambda}} + \frac{d_2}{(\sqrt{\lambda})^2} + \dots \right) \log(t_{12}^2) \right. \\ \left. + \left(\frac{d_1^2}{2(\sqrt{\lambda})^2} + \dots \right) \log^2(t_{12}^2) + \dots \right], \quad (4.1)$$

$$\Delta = \frac{d_1}{\sqrt{\lambda}} + \frac{d_2}{(\sqrt{\lambda})^2} + \frac{d_3}{(\sqrt{\lambda})^3} + \dots, \quad d_1 = 5, \quad (4.2)$$

where the $d_1 = 5$ is the expected value of the leading anomalous dimension coefficient (1.9). The subleading $\frac{d_2}{(\sqrt{\lambda})^2}$ contribution to log term and thus to Δ should come from the 1-loop diagrams involving also the fermions (see below).

Note that the normalization of the 2-point function of the conformal operator dual to Y^A is scheme dependent and hence arbitrary. On the string side, since the two-point function starts with $\langle n^A n^B \rangle = \frac{1}{6} \delta^{AB}$, it appears to be natural to choose a scheme where to all orders

$$C_Y = \frac{1}{6} \quad (4.3)$$

so that the condition $Y^A Y^A = 1$ at coincident points is preserved.¹⁵ This should correspond to fixing a particular choice of 2-point function normalization of the dual operator Φ^A inserted on the WL.

4.1 Leading logarithmic correction

Using (3.8), (3.11) and (3.16) we find $(T^{-1} = \frac{2\pi}{\sqrt{\lambda}})$

$$\langle Y^A(\sigma_1) Y^B(\sigma_2) \rangle = \langle [n^A + \zeta^A + \dots] [n^B + \zeta^B + \dots] \rangle = \frac{1}{6} \delta^{AB} [1 + 5 T^{-1} G_N(\sigma_1, \sigma_2) + \dots]. \quad (4.4)$$

¹⁵One may ensure the expected normalization of (4.1) at the coinciding points $\langle Y^A(t) Y^A(t) \rangle = 1$ by explicitly keeping track of the boundary UV cutoff dependence as in $\langle Y^A(t_1) Y^B(t_2) \rangle = \frac{1}{6} \delta^{AB} [\frac{\varepsilon^2}{|t_{12}|^2 + \varepsilon^2}]^\Delta$. We will not do this below.

Setting $z_1, z_2 \rightarrow 0$ in the propagator in (3.12),(3.13) we thus readily reproduce the value $d_1 = 5$ in (4.1). We have ignored the contribution of the $-\frac{1}{2}\zeta^2 n^A$ term in Y^A in (3.8) as it leads (to the leading order) only to a cutoff-dependent constant.

As discussed in [3], this value is the $J = 1$ case of the $J(J+4)$ eigenvalue corresponding to the S^5 scalar spherical harmonic with angular momentum J . One may, indeed, generalize the computation in (4.4) to the correlator $\langle V^{A_1 \dots A_J}(\sigma_1) V^{B_1 \dots B_J}(\sigma_2) \rangle$ where $V^{A_1 \dots A_J} = Y^{\{A_1 \dots A_J\}}$ is a totally symmetric traceless tensor. It is sufficient to consider the correlator of two primary fields $\langle Z^J \bar{Z}^J \rangle$ where $Z = u_A Y^A$ with constant complex null vector u_A ($u^2 = 0$). For example, we may use $Z = Y_1 + iY_2$ and then

$$\langle Z^J(\sigma_1) \bar{Z}^J(\sigma_2) \rangle = \langle [M_J - J^2 (M_J - 2M_{J-1}) T^{-1} G_N(\sigma_1, \sigma_2)] \rangle + \dots, \quad M_J \equiv |n_1 + i n_2|^{2J}, \quad (4.5)$$

where the remaining S^5 average can be done, e.g., by using the explicit spherical angle parametrization of n^A .¹⁶ As a result, $\langle M_J \rangle = \frac{2}{(J+1)(J+2)}$ and thus

$$\langle (Y_1 + i Y_2)^J(\sigma_1) (Y_1 - i Y_2)^J(\sigma_2) \rangle = \frac{2}{(J+1)(J+2)} [1 + J(J+4) T^{-1} G_N(\sigma_1, \sigma_2)] + \dots, \quad (4.6)$$

with $J(J+4)$ thus replacing 5 in (4.4).

4.2 Subleading corrections

The order $\frac{1}{(\sqrt{\lambda})^2}$ corrections to the 2-point function will be given by the sum of the log and \log^2 terms in (4.1). The d_2 log term should originate from the bosonic (ζ^A and x^i , cf. (2.8)) and fermionic 1-loop diagrams – the second and third diagrams in Fig. 3. We will not systematically include fermions and thus will not determine d_2 here.

The 1d conformal invariance of (4.1) implies that the leading logs at each order in $\frac{1}{(\sqrt{\lambda})^n}$ should exponentiate. Thus at order $\frac{1}{(\sqrt{\lambda})^2}$ we should find the $\log^2(t_{12}^2)$ term with the coefficient being precisely $\frac{d_1^2}{2} = \frac{25}{2}$. To demonstrate this requires to go beyond the tree approximation and include the loop contributions of the interacting vertices in (3.9).¹⁷

At order $\frac{1}{(\sqrt{\lambda})^2}$ we need to consider the 1-loop contributions from the vertices in L_4 in (3.10) and these require UV regularization. In general, the coefficients in the finite contributions will depend on a scheme and, as usual, the scheme should be chosen so that to preserve the required (world-sheet and target space) symmetries (cf. Appendix D).

There are three types of diagrams contributing to the 2-point function (4.1) at order $\frac{1}{(\sqrt{\lambda})^2}$ are shown in Fig. 3: (i) the tree-level one with the contraction of the $\zeta^2 n^A$ terms in Y^A in (3.8) that does not involve interaction vertices; (ii) bosonic 1-loop diagrams with quartic vertices from L_4 in (3.10); (iii) fermionic 1-loop diagrams with vertices from the fermionic terms in the full $\text{AdS}_5 \times S^5$ superstring action (which were ignored in (2.5)).

While the fermionic loop contribution is important for computing the subleading d_2 coefficient in the scaling dimension (4.2), given that d_1 in (4.2) receives contribution only from bosons it might be

¹⁶Explicitly, $\langle M_J \rangle = \frac{1}{\pi^3} \int_0^{2\pi} d\phi \int_0^\pi d\theta_1 \dots d\theta_4 \sin^4 \theta_1 \sin^3 \theta_2 \sin^2 \theta_3 \sin \theta_4 |\cos \theta_1 + i \sin \theta_1 \cos \theta_2|^{2J} = \frac{2}{(J+1)(J+2)}$.

¹⁷It is useful to compare the present case with that of a free scalar 2d theory which also has a logarithmic propagator, $\langle XX \rangle \sim \log |z_{12}|$. Here a primary operator without derivatives which will have $\langle OO \rangle \sim |z_{12}|^{-2\Delta}$ is $O = e^{aX}$. The choice of the exponential function is essential for the right combinatorics. One may of course redefine $X \rightarrow X'$, $X = a^{-1} \log(1 + aX')$ so that $O = 1 + aX'$ but then the required contributions will come from the expansion of the redefined action $L = (\partial X)^2 = \frac{(\partial X')^2}{(1+aX')^2}$. Similarly, in the present case of $Y^A(\zeta) = \sqrt{1 - z^2 n^A} + \zeta^A = n^A + \zeta^A - \frac{1}{2} z^2 n^A + \dots$ with the propagator of ζ given by (3.14) we will not get the correct exponentiation of $\log t_{12}^2$ without including extra contributions from loop diagrams with the interacting vertices from the action.

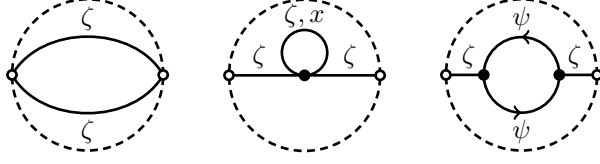


Figure 3. Diagrams contributing the 2-point function $\langle YY \rangle$ at order $\frac{1}{(\sqrt{\lambda})^2}$.

natural to expect that finite $\frac{1}{(\sqrt{\lambda})^2} \log^2(t_{12}^2)$ terms in (4.1) should also come only from the bosonic 1-loop contributions. Still, given that the fermionic contribution is crucial for ensuring the UV finiteness of the 2d theory (and given that, in general, there are power-like divergences in the purely bosonic theory) this issue may be regularization scheme dependent. Below we shall assume that there is no $\log^2(t_{12}^2)$ term coming from the fermionic loop in Fig. 3 and concentrate only on the bosonic contributions, i.e. the first two diagrams in Fig. 3.

The contribution of the first diagram in Fig. 3 is $\langle \frac{1}{2} \zeta^2(t_1) n^A \frac{1}{2} \zeta^2(t_2) n^B \rangle$ so it should correct (4.4) (restricted to the boundary points $\sigma_a = (t_a, 0)$) by $\gamma_2 T^{-2} [\mathbb{G}_N(t_1, t_2)]^2$ term. In general, we should find $(\mathbb{G}_N(t_1, t_2) = -\frac{1}{2\pi} N_{12}$, see (3.14))

$$\langle Y^A(t_1) Y^B(t_2) \rangle = \frac{1}{6} \delta^{AB} \left[1 + \frac{\gamma_1}{\sqrt{\lambda}} N_{12} + \frac{\gamma_2}{(\sqrt{\lambda})^2} (N_{12})^2 + \frac{\gamma_3}{(\sqrt{\lambda})^3} (N_{12})^3 + \dots \right], \quad N_{12} = \log(t_{12}^2) \quad (4.7)$$

$$\gamma_1 = -d_1 = -5, \quad \gamma_2 = \gamma_2^{(0)} + \gamma_2^{(1)}, \quad \gamma_2^{(0)} = \frac{5}{2}. \quad (4.8)$$

The tree-level contribution $\gamma_2^{(0)} = \frac{5}{2}$ here should be part of the total coefficient $\gamma_2 = \frac{d_1^2}{2} = \frac{25}{2}$ in (4.1); the additional term $\gamma_2^{(1)} = \frac{20}{2} = 10$ should come from the 1-loop diagrams.

As we shall see below, it is only the first (“sigma-model”) quartic vertex in L_4 in (3.10) that will contribute to the leading \log^2 term in (4.7). It will lead to several 1-loop contributions to the correlator

$$\langle \zeta^A(t_1) \zeta^B(t_2) \rangle = \frac{1}{6} \delta^{AB} \Pi(t_{12}). \quad (4.9)$$

One comes from the contraction $\int d^2\sigma \sqrt{g} \langle \overline{\zeta^A(t_1)} \overline{\zeta^B(t_2)} \overline{\zeta^C} \zeta^D (\partial \overline{\zeta^C} \cdot \partial \zeta^D) \rangle$ (plus permutations). Its contribution is found to be

$$\Pi_1 = -\frac{\sqrt{\lambda}}{2\pi} \times 5 \times \left(\frac{2\pi}{\sqrt{\lambda}}\right)^3 \times X_2 \times I_2, \quad I_2 = \int \frac{dz dt}{z^2} \mathbb{G}_N(t, z; t_1) \mathbb{G}_N(t, z; t_2) = \frac{1}{4\pi} \log^2(t_{12}^2), \quad (4.10)$$

$$X_2 = \lim_{\sigma' \rightarrow \sigma} g^{\mu\mu'} \partial_\mu \partial_{\mu'} \mathbb{G}_N(\sigma, \sigma') = \frac{k}{4\pi}, \quad (4.11)$$

where $\mathbb{G}_N(t, z; t')$ is the bulk-to-boundary propagator (3.13). X_2 originates from $\langle \partial \zeta(\sigma) \cdot \partial \zeta(\sigma) \rangle$ and its value, in general, depends on a scheme: such correlators are, in general, power divergent and in (4.11) we dropped quadratic divergence (cf. (4.22), (D.13)). The value of k (4.11) found using the naive point-splitting is $k = 1$ but in AdS₂ case (in the presence of the boundary) a more natural value is $k = 2$ (see discussion at the end of Appendix D and (D.14)).

The bulk integral I_2 in (4.10) is computed using that $\log X = -\lim_{\varepsilon \rightarrow 0} X^{-\varepsilon}$ and thus $I_2 = \frac{1}{(2\pi)^2} \lim_{\varepsilon_1, \varepsilon_2 \rightarrow 0} \bar{I}_2$, where

$$\bar{I}_2 = \frac{\partial^2}{\partial \varepsilon_1 \partial \varepsilon_2} \frac{\Gamma(\varepsilon_1 + \varepsilon_2)}{\Gamma(\varepsilon_1) \Gamma(\varepsilon_2)} \int_{-\infty}^{\infty} dt \int_0^{\infty} \frac{dz}{z^2} \int_0^1 dx \frac{x^{\varepsilon_1 - 1} (1-x)^{\varepsilon_2 - 1}}{[x((t-t_1)^2 + z^2) + (1-x)((t-t_2)^2 + z^2)]^{\varepsilon_1 + \varepsilon_2}} \quad (4.12)$$

The resulting contribution to γ_2 in (4.7) is $(\gamma_2^{(1)})_1 = -\frac{5}{4}k$.

Another contribution originates from the contractions $\int d^2\sigma \sqrt{g} \langle \overbrace{\zeta^A(t_1) \zeta^B(t_2) \zeta^C \zeta^D} (\partial \zeta^C \cdot \partial \zeta^D) \rangle$ and $\int d^2\sigma \sqrt{g} \langle \overbrace{\zeta^A(t_1) \zeta^B(t_2) \zeta^C \zeta^D} (\partial \zeta^D \cdot \partial \zeta^C) \rangle$. Using that from (3.12)

$$\left[\partial_\mu G_N(\sigma, \sigma') \right]_{\sigma=\sigma'} = \begin{cases} 0, & \mu = 0 \\ -\frac{1}{2\pi z}, & \mu = 1 \end{cases}, \quad (4.13)$$

we get the following analog of (4.10) (with averaging over n_A computed using (3.16) and $P^{CC} = 5$)

$$\Pi_2 = -\frac{\sqrt{\lambda}}{2\pi} \times \frac{1}{2} \times 2^2 \times 30 \times \frac{1}{\sqrt{\lambda}} \left(\frac{2\pi}{\sqrt{\lambda}}\right)^2 \times I'_2, \quad (4.14)$$

where the bulk integral I'_2 is related to I_2 in (4.10) via integration by parts

$$I'_2 = -\int \frac{dzdt}{z^2} z \partial_z G_N(t, z; t_1) G_N(t, z; t_2) = -\frac{1}{2} \int \frac{dzdt}{z} \partial_z \left[G_N(t, z; t_1) G_N(t, z; t_2) \right] = -\frac{1}{2} I_2. \quad (4.15)$$

As a result, we get an extra contribution to γ_2 in (4.7): $(\gamma_2^{(1)})_2 = 15$.

The remaining term from the first vertex in (3.10) $\int d^2\sigma \sqrt{g} \langle \overbrace{\zeta^A(t_1) \zeta^B(t_2) \zeta^C \zeta^D} (\partial \zeta^C \cdot \partial \zeta^D) \rangle$ contains the logarithmically divergent contribution (ε is the covariant bulk UV cutoff, see (3.12),(D.7))

$$G_N(\sigma, \sigma) = -\frac{1}{2\pi} \log(2\varepsilon^2) - \frac{1}{\pi} \log z. \quad (4.16)$$

The UV divergent term should be absorbed into the renormalization of the radius of S^5 in the purely bosonic model but should be cancelled by the fermionic loop contribution in the superstring case. If we assume that the fermionic contribution cancels $\log \varepsilon^2$ term but does not change the coefficient of the finite $\log z$ term in (4.16) we will get the following additional contribution to (4.9)

$$\Pi_3 = -\frac{\sqrt{\lambda}}{2\pi} \times \frac{1}{2} \times 2 \times 5 \times \left(-\frac{2}{\sqrt{\lambda}}\right) \left(\frac{2\pi}{\sqrt{\lambda}}\right)^2 \int \frac{dzdt}{z^2} \log z z^2 \sum_{\mu=1}^2 \partial_\mu G_N(t, z; t_1) \partial_\mu G_N(t, z; t_2). \quad (4.17)$$

Integrating by parts and using that $\partial_\mu \partial_\mu G_N = 0$ we get as in (4.10),(4.15)

$$\begin{aligned} \Pi_3 &= -\frac{5}{6\pi} \left(\frac{2\pi}{\sqrt{\lambda}}\right)^2 \int \frac{dzdt}{z} G_N(t, z; t_1) \partial_z G_N(t, z; t_2) = -\frac{5}{12\pi} \left(\frac{2\pi}{\sqrt{\lambda}}\right)^2 \int \frac{dzdt}{z} \partial_z \left[G_N(t, z; t_1) G_N(t, z; t_2) \right] \\ &= -\frac{5}{12(\sqrt{\lambda})^2} \log^2(t_{12}^2). \end{aligned} \quad (4.18)$$

The additional contribution to γ_2 in (4.7) is thus $(\gamma_2^{(1)})_3 = -\frac{5}{2}$.

Thus in total we get (adding also the ‘‘tree-level’’ contribution $\gamma_2^{(0)} = \frac{5}{2}$)

$$\gamma_2 = \gamma_2^{(0)} + \gamma_2^{(1)} = \frac{5}{2} + \left(-\frac{5}{4}k + 15 - \frac{5}{2}\right) \Big|_{k=2} = \frac{5}{2} + 10 = \frac{25}{2}, \quad (4.19)$$

which agrees with (4.1) in the scheme where $k = 2$ in (4.11).¹⁸

¹⁸That this value is indeed the natural one can be seen by generalizing the bosonic $SO(6)$ computation to the $SO(N)$ case. Then d_1 in (4.1) becomes $N - 1$ and thus $\frac{d_1^2}{2} = \frac{(N-1)^2}{2}$. The corresponding analog of (4.19) is then $\gamma_2 = \frac{N-1}{2} - \frac{N-1}{4}k + \frac{N(N-1)}{2} - \frac{N-1}{2}$ which is equal to $\frac{(N-1)^2}{2}$ precisely if $k = 2$.

Finally, let us check that 1-loop diagrams with the other two (4-derivative) vertices in L_4 in (3.10) do not contribute to the \log^2 terms in (4.7),(4.9). The second vertex in (3.10) leads to two types of contractions. The first is $\int d^2\sigma \sqrt{g} \langle \zeta^A(t_1) \overline{\zeta^B(t_2)} \overline{\partial\zeta^C} \cdot \overline{\partial\zeta^D} \cdot \overline{\partial\zeta^D} \rangle$; using (4.11) and doing the bulk integral we find its contribution to (4.9) to be

$$\Pi_4 = -\frac{\sqrt{\lambda}}{2\pi} \times \frac{1}{8} \times k \times 2^2 \times 25 \times \left[-\frac{\pi}{(\sqrt{\lambda})^3} \log(t_{12}^2) \right]. \quad (4.20)$$

It thus contributes to the first power of \log , i.e. to the coefficient d_2 in the scaling dimension (4.2). In the second contraction $\int d^2\sigma \sqrt{g} \langle \zeta^A(t_1) \overline{\zeta^B(t_2)} \overline{\partial\zeta^C} \cdot \overline{\partial\zeta^C} \overline{\partial\zeta^D} \cdot \overline{\partial\zeta^D} \rangle$ we need to use that (see (D.11),(D.13))

$$G_N(\sigma, \sigma') = -\frac{1}{4\pi} \log u(u+1), \quad u = \frac{1}{2} \frac{(t-t')^2 + (z-z')^2}{2zz'} + \varepsilon^2, \quad (4.21)$$

$$\partial_\mu \partial'_\nu G_N(\sigma, \sigma') \Big|_{\sigma \rightarrow \sigma'} = \frac{1}{8\pi z^2} \left(\frac{1}{\varepsilon^2} + 1 \right) \delta_{\mu\nu}. \quad (4.22)$$

Then the bulk integral gives again only a \log term. The third vertex in (3.10) that has a different $SO(6)$ contraction structure leads to the same bulk integral and thus also does not produce \log^2 contributions to (4.9).

Similar conclusions are reached for the 1-loop diagrams with the x^i loop coming from the $\partial x \partial x \partial y \partial y$ vertex in (2.8) (where one can replace $y^a \rightarrow Y^A$). Here we will need to use that the bulk-to-bulk AdS₂ Green's function for the massive scalar x^i satisfies (cf. (4.21),(D.7))

$$G_D^{(m^2=2)}(\sigma, \sigma') = -\frac{1}{4\pi} \left[(2u+1) \log \frac{u}{u+1} + 2 \right], \quad (4.23)$$

$$\partial_\mu \partial'_\nu G_D^{(m^2=2)}(\sigma, \sigma') \Big|_{\sigma \rightarrow \sigma'} = \frac{1}{8\pi z^2} \left(\frac{1}{\varepsilon^2} + 1 + 2 \log \varepsilon^2 \right) \delta_{\mu\nu}. \quad (4.24)$$

As (4.24) scales with z in the same way as (4.21) the corresponding 1-loop diagram also does not contribute to \log^2 term (while the UV \log divergence should cancel against the contribution of the fermionic loop).

At the next $\frac{1}{(\sqrt{\lambda})^3}$ order the $(N_{12})^3 = \log^3(t_{12}^2)$ term in (4.1),(4.7) should have the coefficient $\gamma_3 = -\frac{d_3^3}{3!} = -\frac{125}{6}$. As the expansion of Y^A in (3.8) does not contain a ζ^3 term (while the ζ^4 term in Y^A will start contributing only at order $\frac{1}{(\sqrt{\lambda})^4}$) all contributions to γ_3 should come from loop diagrams. The first type of them is the first diagram in Fig. 3 where one of the two tree propagators is replaced by the 1-loop corrected one (i.e. the one with the corrections from the 1-loop graphs in Fig. 3 included), see Fig. 4(a). In view of the above discussion this 1-loop ‘‘self-energy’’ dressing amounts to the following replacement of each \log factor in (4.7) (cf. the first and the second terms in (4.7) with $\gamma_2^{(1)} = 5 \times 2$ according to (4.19))¹⁹

$$N_{12} \rightarrow N_{12} - \frac{2}{\sqrt{\lambda}} (N_{12})^2. \quad (4.25)$$

Applied to the tree-level $\gamma_2^{(0)}$ term in (4.7) this will give the following contribution to γ_3 : $\gamma_3^{(1)} = \frac{5}{2} \times 2 \times (-2) = -10$.

¹⁹This shift accounts just for the leading \log contributions; in addition, there will be also subleading ones that can be accounted for by a shift like in (G.7).

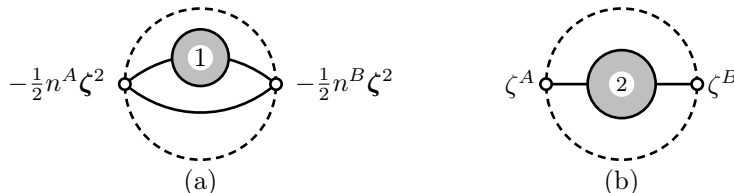


Figure 4. Loop diagrams contributing to $\frac{1}{(\sqrt{\lambda})^3} \log^3$ term in the 2-point correlator. In (a) the blob stands for the bosonic and fermionic one-loop diagrams in Fig. 3. In (b) it stands for the two-loop irreducible contributions like \ominus or reducible iterations of one-loop diagrams as in $\underline{\bigcirc} \underline{\bigcirc}$.

The second type of contributions should come from the 2-loop corrections to the ζ^A -propagator which are: (i) irreducible 2-loop generalizations of the second and third graphs in Fig. 3; (ii) reducible iterations of these 1-loop graphs, see Fig.4(b). These 2-loop corrections (which we will not compute here) should produce the remaining contribution $\gamma_3^{(2)}$

$$\gamma_3 = \gamma_3^{(1)} + \gamma_3^{(2)} = -\frac{125}{6}, \quad \gamma_3^{(1)} = -10, \quad \gamma_3^{(2)} = -\frac{65}{6}. \quad (4.26)$$

5 Mixed four-point function $\langle x^i x^j Y^A Y^B \rangle$

As was mentioned in the Introduction, the correlators of the three AdS₅ transverse fluctuations x_i (scalars with $m^2 = 2$) dual to the correlator of the field strengths F_{ti} at leading order in strong-coupling expansion should be the same in both WML and WL cases as they are described by the same classical string action (2.5) with the same (Dirichlet) boundary conditions for x_i . The corresponding tree-level 2- and 4-point functions $\langle xx \rangle$ or $\langle xxx \rangle$ were computed in [11]. As the boundary operator $F_t^i \equiv iF_t^i$ dual to x^i has the interpretation of the displacement operator, its dimension $\Delta = 2$ will be protected also in the non-supersymmetric WL case, i.e. it should not receive corrections in the strong-coupling expansion

$$\langle\langle F_t^i(t_1) F_t^j(t_2) \rangle\rangle = \langle x^i(t_1) x^j(t_2) \rangle = \delta^{ij} \frac{C'_x}{(t_{12})^4}. \quad (5.1)$$

While in the WML case the normalization factor $C_x = C_{\mathbb{F}}(\lambda)$ in the analog of (5.1) is known exactly (being equal to 12 times the Bremsstrahlung function), the expression for $C'_x = C_F(\lambda)$ at strong coupling (which should have a scheme-independent meaning, see footnote 4) is not known at present.²⁰ The 4-point correlators $\langle xxx \rangle$ in the supersymmetric and non-supersymmetric cases may start to differ at the first subleading order in $\frac{1}{\sqrt{\lambda}}$.

In the case of the 4-point correlator of two AdS fluctuations and two S^5 fluctuations the difference should appear already at the leading order at strong coupling. In the supersymmetric WML case when S^5 coordinates were subject to the Dirichlet b.c. it was computed in [11]. In the WL case with Neumann b.c. in S^5 directions this correlator should have $SO(3) \times SO(6)$ symmetry and should represent the strong-coupling limit of the 4-point function of two displacement operators and two 6-scalars (cf. (1.3))

$$\langle\langle F_t^i(t_1) F_t^i(t_2) \Phi_A(t_3) \Phi_B(t_4) \rangle\rangle = \langle x^i(t_1) x^j(t_2) Y_A(t_3) Y_B(t_4) \rangle$$

²⁰It should be easy to compute the leading strong-coupling correction to it as $C'_x - C_x = C_F - C_{\mathbb{F}}$ should be given by the loop of S^5 scalars with the internal line being the difference of the Neumann and Dirichlet propagators.

$$= \frac{1}{6} \delta^{ij} \delta_{AB} \frac{C'_x}{(t_{12})^4 (t_{34})^{2\Delta}} G(\chi) , \quad G(\chi) = 1 + \frac{1}{\sqrt{\lambda}} G^{(1)} + \frac{1}{(\sqrt{\lambda})^2} G^{(2)} \dots , \quad (5.2)$$

where $\Delta = \frac{5}{\sqrt{\lambda}} + \dots$ is given by (4.2) and as in (4.3) we choose a scheme where $C_Y = \frac{1}{6}$.

Recalling that $Y_A = n_A + \zeta_A - \frac{1}{2} \zeta^2 n_A + \dots$ (see (3.8)) the leading order contributions to (5.2) will come from the disconnected diagrams $\langle xx \rangle \langle YY \rangle$ (see Fig. 5) that will contribute to the prefactor $\frac{1}{(t_{12})^4 (t_{34})^{2\Delta}}$ in (5.2). Here the bulk-to-boundary propagator for x (given by (2.30) with $\Delta = 2$) and

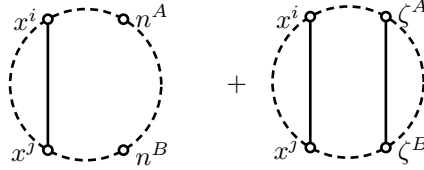


Figure 5. Leading order disconnected contributions to $\langle x^i x^j Y^A Y^B \rangle$.

the bulk-to-boundary propagator for the massless field ζ given by (3.13), i.e.

$$K_2(t, z; t') = \mathcal{C}_2 K_2(t, z; t') , \quad K_2(t, z; t') \equiv \left[\frac{z}{(t-t')^2 + z^2} \right]^2 , \quad \mathcal{C}_2 = \frac{2}{3\pi} , \quad (5.3)$$

$$G_N(t, z; t') = \mathcal{C}_N N(t, z; t') , \quad N(t, z; t') \equiv \log[(t-t')^2 + z^2] , \quad \mathcal{C}_N \equiv -\frac{1}{2\pi} , \quad (5.4)$$

so that (ignoring an infinite rescaling of x^i by a $z \rightarrow 0$ factor)

$$\langle x^i(t_1) x^j(t_2) \rangle = \frac{C'_x}{(t_{12})^4} , \quad C'_x = \frac{2\pi}{\sqrt{\lambda}} \mathcal{C}_2 + \mathcal{O}\left(\frac{1}{(\sqrt{\lambda})^2}\right) . \quad (5.5)$$

One may normalize the 4-point function on the 2-point function of x^i , i.e. absorb the factor of C'_x into a redefinition of the operator x ; we will not do this here.

To compute the non-trivial correction to $\langle xxYY \rangle$ we need to use the 4-vertices in (2.8) where we may replace $\partial_\mu y_a \partial_\nu y_a \rightarrow \partial_\mu Y_A \partial_\nu Y_A$ (the two expressions are the same to quartic order in the fields). The leading connected contribution to $G(\chi)$ will come from the connected diagram in Fig. (6).

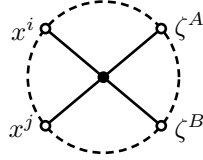


Figure 6. Connected contribution to $\langle x^i x^j Y^A Y^B \rangle$. The 4-vertex comes from the quartic Lagrangian (2.8).

There is also another connected contribution to $\langle x^i x^j Y^A Y^B \rangle$ when Y^A is replaced by n^A and Y^B by $-\frac{1}{2} \zeta^2 n^B$ (or vice versa), see Fig. 7.

We get for the tree-level connected contribution of the diagram in Fig. (6) to the correlator in (5.2)²¹

$$\frac{G_{\text{conn}}(\chi)}{t_{12}^4 t_{34}^{2\Delta}} = -5 \times \left(\frac{2\pi}{\sqrt{\lambda}}\right)^2 \mathcal{C}_2 (\mathcal{C}_N)^2 \mathcal{Q}_{xy} , \quad (5.6)$$

²¹Here the vertex (2.8) in the string action (2.5) contributes $\frac{\sqrt{\lambda}}{2\pi}$ and four propagators $(\frac{2\pi}{\sqrt{\lambda}})^4$. One power of normalization factor $\frac{2\pi}{\sqrt{\lambda}} \mathcal{C}_2$ of the x -propagator is extracted to represent C'_x in (5.2).

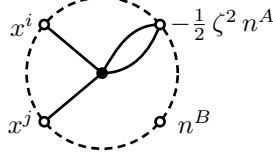


Figure 7. Connected contribution with Y^A replaced by $-\frac{1}{2}\zeta^2 n^A$. There is a similar diagram with $A \leftrightarrow B$.

$$\begin{aligned} \mathbf{Q}_{xy} \equiv \int \frac{dt dz}{z^2} & \left[\partial \mathbf{K}_2(t_1) \cdot \partial \mathbf{K}_2(t_2) \partial \mathbf{N}(t_3) \cdot \partial \mathbf{N}(t_4) - \partial \mathbf{K}_2(t_1) \cdot \partial \mathbf{N}(t_3) \partial \mathbf{K}_2(t_2) \cdot \partial \mathbf{N}(t_4) \right. \\ & \left. - \partial \mathbf{K}_2(t_1) \cdot \partial \mathbf{N}(t_4) \partial \mathbf{K}_2(t_2) \cdot \partial \mathbf{N}(t_3) \right], \end{aligned} \quad (5.7)$$

where the factor 5 came from (3.16), $\partial A \cdot \partial B \equiv g^{\mu\nu} \partial_\mu A \cdot \partial_\nu B$, and $\mathbf{K}_2(t_1) \equiv \mathbf{K}_2(t, z; t_1)$, etc. The expression (5.7) can be simplified using the relations (cf. (C.2))

$$\begin{aligned} \partial \mathbf{K}_2(t_1) \cdot \partial \mathbf{K}_2(t_2) &= 4 [\mathbf{K}_2(t_1) \mathbf{K}_2(t_2) - 2(t_{12})^2 \mathbf{K}_3(t_1) \mathbf{K}_3(t_2)], \\ \partial \mathbf{N}(t_1) \cdot \partial \mathbf{N}(t_2) &= 2z [\mathbf{K}_1(t_1) + \mathbf{K}_1(t_2)] - 2(t_{12})^2 \mathbf{K}_1(t_1) \mathbf{K}_1(t_2), \\ \partial \mathbf{K}_2(t_1) \cdot \partial \mathbf{N}(t_2) &= -4z \mathbf{K}_3(t_1) + 4(t_{12})^2 \mathbf{K}_3(t_1) \mathbf{K}_1(t_2), \quad \mathbf{K}_n(t_1) \equiv \mathbf{K}_n(t, z; t_1) = \left[\frac{z}{(t-t')^2 + z^2} \right]^n. \end{aligned} \quad (5.8)$$

The contribution of the diagram in Fig. 7 is similar: including it gives the total connected contribution by replacing $\mathbf{Q}_{xy}(1, 2, 3, 4)$ with

$$\mathbf{Q}_{xy}^{(\text{tot})}(t_1, t_2, t_3, t_4) = \mathbf{Q}_{xy}(t_1, t_2, t_3, t_4) - \frac{1}{2} \mathbf{Q}_{xy}(t_1, t_2, t_3, t_3) - \frac{1}{2} \mathbf{Q}_{xy}(t_1, t_2, t_4, t_4). \quad (5.9)$$

This results in the following replacement in (5.7)²²

$$\partial_{(\mu} \mathbf{N}(t_3) \partial_{\nu)} \mathbf{N}(t_4) \rightarrow -\frac{1}{2} \partial_{(\mu} [\mathbf{N}(t_3) - \mathbf{N}(t_4)] \partial_{\nu)} [\mathbf{N}(t_3) - \mathbf{N}(t_4)], \quad (5.10)$$

and we find from (5.7),(5.8)

$$\begin{aligned} \mathbf{Q}_{xy}^{(\text{tot})} &= \int \frac{dt dz}{z^2} \left[16 \mathbf{K}_2(t_3) \mathbf{K}_3(t_1) \mathbf{K}_3(t_2) t_{13}^2 t_{23}^2 + 16 \mathbf{K}_2(t_4) \mathbf{K}_3(t_1) \mathbf{K}_3(t_2) t_{14}^2 t_{24}^2 \right. \\ &\quad - 16 \mathbf{K}_1(t_3) \mathbf{K}_1(t_4) \mathbf{K}_3(t_1) \mathbf{K}_3(t_2) t_{14}^2 t_{23}^2 - 8 \mathbf{K}_1(t_3) \mathbf{K}_1(t_4) \mathbf{K}_2(t_1) \mathbf{K}_2(t_2) t_{34}^2 \\ &\quad \left. - 16 \mathbf{K}_1(t_3) \mathbf{K}_1(t_4) \mathbf{K}_3(t_1) \mathbf{K}_3(t_2) t_{13}^2 t_{24}^2 + 16 \mathbf{K}_1(t_3) \mathbf{K}_1(t_4) \mathbf{K}_3(t_1) \mathbf{K}_3(t_2) t_{12}^2 t_{34}^2 \right] \\ &= 16 t_{13}^2 t_{23}^2 T_{2,3,3}(t_3, t_1, t_2) + 16 t_{14}^2 t_{24}^2 T_{2,3,3}(t_4, t_1, t_2) \\ &\quad - 16 D_{3,3,1,1} t_{14}^2 t_{23}^2 - 8 D_{2,2,1,1} t_{34}^2 - 16 D_{3,3,1,1} t_{13}^2 t_{24}^2 + 16 D_{3,3,1,1} t_{12}^2 t_{34}^2. \end{aligned} \quad (5.11)$$

Here $T_{\Delta_1, \Delta_2, \Delta_3}(t_1, t_2, t_3)$ is the standard AdS scalar 3-point function (see, e.g., [48])

$$T_{\Delta_1, \Delta_2, \Delta_3}(t_1, t_2, t_3) = \int \frac{dt dz}{z^2} \mathbf{K}_{\Delta_1}(z, t; t_1) \mathbf{K}_{\Delta_2}(z, t; t_2) \mathbf{K}_{\Delta_3}(z, t; t_3) = \frac{A}{t_{12}^{\Delta_{12}} t_{23}^{\Delta_{23}} t_{31}^{\Delta_{31}}}, \quad (5.12)$$

$$A = \frac{\sqrt{\pi}}{2} \frac{\Gamma[\frac{\Delta_{12}}{2}] \Gamma[\frac{\Delta_{23}}{2}] \Gamma[\frac{\Delta_{31}}{2}]}{\Gamma(\Delta_1) \Gamma(\Delta_2) \Gamma(\Delta_3)} \Gamma[\frac{1}{2}(\Delta_1 + \Delta_2 + \Delta_3 - 1)], \quad \Delta_{12} \equiv \Delta_1 + \Delta_2 - \Delta_3, \text{ etc.}, \quad (5.13)$$

²²Since this depends only on the difference $\mathbf{N}(t_3) - \mathbf{N}(t_4) = \log \frac{(t-t_3)^2 + z^2}{(t-t_4)^2 + z^2}$ the same result is found if we start with the manifestly AdS₂ (or conformally) invariant bulk-to-boundary propagator corresponding to (D.11), i.e. $\mathbf{N}(t, z; t') = \log \frac{(t-t')^2 + z^2}{z}$. This ensures that the resulting integral is conformally invariant.

and the D -functions are defined in (C.1). Expressing the latter in terms of \bar{D} functions according to (C.3) we may use that in the AdS₂ case (cf. (C.5))

$$\begin{aligned}\bar{D}_{2,2,1,1} &= \frac{1}{3(1-\chi)\chi^2} - \frac{2+\chi}{3\chi^3} \log(1-\chi) + \frac{1}{3(1-\chi)^2} \log \chi, \\ \bar{D}_{3,3,1,1} &= -\frac{2\chi^2+3\chi-3}{15(\chi-1)^2\chi^4} - \frac{2(\chi^2+3\chi+6)}{15\chi^5} \log(1-\chi) - \frac{2}{15(1-\chi)^3} \log \chi.\end{aligned}\quad (5.14)$$

As a result,

$$\mathbf{Q}_{xy}^{(\text{tot})} = \frac{6\pi}{t_{12}^4} \left[1 - \left(\frac{1}{2} - \frac{1}{\chi} \right) \log(1-\chi) \right]. \quad (5.15)$$

We thus find for the leading-order contribution to the G -function in (5.2)

$$G(\chi) = 1 + \frac{1}{(\sqrt{\lambda})^2} G^{(2)}(\chi) + \mathcal{O}\left(\frac{1}{(\sqrt{\lambda})^3}\right), \quad (5.16)$$

$$G^{(2)}(\chi) = -5(2\pi)^2 \mathcal{C}_2 (\mathcal{C}_N)^2 t_{12}^4 \mathbf{Q}_{xy}^{(\text{tot})} = -20 \left[1 - \left(\frac{1}{2} - \frac{1}{\chi} \right) \log(1-\chi) \right]. \quad (5.17)$$

We observe that the strong-coupling contribution to the connected part of G in (5.2) first appears at order $\frac{1}{(\sqrt{\lambda})^2}$ and, remarkably, that $G^{(2)}$ is proportional to the corresponding expression (2.37),(2.38) for the tree-level $\langle x^i x^j y^a y^b \rangle$ correlator found in the supersymmetric line case in [11]. Using the label D for the G -function in the supersymmetric (Dirichlet propagator) case we thus get in the non-supersymmetric case

$$G^{(2)} = 5 G_D^{(1)}, \quad G_D^{(1)} = -4 \left[1 - \left(\frac{1}{2} - \frac{1}{\chi} \right) \log(1-\chi) \right]. \quad (5.18)$$

We will explain the reason for this coincidence in section 6.2 below.

Let us comment on the OPE interpretation of the function $G(\chi)$ in (5.2),(5.16, 5.17). Exchanging $t_2 \leftrightarrow t_3$ in (5.2) we get (cf. (2.13),(2.13))

$$\begin{aligned}\langle F_t^i(t_1) \Phi_A(t_2) F_t^i(t_3) \Phi_B(t_4) \rangle &= \frac{1}{6} \delta^{ij} \delta_{AB} \frac{C'_x}{(t_{12} t_{34})^{2+\Delta}} \left| \frac{t_{24}}{t_{13}} \right|^{2-\Delta} \mathbb{G}(\chi), \\ \mathbb{G}(\chi) &\equiv \chi^{2+\Delta} G(\chi^{-1}) = \chi^{2+\Delta} \left(1 - \frac{20}{(\sqrt{\lambda})^2} \left[1 + \left(\chi - \frac{1}{2} \right) \log \frac{1-\chi}{\chi} \right] + \mathcal{O}\left(\frac{1}{(\sqrt{\lambda})^3}\right) \right),\end{aligned}\quad (5.19)$$

where Δ is given by (4.2). The corresponding conformal block expansion is²³

$$\mathbb{G}(\chi) = \sum_h c_h \chi^h {}_2F_1(h+2-\Delta, h-2+\Delta, 2h, \chi). \quad (5.20)$$

Comparing (5.19) with (5.20), and using the expansion (4.2) for Δ , we find the following results for the corresponding intermediate operator dimensions and coefficients c_h consistent content in (5.20)

$$\begin{aligned}h_0 &= 2 + \frac{5}{\sqrt{\lambda}} - \frac{10-d_2}{(\sqrt{\lambda})^2} + \dots, & c_{h_0} &= 1 - \frac{20}{(\sqrt{\lambda})^2} + \dots, \\ h_1 &= 3 + \frac{3}{\sqrt{\lambda}} + \dots, & c_{h_1} &= -\frac{10}{\sqrt{\lambda}} + \frac{25-2d_2}{(\sqrt{\lambda})^2} + \dots, \\ h_2 &= 4 + \frac{0}{\sqrt{\lambda}} + \dots, & c_{h_2} &= \frac{10}{3\sqrt{\lambda}} + \left(\frac{80}{3} + \frac{2d_2}{3} \right) \frac{1}{(\sqrt{\lambda})^2} + \dots,\end{aligned}$$

²³ c_h is related to the coefficient in the 3-point function between F , Φ , and the exchanged operator \mathcal{O}_h of conformal dimension h . Let us recall that in the supersymmetric case (cf. (2.37)) the operator \mathcal{O}_h takes a schematic form $\Phi \partial_i^n \mathbb{F}$, and has dimension $h_n = 3 + n - \frac{1}{2\sqrt{\lambda}} (n+1)(n+4) + \dots$ [11]. The normalization of c_h in (5.21) below takes into account that in the present case in (5.16) we have $G(\chi) = 1 + \dots$.

$$h_3 = 5 - \frac{4}{\sqrt{\lambda}} + \dots, \quad c_{h_3} = -\frac{25}{21\sqrt{\lambda}} + \left(-\frac{8125}{441} - \frac{5d_2}{21}\right) \frac{1}{(\sqrt{\lambda})^2} + \dots, \quad \text{etc.} \quad (5.21)$$

For $n \geq 2$ the general expression for the leading order $\frac{1}{\sqrt{\lambda}}$ correction is

$$h_n = 2 + n - \frac{(n+5)(n-2)}{2} \frac{1}{\sqrt{\lambda}} + \dots, \quad c_{h_n} = \frac{20}{3} \frac{n+2}{n} \left(-\frac{1}{4}\right)^{n+2} \frac{\sqrt{\pi}(n+3)!}{\Gamma(n+\frac{3}{2})} \frac{1}{\sqrt{\lambda}} + \dots. \quad (5.22)$$

Notice that for large n the dimension h_n of the intermediate operator $\Phi \partial_t^n \mathbf{F}$ has the same universal behaviour as in the supersymmetric line case in [11]: $h_n \rightarrow n - \frac{n^2}{2\sqrt{\lambda}} + \dots$ (compared to (2.36),(B.6) where the operator contains ∂_t^{2n} here $n \rightarrow \frac{1}{2}n$). This universality supports the existence of a semiclassical explanation of this large n asymptotics (indeed, possibly related classical string solution should not be sensitive to boundary conditions in S^5).

6 Four-point function $\langle Y^A Y^B Y^C Y^D \rangle$

Given the 2-point function (4.1), the general structure of the $SO(6)$ scalar 4-point function controlled by the 1d conformal invariance and crossing should be as in (2.14),(2.15), i.e.

$$\langle Y^A(t_1) Y^B(t_2) Y^C(t_3) Y^D(t_4) \rangle = \frac{C_Y^2}{|t_{12} t_{34}|^{2\Delta}} G^{ABCD}(\chi), \quad (6.1)$$

$$G^{ABCD} = G_S \delta^{AB} \delta^{CD} + G_T \left[\delta^{AC} \delta^{BD} + \delta^{BC} \delta^{AD} - \frac{1}{3} \delta^{AB} \delta^{CD} \right] + G_A \left[\delta^{AC} \delta^{BD} - \delta^{BC} \delta^{AD} \right]. \quad (6.2)$$

Here $G_S(\chi)$ is the basic function with G_T and G_A expressed in terms of it via leg interchange, i.e. using the crossing relations (2.23),(2.24). In what follows we shall set $C_Y = \frac{1}{6}$ as in (4.3).

To compute G_S it is sufficient to consider the singlet correlator as in (2.17), i.e.

$$\langle Y^A(t_1) Y^A(t_2) Y^B(t_3) Y^B(t_4) \rangle = \frac{1}{|t_{12} t_{34}|^{2\Delta}} G_S. \quad (6.3)$$

Here n^A dependence drops out (so the integration over S^5 is trivial). Thus (6.3) can be computed in any explicit parametrization of Y_A and we shall again use (3.8), i.e. $Y^A = n^A + \zeta^A - \frac{1}{2} n^A \zeta^2 + \mathcal{O}(\zeta^4)$ with $n_A \zeta_A = 0$, $n_A n_A = 1$.

6.1 Leading-order contributions

Let us first consider the simplest – leading order – contributions to (6.3)

$$\langle Y^A(t_1) Y^A(t_2) Y^B(t_3) Y^B(t_4) \rangle = 1 + \frac{1}{\sqrt{\lambda}} Q^{(1)} + \frac{1}{(\sqrt{\lambda})^2} Q^{(2)} + \frac{1}{(\sqrt{\lambda})^3} Q^{(3)} + \dots. \quad (6.4)$$

At order $\frac{1}{\sqrt{\lambda}}$ these are just the tree-level terms $\langle \zeta_A \zeta_A n_B n_B \rangle + \langle n_A n_A \zeta_B \zeta_B \rangle$, giving as in (4.1),(4.7)

$$Q^{(1)} = -5(N_{12} + N_{34}), \quad N_{12} = \log t_{12}^2. \quad (6.5)$$

$Q^{(1)}$ thus corresponds to the leading term in the expansion of the prefactor $(t_{12} t_{34})^{-2\Delta}$ in (6.1),(6.3) with $\Delta = \frac{5}{\sqrt{\lambda}} + \dots$. At the next $\frac{1}{(\sqrt{\lambda})^2}$ order we will get several contributions from tree-level diagrams with four ζ and two contractions (see Fig. 8). Denoting their contribution to $Q^{(2)}$ as $Q_0^{(2)}$ we get

$$Q_0^{(2)} = \frac{5}{2} (N_{12}^2 + N_{34}^2 + N_{13}^2 + N_{14}^2 + N_{23}^2 + N_{24}^2) + 25 N_{12} N_{34} - 5(N_{13} N_{14} + N_{23} N_{24} + N_{13} N_{23} + N_{14} N_{24}) + 5(N_{13} N_{24} + N_{14} N_{23}). \quad (6.6)$$

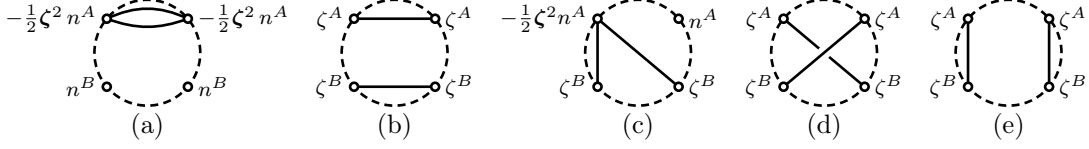


Figure 8. Types of diagrams contributing to (6.6). Other diagrams are obtained by interchanging points.

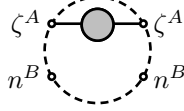


Figure 9. A disconnected diagram contributing $\langle Y^A Y^A Y^B Y^B \rangle$. The ζ -propagator includes loop corrections, with 1-loop ones corresponding to the second and third diagram in Fig. 3.

Here the first group of terms comes from diagrams like Fig. 8(a), the second from Fig. 8(b), the third from Fig. 8(c) and the fourth from Fig. 8(d) and Fig. 8(e). The terms $\frac{5}{2}(N_{12}^2 + N_{34}^2)$ and $25N_{12}N_{34}$ with 12 and 34 propagators should correspond again to the \log^2 terms appearing from the expansion of the prefactor $(t_{12}^2 t_{34}^2)^{-\frac{5}{\sqrt{\lambda}} + \dots}$ in (6.3).

In addition, there are also similar terms coming from the 1-loop propagator correction diagrams like in Fig. 9. As follows from the structure of the loop-corrected propagator in (4.1) there will be a log correction to $Q^{(2)}$ given by

$$Q_{\log}^{(2)} = -d_2(N_{12} + N_{34}) . \quad (6.7)$$

From the analysis of the $\langle YY \rangle$ correlator in section 4 we know that these loop diagrams also contribute the $\log^2(t_{12}) + \log^2(t_{34})$ terms (cf. (4.7)) necessary to build up the prefactor $|t_{12} t_{34}|^{-2\Delta}$ as required by conformal invariance. The coefficient of these terms is given by $\gamma_2^{(1)} = \frac{25}{2} - \frac{5}{2} = 10$ in (4.19). Thus we get for the additional 1-loop contribution to $Q^{(2)}$

$$Q_1^{(2)} = 10(N_{12}^2 + N_{34}^2) . \quad (6.8)$$

Equivalently, this term is found from the $\frac{1}{\sqrt{\lambda}}Q^{(1)}$ term in (6.4) upon the substitution (4.25). Thus

$$\begin{aligned} Q^{(2)} &= Q_{\log}^{(2)} + Q_0^{(2)} + Q_1^{(2)} = Q_{\log}^{(2)} + \frac{25}{2}(N_{12} + N_{34})^2 + \bar{Q}^{(2)} , \\ \bar{Q}^{(2)} &= \frac{5}{2}(N_{13} + N_{24} - N_{14} - N_{23})^2 . \end{aligned} \quad (6.9)$$

Multiplying (6.4) by $|t_{12} t_{34}|^{2\Delta} = 1 + \frac{5}{\sqrt{\lambda}}(N_{12} + N_{34}) + \frac{25}{2(\sqrt{\lambda})^2}(N_{12} + N_{34})^2 + \dots$ (cf. (6.4),(6.3)) we conclude that all N_{12} and N_{34} dependent terms cancel out (in particular, log term in (6.7) does not contribute) so that the leading contribution to G_S is given by

$$G_S(\chi) = 1 + \frac{1}{(\sqrt{\lambda})^2}\bar{Q}^{(2)} + \mathcal{O}\left(\frac{1}{(\sqrt{\lambda})^3}\right) = 1 + \frac{1}{(\sqrt{\lambda})^2}G_S^{(2)}(\chi) + \mathcal{O}\left(\frac{1}{(\sqrt{\lambda})^3}\right) , \quad (6.10)$$

$$G_S^{(2)} = 10\log^2(1 - \chi) . \quad (6.11)$$

There is no $\frac{1}{\sqrt{\lambda}}$ term as the leading-order correction (6.5) correspond just to the prefactor in (6.3). As there is no other “connected” contribution at order $\frac{1}{(\sqrt{\lambda})^2}$ the expression in (6.11) gives the full conformally invariant expression for G_S to this order.

To find G_T and G_A in (6.2) we may use the general crossing relations(2.23),(2.24) with $N = 6$ and Δ given by (4.2), i.e. $\Delta = \frac{5}{\sqrt{\lambda}} + \frac{d_2}{(\sqrt{\lambda})^2} + \dots$. As a result,

$$G_T(\chi) = \frac{3}{4} + \frac{9}{2\sqrt{\lambda}} \log \frac{\chi^2}{1-\chi} + \frac{3}{2(\sqrt{\lambda})^2} \left(9 \log^2 \frac{\chi^2}{1-\chi} + 8 \log^2(1-\chi) + \frac{3}{5} d_2 \log \frac{\chi^2}{1-\chi} \right) + \mathcal{O}\left(\frac{1}{(\sqrt{\lambda})^3}\right), \quad (6.12)$$

$$G_A(\chi) = \frac{6}{\sqrt{\lambda}} \log(1-\chi) + \frac{6}{(\sqrt{\lambda})^2} \log(1-\chi) \left(4 \log \frac{\chi^2}{1-\chi} + \frac{1}{5} d_2 \right) + \mathcal{O}\left(\frac{1}{(\sqrt{\lambda})^3}\right). \quad (6.13)$$

The $\frac{1}{\sqrt{\lambda}}$ terms here originated from the Δ -dependence in (2.23),(2.24). The appearance of the second anomalous dimension coefficient d_2 in (6.12),(6.13) is not surprising: it means that in order to determine the $\frac{1}{(\sqrt{\lambda})^2}$ terms in $G^{ABCD}(\chi)$ one needs to compute also the 1-loop graphs (bosonic and fermionic ones, cf. Fig. 3) that contribute not only to Δ but effectively also to G_T and G_S . Similarly, the $\frac{1}{(\sqrt{\lambda})^3}$ terms in (6.12),(6.13) will depend not only on the $\frac{1}{(\sqrt{\lambda})^3}$ correction to (6.11) but also on the $\frac{d_3}{(\sqrt{\lambda})^3}$ term in Δ .

It is important to stress that in contrast to the supersymmetric ($SO(5)$ invariant) case in [11] here the presence of the n_A ‘‘condensate’’ in Y_A implies that the disconnected graphs are not described just by a generalized free field perturbation theory (cf. Appendix A). For example, the averages over S^5 do not factorize: $\langle n^A n^B n^C n^D \rangle \neq \langle n^A n^B \rangle \langle n^C n^D \rangle$, etc. Thus even $\frac{1}{\sqrt{\lambda}}$ corrections in (6.12),(6.13) are not those of a free field theory. For example, setting $\Delta = \frac{5}{\sqrt{\lambda}} + \dots$ in (A.2) and expanding does not reproduce the single logarithms proportional to (6.12).

6.2 Order $\frac{1}{(\sqrt{\lambda})^3}$ contributions: Dirichlet/Neumann relations

At the next $\frac{1}{(\sqrt{\lambda})^3}$ order we get two different contributions: (i) ‘‘reducible’’ contributions given by tree level diagrams with possible 1-loop or 2-loop propagator corrections; (ii) ‘‘irreducible’’ connected tree-level contributions where all four points are connected to the bulk vertex. The 3-loop propagator corrections (like in Fig. 4(b)) can appear only in the disconnected parts $\langle \zeta^A \zeta^A n^B n^B \rangle + \langle n^A n^A \zeta^B \zeta^B \rangle$ (see Fig. 9) and thus contribute only to the prefactor $|t_{12} t_{34}|^{-2\Delta}$ in (6.3) but not to G_S .

Non-trivial reducible contributions come from connected tree diagrams with 3 propagators like the one in Fig. 10 and also from the leading order diagrams in Fig. 8 with one of the propagators being ‘‘dressed’’ by 1-loop correction as in Fig. 3 or Fig. 9. We will discuss these reducible contributions in detail in Appendix G.

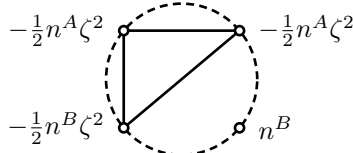


Figure 10. ‘‘Reducible’’ tree-level diagram contributing at order $\frac{1}{(\sqrt{\lambda})^3}$.

In addition, there is also an ‘‘irreducible’’ connected contribution to (6.1),(6.3) that comes from the contact tree diagram in Fig. 11 where all four fields in $\langle \zeta^A(t_1) \zeta^A(t_2) \zeta^B(t_3) \zeta^B(t_4) \rangle$ are attached to a quartic vertex from L_4 in (3.10). The analog of it (see Fig. 2) was the only leading connected contribution (2.33) in the supersymmetric line case with the Dirichlet bulk-to-boundary propagators [11].

Having one bulk 4-vertex in (3.10) (proportional to $\sqrt{\lambda}$) and four ζ -propagators (each bringing a $\frac{1}{\sqrt{\lambda}}$ factor) this connected contribution should scale as $\frac{1}{(\sqrt{\lambda})^3} G_{S,\text{conn}}^{(3)}$. Note that the normalization

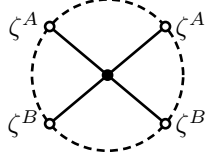


Figure 11. Contact diagram contributing at order $\frac{1}{(\sqrt{\lambda})^3}$.

in the supersymmetric case (2.33) was different, so comparing to it below we shall strip off the $\frac{1}{\sqrt{\lambda}}$ factors. In total, we should find (cf. (6.11), (G.3))

$$G_S = 1 + \frac{1}{(\sqrt{\lambda})^2} G_S^{(2)} + \frac{1}{(\sqrt{\lambda})^3} G_S^{(3)} + \mathcal{O}\left(\frac{1}{(\sqrt{\lambda})^4}\right), \quad (6.14)$$

$$G_S^{(3)} = G_{S,\text{red}}^{(3)} + G_{S,\text{conn}}^{(3)}, \quad G_{S,\text{red}}^{(3)} = G_{S,\log^2}^{(3)} + G_{S,\log^3}^{(3)}, \quad (6.15)$$

where $G_{S,\log^2}^{(3)}$ and $G_{S,\log^3}^{(3)}$ are given in (G.9) and (G.17).

Trying to compute $G_{S,\text{conn}}^{(3)}$ directly one observes that the logarithmic form of the Neumann bulk-to-boundary propagator (3.13) leads to complicated AdS₂ integrals. A useful observation is that applying boundary-point ∂_{t_i} derivatives to the contact contribution to the correlator $\langle YYY Y \rangle$ it is possible to relate the expressions for the integrands with the differentiated Neumann propagators to the similar ones in the Dirichlet propagator case.

Let us define (see (2.32), (5.4); below $\partial_\mu = (\partial_t, \partial_z)$, $\partial^\mu A \partial_\mu B = z^2 \partial_\mu A \partial_\mu B$, $\epsilon_{\mu\nu} = \pm \epsilon_{tz} = \pm 1$; repeated low indices are contracted with $\delta_{\mu\nu}$)

$$N'(t_a) \equiv \partial_{t_a} N(t_a) = 2 \frac{t_a - t}{(t - t_a)^2 + z^2} = \frac{2(t_a - t)}{z} K_1(t_a), \quad (6.16)$$

$$N(t_a) = \log [(t - t_a)^2 + z^2], \quad K_1(t_a) = \frac{z}{(t - t_a)^2 + z^2} = \frac{1}{2} \partial_z N(t_a), \quad (6.17)$$

$$\partial_\mu N'(t_a) = 2 \epsilon_{\mu\nu} \partial_\nu K_1(t_a), \quad \partial_\mu = (\partial_t, \partial_z). \quad (6.18)$$

Using (6.18) we may thus relate the expressions containing bulk-point derivatives of $N'(t_a)$ to the ones with bulk-point derivatives of $K_1(t_a)$. For example, we get

$$\partial_\mu N'(t_1) \partial_\mu N'(t_2) = 4 \partial_\mu K_1(t_1) \partial_\mu K_1(t_2). \quad (6.19)$$

Equivalently, (6.19) follows simply from the complex coordinate decomposition of K_1 and N'

$$K_1(t_a) = -\frac{1}{2i} \left(\frac{1}{w} - \frac{1}{\bar{w}} \right), \quad N'(t_a) = -\left(\frac{1}{w} + \frac{1}{\bar{w}} \right), \quad w \equiv t - t_a + iz, \quad (6.20)$$

using that $\partial_\mu A \partial_\mu B = 4 \partial_w A \partial_{\bar{w}} B$ (cf. (D.6)).

From (6.19), we see that the contact diagram associated to the $(\partial\zeta)^4$ term in (3.10) contributing to the 4-point function in the Neumann propagator theory is simply proportional to the same diagram in the theory with the Dirichlet propagator. A similar relation is true for the contributions of the mixed $xxYY$ 4-derivative vertices in (2.8). There is also a close relation between the two cases for the contribution of the 2-derivative $\zeta^2(\partial\zeta)^2$ vertex in (3.10). Explicitly, one finds (see Appendix F)

$$\int dz dt N'(t_1) N'(t_2) \partial_\mu N'(t_3) \partial_\mu N'(t_4) = 16 \int dz dt K_1(t_1) K_1(t_2) \partial_\mu K_1(t_3) \partial_\mu K_1(t_4) + \omega, \quad (6.21)$$

$$\omega(t_1, t_2, t_3, t_4) = -\frac{8\pi}{t_{34}^2} \left(\frac{1}{t_{13}t_{23}} + \frac{1}{t_{14}t_{24}} \right), \quad t_{ij} = t_i - t_j. \quad (6.22)$$

which may be proved by using (6.16)–(6.20) and performing the integrals. The “deficit” ω -term here corresponds to the non-zero boundary contribution that survives upon manipulating one integral into the other using integration by parts (see (F.4)–(F.7)).

We then arrive at the following symbolic relations between the G -functions appearing in the corresponding connected contributions to the correlators in (5.2) and (6.1), (6.2) in the Dirichlet and Neumann cases²⁴

$$\langle x^i(t_1)x^j(t_2)Y^A(t_3)Y^B(t_4) \rangle : \quad \partial_{t_3}\partial_{t_4}\widehat{G} = -2\frac{1}{t_{34}^2}G_D(\chi), \quad (6.23)$$

$$\langle Y^A(t_1)Y^B(t_2)Y^C(t_3)Y^D(t_4) \rangle : \quad \partial_{t_1}\partial_{t_2}\partial_{t_3}\partial_{t_4}\widehat{G} = 4\frac{1}{t_{12}^2t_{34}^2}G_D(\chi) + \Omega. \quad (6.24)$$

Here \widehat{G} and G_D stand for the contact diagram $\frac{1}{(\sqrt{\lambda})^3}$ contributions in the Neumann and Dirichlet cases respectively with all symmetry group factors stripped off before averaging over n^A in the N-case (\widehat{G} -functions are related to G -functions in (6.2) as in (6.29) below). For simplicity, in this section shall often omit the label “(3)” on $G^{(3)}$. Ω in (6.24) is the total contribution of the ω -terms in the relation like (6.21). The basic idea behind (6.23),(6.24) is that after the differentiation over the boundary points the Neumann propagator contributions get related to the Dirichlet ones as in (6.19),(6.21). To find the conformally-invariant solution for the total G we will need to add also the “reducible” contribution as in (6.15) that will cancel non-invariant terms in Ω .

More explicitly, to compare to the supersymmetric line case with $SO(5)$ scalars in (2.33),(2.37) one is to replace Y^A by y^a and postpone the averaging over n^A till the end. For the mixed correlator in (6.23) we will have (cf. (3.16))

$$G_D^{ab} = \delta^{ab}G_D, \quad \widehat{G}^{AB} = P^{AB}\widehat{G} \rightarrow G^{AB} = \frac{1}{6}\delta^{AB}G, \quad G = 5\widehat{G}. \quad (6.25)$$

In the massless 4-scalar correlator case, starting with the expression (2.33) in the supersymmetric line case we are first to replace $\delta^{ab} \rightarrow P^{AB} = \delta^{AB} - n^A n^B$ and $K_1 = \mathcal{C}_1 K_1 \rightarrow G_N = \mathcal{C}_N N$ in the $SO(5)$ version of (2.15) getting (cf. (6.24))

$$\begin{aligned} \widehat{G}^{ABCD} &= \widehat{G}_S(\chi)P^{AB}P^{CD} + \widehat{G}_T(\chi)\left[P^{AC}P^{BD} + P^{BC}P^{AD} - \frac{2}{5}P^{AB}P^{CD}\right] \\ &\quad + \widehat{G}_A(\chi)\left[P^{AC}P^{BD} - P^{BC}P^{AD}\right], \end{aligned} \quad (6.26)$$

$$\partial_{t_1}\partial_{t_2}\partial_{t_3}\partial_{t_4}\widehat{G}_c = 4\frac{1}{t_{12}^2t_{34}^2}G_{D,c}(\chi) + \Omega_c, \quad c = S, T, A. \quad (6.27)$$

Here the functions $G_{D,c}(\chi)$ are given by the leading-order connected expressions (2.34). Averaging (6.26) over n^A according to (3.15),(3.16) we end up with (cf. (6.2) and (2.16)–(2.18))

$$\begin{aligned} \widehat{G}^{ABCD} &\rightarrow \frac{1}{36}G^{ABCD}, \quad (6.28) \\ G^{ABCD} &= G_S\delta^{AB}\delta^{CD} + G_T\left[\delta^{AC}\delta^{BD} + \delta^{BC}\delta^{AD} - \frac{2}{6}\delta^{AB}\delta^{CD}\right] + G_A\left[\delta^{AC}\delta^{BD} - \delta^{BC}\delta^{AD}\right], \end{aligned}$$

²⁴While in the D-case it is natural to strip off normalization factors of all 2-point functions in the correlator in the N-case this is not natural as the 2-point function of Y^A expanded in $\frac{1}{\sqrt{\lambda}}$ starts with constant rather than the tree-level propagator. We may still formally do this but without changing sign, so the factor associated to the N-propagator in (5.4) will be $\frac{2\pi}{\sqrt{\lambda}}|\mathcal{C}_N| = \frac{1}{\sqrt{\lambda}}$. Finally, when relating the expressions in the D and N cases we omit the $\frac{1}{\sqrt{\lambda}}$ factors. This formal identification requires the -1 factor in (6.23).

$$G_S = 25 \widehat{G}_S, \quad G_T = \frac{3}{4} \widehat{G}_S + \frac{126}{5} \widehat{G}_T, \quad G_A = 24 \widehat{G}_A. \quad (6.29)$$

Before turning to the case of $\langle YYY Y \rangle$ let us first demonstrate how the above D/N relation (6.23) explains the proportionality of the expressions for the leading connected part of the mixed correlator $\langle x^i(t_1)x^j(t_2)Y^A(t_3)Y^B(t_4) \rangle$ in the supersymmetric (D) (2.38) and non-supersymmetric (N) (5.16),(5.18) cases. The leading order term in G_D is $G^{(1)}$ in (2.38). To find the corresponding term in G_N we may integrate the relation in (6.23).

The double derivative operator in (6.23) has a nice interpretation in terms of the quadratic Casimir operator of the 1d conformal group (i.e. J^2 for $SO(1,2)$). Indeed, $t_{34}^2 \partial_{t_3} \partial_{t_4}$ is invariant under the scale transformations, translations, and also the inversion. When acting on a function of the cross-ratio $\chi = \frac{t_{12}t_{34}}{t_{13}t_{24}}$ it becomes

$$t_{34}^2 \partial_{t_3} \partial_{t_4} f(\chi) = -\mathcal{D}f(\chi), \quad \mathcal{D} \equiv \chi^2(1-\chi)\partial_\chi^2 - \chi^2\partial_\chi, \quad (6.30)$$

where \mathcal{D} is the conformal Casimir operator (see, e.g., [43, 49]). The eigenfunctions of \mathcal{D} are the $SL(2, R)$ conformal blocks (cf. (B.1))

$$\mathcal{D}F_h = h(h-1)F_h, \quad F_h = \chi^h F_h(\chi), \quad F_h \equiv {}_2F_1(h, h, 2h, \chi). \quad (6.31)$$

From (6.23),(6.25) we have (cf. (2.38))

$$t_{34}^2 \partial_{t_3} \partial_{t_4} G(\chi) = -\mathcal{D}G(\chi) = -10 G_D(\chi). \quad (6.32)$$

One can check that

$$F_2 = \chi^2 {}_2F_1(2, 2, 4, \chi) = -12 \left[1 - \left(\frac{1}{2} - \frac{1}{\chi} \right) \log(1-\chi) \right] = 3G_D(\chi), \quad \mathcal{D}G_D(\chi) = 2G_D(\chi). \quad (6.33)$$

Thus $G_D = G^{(1)}$ in (2.38) is given just by a single conformal block corresponding to the dimension $h = 2$. This means that in the supersymmetric line case the only operator that can appear in the OPE channel $12 \rightarrow 34$ (besides the identity which contributes to the disconnected part) is the $h = 2$ singlet $\sim y^a y^a$. Integrating (6.32) for G using (6.33) we get

$$G(\chi) = 5 G_D(\chi) + c_1 + c_2 \log(1-\chi), \quad (6.34)$$

where the last two terms are the zero modes of the Casimir operator \mathcal{D} , i.e. a linear combination of the $h = 0$ and $h = 1$ conformal blocks.

Let us argue that this “zero-mode” part is to be omitted, i.e. one should set $c_1 = c_2 = 0$. The leading order term in the small χ expansion of generic $G(\chi)$ in (2.10) should be determined by the minimal dimension of the fields appearing in the corresponding OPE. In the present case of connected part of G this is the $\Delta = 2$ operator suggesting that $G(0) = 0$. Assuming the symmetry under $t_3 \leftrightarrow t_4$, i.e. under $\chi \rightarrow -\frac{\chi}{1-\chi}$, we get also $G'(0) = 0$. Then a (connected part of) $G(\chi)$ should have the small χ expansion²⁵

$$G(0) = G'(0) = 0. \quad (6.35)$$

This property is readily checked for $G_D = G^{(1)}$ in (2.38) and should hold also for G in (6.34), implying that $c_1 = c_2 = 0$. As a result, we find that G in (6.34) coincides with the expression in (5.17),(5.18) that we found above by the direct computation in the Neumann propagator case.

²⁵This will also apply to the singlet part of the 4-scalar correlator below but will not be true in general in the T- and A- channels.

6.3 Contact diagram contribution and $G_{S,T,A}$ functions at order $\frac{1}{(\sqrt{\lambda})^3}$

The four-point function $\langle Y^A Y^B Y^C Y^D \rangle$ in the $SO(6)$ Neumann theory (6.1),(6.2) is expressed in terms of the three functions G_c ($c = S, T, A$). The main task is to determine G_S as then G_T and G_A can be found using the crossing relations (2.23),(2.24) (with $N = 6$)

$$G_T(\chi) = -\frac{3}{20} \left[G_S(\chi) - 3\chi^{2\Delta} G_S\left(\frac{1}{1-\chi}\right) - 3\left(\frac{\chi}{\chi-1}\right)^{2\Delta} G_S(1-\chi) \right], \quad (6.36)$$

$$G_A(\chi) = \frac{3}{5} \left[\chi^{2\Delta} \widehat{G}_S\left(\frac{1}{1-\chi}\right) - \left(\frac{\chi}{\chi-1}\right)^{2\Delta} \widehat{G}_S(1-\chi) \right], \quad \Delta = \frac{5}{\sqrt{\lambda}} + \frac{d_2}{(\sqrt{\lambda})^2} + \frac{d_3}{(\sqrt{\lambda})^3} + \dots \quad (6.37)$$

One may try to determine G_S by integrating the relation (6.27) of its connected part to the corresponding function in the Dirichlet theory (2.34)

$$t_{12}^2 t_{34}^2 \partial_{t_1} \partial_{t_2} \partial_{t_3} \partial_{t_4} (G_S)_{\text{conn}} = 100 G_{D,S}(\chi) + U_S, \quad U_S = t_{12}^2 t_{34}^2 \Omega_S. \quad (6.38)$$

The normalization of the U_S contribution is chosen such that it directly contributes to G_S . Here we restored the label ‘‘conn’’ on G_S to indicate that this contribution comes from the contact connected diagram. By the explicit computation from the 4-vertex in first term in (3.10) one finds that in the S-channel the total combination Ω_S of ω -terms coming from relations like (6.21) is such that

$$U_S(t_1, t_2, t_3, t_4) = 40 t_{12}^2 t_{34}^2 \left(\frac{1}{t_{12}^2 t_{23} t_{24}} - \frac{5}{t_{12} t_{23}^2 t_{24}} - \frac{6}{t_{12} t_{23} t_{24}^2} + \frac{1}{t_{12}^2 t_{14} t_{13}} - \frac{1}{t_{23}^2 t_{34} t_{13}} + \frac{6}{t_{12} t_{14}^2 t_{13}} \right. \\ \left. + \frac{2}{t_{23} t_{34}^2 t_{13}} + \frac{5}{t_{12} t_{14} t_{13}^2} - \frac{1}{t_{23} t_{34} t_{13}^2} \right). \quad (6.39)$$

Since U_S is not conformally invariant, the contact diagram contribution to G_S is also not just a function of χ so we cannot simply replace $t_{12}^2 t_{34}^2 \partial_{t_1} \partial_{t_2} \partial_{t_3} \partial_{t_4}$ in (6.38) by the square of the Casimir operator \mathcal{D} (6.30). However, the conformal invariance is restored in the total expression for G_S , i.e. once we add the ‘‘reduced’’ diagram contributions as in (6.15). Indeed, the expression for $t_{12}^2 t_{34}^2 \partial_{t_1} \partial_{t_2} \partial_{t_3} \partial_{t_4}$ applied to the reduced part $(G_S)_{\text{red}}$ is given by the sum of (G.11) and (G.18). As a result, we find that non-invariant terms in (G.18) cancel against those in (6.39) and we are left with

$$t_{12}^2 t_{34}^2 \partial_{t_1} \partial_{t_2} \partial_{t_3} \partial_{t_4} (G_S)_{\text{conn}} = \mathcal{D}^2 (G_S)_{\text{conn}} = 100 G_{D,S}(\chi) + R_S(\chi), \quad (6.40)$$

$$G_S = (G_S)_{\text{conn}} + (G_S)_{\text{red}}, \quad (G_S)_{\text{red}} = (G_S)_{\log^2} + (G_S)_{\log^3}, \quad (6.41)$$

$$R_S = 8d_2 \left[\chi^2 + \frac{\chi^2}{(1-\chi)^2} \right] + 320 \frac{\chi^2}{(1-\chi)^2} \left([1 + (1-\chi)^2] \left(1 + \frac{1}{2} \log \chi \right) - \frac{1}{2} \log(1-\chi) \right). \quad (6.42)$$

Here R_S is the combination of U_S with the contributions (G.11), (G.18) of the ‘‘reduced’’ terms in which all non-invariant terms happen to cancel out. The d_2 term in (6.42) is the contribution of the \log^2 reduced term in (G.11); as its contribution to the invariant part of G_S is known already (see (G.10)) in what follows we will simply omit it, concentrating on other invariant terms in G_S solving (6.40).

We may formally split $(G_S)_{\text{conn}}$ into the sum $\overline{G}_S + \widetilde{G}_S$ of the solution of $\mathcal{D}^2 \overline{G}_S = 100 G_{D,S}(\chi)$ where $G_{D,S} = G_S^{(1)}$ in (2.34) and the solution of $\mathcal{D}^2 \widetilde{G}_S = R_S(\chi)$ where R_S is given by (6.42),

$$(G_S)_{\text{conn}} = \overline{G}_S + \widetilde{G}_S, \quad \mathcal{D}^2 \overline{G}_S = 100 G_{D,S}(\chi), \quad \mathcal{D}^2 \widetilde{G}_S = R_S(\chi). \quad (6.43)$$

Explicitly, one finds that the most general solution for \widetilde{G}_S may be written as²⁶

$$\widetilde{G}_S = -320 \text{Li}_3(1-\chi) + 320 \text{Li}_2(1-\chi) \log(1-\chi) + 160 \text{Li}_2(\chi) \log(1-\chi)$$

²⁶The appearance of Li_n functions here (absent in the ‘‘reduced’’ \log^3 contribution in (G.17)) should be attributed to the contribution of the Ω -part of the contact diagram contribution to R_S : for example, the 4 times integrated expression of the ω in (6.22) can be seen to be given by a combination of the polylogarithmic functions.

$$-\frac{80}{3} \log^3(1-\chi) + 240 \log \chi \log^2(1-\chi) + \sum_{n=1}^4 c_n \psi_n(\chi) , \quad (6.44)$$

$$\psi_1 = 1, \quad \psi_2 = \log(1-\chi), \quad \psi_3 = \log \chi, \quad \psi_4 = \text{Li}_2(\chi) + \frac{1}{2} \log \chi \log(1-\chi) , \quad (6.45)$$

where c_n are constants multiplying the zero modes $\psi_n(\chi)$ of the \mathcal{D}^2 operator (cf. (6.34)). Expanding (6.44) for small χ we get

$$\tilde{G}_S = [c_3 \log \chi + c_1 - 320\zeta_R(3)] + (c_4 - c_2 - \frac{1}{2}c_4 \log \chi)\chi + [\frac{1}{4}c_4 - \frac{1}{2}c_2 - 80 + (80 - \frac{1}{4}c_4) \log \chi]\chi^2 + \mathcal{O}(\chi^3) . \quad (6.46)$$

Imposing the condition (6.35) fixes

$$c_1 = 320\zeta_R(3) , \quad c_2 = c_3 = c_4 = 0 . \quad (6.47)$$

Similarly, we may attempt to solve the equation for $\overline{G}_S(\chi)$ in (6.43) which has a more complicated source term (cf. (2.34)) and try to constrain the zero-mode freedom by imposing the $3 \leftrightarrow 4$ crossing symmetry condition on the total function (cf. (2.19),(2.20))

$$G_S(\chi) = G_S(\frac{\chi}{\chi-1}) , \quad (6.48)$$

and also the condition (6.35). A somewhat complicated structure of ψ_4 in (6.45) suggests that finding a correct analytic continuation of $G_S(\chi)$ out of the perturbative region $\chi \rightarrow 0$ may be non-trivial.²⁷

To avoid these issues let us start from the very beginning and consider not the fourth derivative (as in (6.27)), but just the second derivative of the singlet correlator

$$\partial_{t_1} \partial_{t_2} \langle Y^A(t_1) Y^A(t_2) Y^B(t_3) Y^B(t_4) \rangle . \quad (6.49)$$

Computing it using the relations between the N and D propagators like (6.18) we may then integrate the resulting analog of (6.23), i.e. follow the same approach as described above in the case of the mixed correlator $\langle xxYY \rangle$.

Our strategy will be to find the invariant contribution to \overline{G}_S (freely doing integrations by parts and assuming that all non-invariant terms from boundary terms cancel against the “reduced” contributions as discussed above). A consistency test will be that the resulting function will indeed satisfy the correct 4-derivative equation $\mathcal{D}^2 \overline{G}_S = 100 G_{D,S}(\chi)$ in (6.43).

Given the connected correlator with 4-vertices from (3.10) (see Fig. 11), applying $\partial_{t_1} \partial_{t_2}$ to it we will get various contractions with two of the four bulk-to-boundary Neumann propagators (5.4),(6.13) differentiated over the boundary point. For example, the 4-derivative vertices in (3.10) will lead to (cf. (6.21))

$$\partial_\mu N'(t_1) \partial_\mu N'(t_2) \partial_\nu N(t_3) \partial_\nu N(t_4), \quad \text{etc.} \quad (6.50)$$

Using (6.18) or $\partial_\mu N' = 2 \varepsilon_{\mu\nu} \partial_\nu K_1$ we can replace N' with K_1 and also apply the relations similar to (5.8), i.e.

$$\partial K_1(t_1) \cdot \partial K_1(t_2) = K_1(t_1) K_1(t_2) - 2 t_{12}^2 K_2(t_1) K_2(t_2) , \quad (6.51)$$

$$\partial K_1(t_1) \cdot \partial N(t_2) = -2 z K_2(t_1) + 2 t_{12}^2 K_2(t_1) K_1(t_2) . \quad (6.52)$$

²⁷A possible solution of the analytic continuation problem may be based on the following relations

$$\mathcal{D}^2 [f(1-\chi)] = \frac{\chi^2}{(1-\chi)^2} [\mathcal{D}^2 f(\chi)]_{\chi \rightarrow 1-\chi} , \quad \mathcal{D}^2 [f(\frac{1}{1-\chi})] = \chi^2 [\mathcal{D}^2 f(\chi)]_{\chi \rightarrow \frac{1}{1-\chi}} .$$

Indeed, to determine, for instance, $f(\frac{1}{1-\chi})$ from the solution to $\mathcal{D}^2 f = g$, one simply writes $\mathcal{D}^2 [f(\frac{1}{1-\chi})] = \chi^2 g(\frac{1}{1-\chi})$. If the r.h.s. admits a simple analytic continuation (e.g. using the $\log(\dots) \rightarrow \log|\dots|$ rule) under which it keeps essentially the same complexity, this will then readily give an expression for $f(\frac{1}{1-\chi})$ after the integration.

This allows us to effectively replace all logarithmic N factors by the Dirichlet functions $K_n(t, t_a; z) = \left[\frac{z}{(t-t_a)^2+z^2} \right]^n$, (cf. (2.30)) so that the resulting integrals over the AdS₂ bulk point become the standard ones (see Appendix C).

There is also another type of contractions coming from the 2-derivative vertex in (3.10): after applying $\partial_{t_1}\partial_{t_2}$ to them we get integrals $\int dt dz(\dots)$ like (6.21) with the integrands of the three types

$$V_1 = \text{N N } \partial_\mu \text{N}' \partial_\mu \text{N}', \quad V_2 = \text{N}' \text{N}' \partial_\mu \text{N} \partial_\mu \text{N}, \quad V_3 = \text{N N}' \partial_\mu \text{N} \partial_\mu \text{N}'. \quad (6.53)$$

We can simplify these using $\square \text{N} = \square \text{N}' = \square \text{K}_1 = 0$ (here $\square = \partial_\mu \partial_\mu = \partial_t^2 + \partial_z^2$) and formal integration by parts. Then we get²⁸ $V_1 = 4\text{G}_\text{N}\text{G}_\text{N}'\partial_\mu \text{K}_1 \partial_\mu \text{K}_1 \rightarrow 4\partial_\mu \text{G}_\text{N}'\partial_\mu \text{G}_\text{N}\text{K}_1 \text{K}_1$, and we can use (5.8) to eliminate N in terms of K₁. V_2 in (6.53) can be also reduced to the V_1 -type term: $V_2 = \text{N}'\text{N}'\partial_\mu \text{N} \partial_\mu \text{N} \rightarrow \partial_\mu \text{N}'\partial_\mu \text{N}'\text{N}\text{N}$. The same is also true for $V_3 = \text{N N}'\partial_\mu \text{N} \partial_\mu \text{N}'$ (using the 1 ↔ 2 and 3 ↔ 4 symmetry).

As a result, we find that the second derivative of G_S appearing in (6.49) is given by (see (5.11) and (C.5) for the expressions for the T and \bar{D} functions)²⁹

$$\begin{aligned} \partial_{t_1}\partial_{t_2}\bar{G}_S = & -\frac{1}{2\pi} \left[-400t_{13}^2t_{23}^2 T_{2,2,2}(t_1, t_2, t_3) - 400t_{14}^2t_{24}^2 T_{2,2,2}(t_1, t_2, t_4) \right. \\ & \left. + \frac{150\pi t_{34}^2}{t_{13}^2 t_{24}^2} \bar{D}_{1,1,1,1} - \frac{60\pi \left[(t_{13}^2 - 7t_{14}t_{13} + t_{14}^2)t_{12}^2 + 5t_{13}t_{14}(t_{13} + t_{14})t_{12} - 5t_{13}^2t_{14}^2 \right] t_{34}^2}{t_{13}^4 t_{24}^4} \bar{D}_{2,2,1,1} \right]. \end{aligned} \quad (6.54)$$

Here we again put bar on G_S to indicate that this connected contribution of the contact diagram is computed by formally discarding boundary terms while integrating by parts. Using (5.12), (C.5) gives (cf. (6.30))

$$\begin{aligned} -\mathcal{D}\bar{G}_S(\chi) = & -10 \left[\frac{\chi^2 - 10\chi + 10}{\chi - 1} - \frac{(\chi^2 - 10\chi + 10)\chi^2}{(\chi - 1)^2} \log \chi + \frac{\chi^3 - 8\chi^2 + 5\chi - 10}{\chi} \log(1 - \chi) \right] \\ = & 25(4 \log \chi - \frac{47}{15})\chi^2 + 25(4 \log \chi - \frac{17}{15})\chi^3 + \mathcal{O}(\chi^4). \end{aligned} \quad (6.55)$$

Integrating this as in (6.32),(6.34) and applying the crossing constraint (6.48) and the condition (6.35) of regularity at $\chi \rightarrow 0$ we get³⁰

$$\begin{aligned} \bar{G}_S(\chi) = & -240 \left[\text{Li}_3(\chi) + \text{Li}_3\left(\frac{\chi}{\chi-1}\right) \right] + 50 \left[\frac{1}{2} - \frac{1}{\chi} - \frac{1}{5}\chi + \frac{8}{5} \text{Li}_2(\chi) \right] \log(1 - \chi) \\ & + 40 \left[\log^3(1 - \chi) - \frac{1}{4} \frac{\chi^2}{1-\chi} \log \chi - \log^2(1 - \chi) \log \chi \right] - 50 \\ = & -50 \left(\log \chi - \frac{137}{60} \right) \chi^2 + \mathcal{O}(\chi^3). \end{aligned} \quad (6.56)$$

We have fixed the integration constant to zero using (6.35).³¹ A non-trivial check of (6.56) is that applying \mathcal{D}^2 it does satisfy the second equation in (6.43) with $G_{\text{D},S}(\chi)$ given by (2.34).

It is interesting to note that despite the relative simplicity of the $\zeta^2(\partial\zeta)^2$ vertex contribution to the (6.55) (given by the term $-80 \left[\frac{\chi^2}{\chi-1} \log \chi - \chi \log(1-\chi) \right]$ on the r.h.s.) it is this vertex that produces

²⁸Here we use that for the harmonic functions ($\square H_i = 0$) one has $H_1 H_2 \partial_\mu H_3 \partial_\mu H_4 = \frac{1}{2} H_1 H_2 \square (H_3 H_4) \rightarrow \frac{1}{2} \square (H_1 H_2) H_3 H_4 = \partial_\mu H_1 \partial_\mu H_2 H_3 H_4$ where we dropped a total derivative term.

²⁹In obtaining the expression (6.54) we included the contributions of diagrams with the $-\frac{1}{2}n^A \zeta^2$ term in Y^A at the points t_3 or t_4 (like in Fig. 7 where points x^i are now replaced by Y^A). This amounts to a subtraction of contributions at the coinciding points completely analogous to that in (5.9).

³⁰Let us note two useful relations: $\text{Li}_2(1 - \chi) = \frac{\pi^2}{6} - \log(1 - \chi) \log \chi - \text{Li}_2(\chi)$,

$\text{Li}_3(1 - \chi) = \frac{\pi^2}{6} \log(1 - \chi) + \frac{1}{6} \log^3(1 - \chi) - \frac{1}{2} \log^2(1 - \chi) \log \chi + \zeta_R(3) - \text{Li}_3(\chi) - \text{Li}_3\left(\frac{\chi}{\chi-1}\right)$.

³¹This condition is natural as the connected part of $\langle Y^A(t_1)Y^A(t_2)Y^B(t_3)Y^B(t_4) \rangle$ should vanish for $t_{12} \rightarrow 0$ and $t_{34} \rightarrow 0$ (implying $\chi \rightarrow 0$) as we have $Y^A Y^A = 1$ at the coincident points. Thus in (6.1) we should have $G_S(\chi \rightarrow 0) \rightarrow 1$, i.e. the connected part of G_S should vanish at $\chi = 0$.

the most complicated Li_n dependent part in $\overline{G}_S(\chi)$ in (6.56) while the contribution $(\overline{G}_S)_{(\partial\zeta)^4}$ of the $(\partial\zeta)^4$ vertex is similar in structure to the expression in (2.34) in the Dirichlet theory case:

$$(\overline{G}_S)_{(\partial\zeta)^4} = -50 + 50 \left(\frac{1}{2} - \frac{1}{\chi} - \frac{1}{5}\chi \right) \log(1 - \chi) - 10 \frac{\chi^2}{1-\chi} \log \chi . \quad (6.57)$$

The total expression for the $\frac{1}{(\sqrt{\lambda})^3}$ term in $G_S(\chi)$ in (6.14) is given by the sum of $\tilde{G}_S(\chi)$ in (6.44),(6.47) and $\overline{G}_S(\chi)$ in (6.56) and also the reducible d_2 -contribution in (G.10) (cf. also (6.42)), i.e. explicitly

$$G_S = 1 + \frac{10}{(\sqrt{\lambda})^2} \log^2(1 - \chi) + \frac{1}{(\sqrt{\lambda})^3} G_S^{(3)} + \mathcal{O}\left(\frac{1}{(\sqrt{\lambda})^4}\right) , \quad (6.58)$$

$$\begin{aligned} G_S^{(3)} &= 80 \left[\text{Li}_3(\chi) + \text{Li}_3\left(\frac{\chi}{\chi-1}\right) - \text{Li}_2(\chi) \log(1 - \chi) \right] + 40 \log \frac{\chi}{1-\chi} \log^2(1 - \chi) \\ &\quad - 10 \frac{\chi^2}{1-\chi} \log \chi + 5 \left(5 - \frac{10}{\chi} - 2\chi \right) \log(1 - \chi) - 50 + 4 d_2 \log^2(1 - \chi) \\ &= (30 \log \chi + \frac{205}{6} + 4d_2)\chi^2 + \mathcal{O}(\chi^3) . \end{aligned} \quad (6.59)$$

Let us now compute the $\frac{1}{(\sqrt{\lambda})^3}$ terms in the G_T and G_A functions (complementing the order $\frac{1}{(\sqrt{\lambda})^2}$ expressions in (6.12),(6.13)) using the crossing relations (6.36),(6.37). As a first step, let us replace (6.59) by the following improved form that is equivalent to (6.59) for $0 < \chi < 1$ and represents its real continuation for $\chi > 1$ (cf. footnote 30)

$$\begin{aligned} G_S^{(3)} &= -80 \text{Li}_3(1 - \chi) + \left[80 \text{Li}_2(1 - \chi) - \frac{5(2\chi^2 - 5\chi + 10)}{\chi} \right] \log |1 - \chi| + 10 \frac{\chi^2}{\chi-1} \log \chi \\ &\quad - \frac{80}{3} \log^3 |1 - \chi| + 80 \log \chi \log^2 |1 - \chi| + 10 [8\zeta_R(3) - 5] + 4 d_2 \log^2 |1 - \chi| . \end{aligned} \quad (6.60)$$

Note that using this expression we can consider the analytic continuation to the thermal out of time order correlators, following the procedure described in section 2.4. It is easy to see that the dominant contribution in the limit relevant for chaos comes again from the term $\sim \chi^{-1} \log(1 - \chi)$ in (6.60), leading to a maximal Lyapunov exponent. This term originates, in fact, just from the ‘‘Nambu string’’ $(\partial\zeta)^4$ vertex contribution (6.57) (and not from the S^5 sigma model vertex $\zeta^2(\partial\zeta)^2$ in (3.10)), in full analogy with what happened also in the supersymmetric line case (cf. last term in $G_S^{(1)}$ in (2.34)).

Applying the crossing relations (6.36),(6.37) we can use (6.60) to get the following (real) expressions for G_T and G_A that are valid in the range $0 < \chi < 1$ and depend also on the subleading coefficients in Δ in (4.2)

$$\begin{aligned} G_T^{(3)} &= 48 \text{Li}_3(1 - \chi) + \log(1 - \chi) \left[-12 \text{Li}_2(1 - \chi) + 36 \text{Li}_2(\chi) - \frac{3(17\chi^2 - 11\chi + 1)}{2\chi} - 324 \log^2 \chi \right] \\ &\quad + \frac{3(17\chi^2 - 21\chi + 21)}{2(\chi-1)} \log \chi - 83 \log^3(1 - \chi) + 216 \log^3 \chi + 294 \log \chi \log^2(1 - \chi) \\ &\quad + \frac{3}{2} [16\zeta_R(3) - 25] - 6\pi^2 \log(1 - \chi) + \frac{3}{5} d_2 \left[9 \log^2\left(\frac{\chi^2}{1-\chi}\right) + 8 \log^2(1 - \chi) \right] + \frac{9}{10} d_3 \log\left(\frac{\chi^2}{1-\chi}\right) , \end{aligned} \quad (6.61)$$

$$\begin{aligned} G_A^{(3)} &= 48 \left[\text{Li}_3(1 - \chi) + 2 \text{Li}_3(\chi) \right] + \log(1 - \chi) \left[48 \text{Li}_2(\chi) - 24\chi + 192 \log^2 \chi + 3 \right] \\ &\quad + \left[\frac{24(\chi-2)\chi}{\chi-1} - 96 \text{Li}_2(\chi) \right] \log \chi + 84 \log^3(1 - \chi) - 192 \log \chi \log^2(1 - \chi) - 48\zeta_R(3) \\ &\quad + \frac{48}{5} d_2 \log(1 - \chi) \log\left(\frac{\chi^2}{1-\chi}\right) + \frac{6}{5} d_3 \log(1 - \chi) . \end{aligned} \quad (6.62)$$

The small χ expansions of these expressions read (cf. (6.59))

$$G_T^{(3)} = 216 \log^3 \chi + \frac{108}{5} d_2 \log^2 \chi + \left(-\frac{63}{2} + \frac{9}{5} d_3 \right) \log \chi + 72\zeta_R(3) - 36$$

$$\begin{aligned}
& + \left[324 \log^2 \chi + \frac{108}{5} d_2 \log \chi - \frac{63}{4} + \frac{9}{10} d_3 \right] \chi \\
& + \left[162 \log^2 \chi + \left(\frac{54}{5} d_2 + \frac{513}{2} \right) \log \chi + \frac{51}{5} d_2 + \frac{23}{4} + \frac{9}{20} d_3 \right] \chi^2 + \mathcal{O}(\chi^3), \quad (6.63)
\end{aligned}$$

$$\begin{aligned}
G_A^{(3)} & = \left[-192 \log^2 \chi + \left(-\frac{96}{5} d_2 - 48 \right) \log \chi + 93 - \frac{6}{5} d_3 \right] \chi \\
& + \left[-96 \log^2 \chi + \left(-\frac{48}{5} d_2 - 216 \right) \log \chi - \frac{48}{5} d_2 + \frac{45}{2} - \frac{3}{5} d_3 \right] \chi^2 + \mathcal{O}(\chi^3). \quad (6.64)
\end{aligned}$$

A direct computation of $G_T^{(3)}$ and $G_A^{(3)}$ which is not based on the crossing relations but follows the same approach as used above to find $G_S^{(3)}$ is presented in Appendix H. Up to the Casimir operator zero mode terms (cf. (6.45)) that are not, in general, determined in the approach based on integrating the relations like (6.24) the resulting expressions are found to be equivalent to (6.61) and (6.62).

The reason why this ambiguity was not present in the case of $G_S^{(3)}$ (or, equivalently, was fixed by the condition (6.35)) can be understood from the OPE constraints: in the singlet channel the only non-derivative operator (with dimension $\mathcal{O}(\frac{1}{\sqrt{\lambda}})$) that can appear in the exchange is the identity (due to $Y^A Y^A = 1$), implying $G_S(\chi) = \mathcal{O}(\chi^2)$. At the same time, non-singlet $Y^A Y^B$ operators can appear in the OPE of G_T and G_A .

Finally, let us note that the resulting expressions for $G_{S,T,A}^{(3)}$ in (6.60),(6.61),(6.62) depend on two subleading coefficients d_2 and d_3 in the scalar anomalous dimension (4.2) that receive contributions from the fermion loops and are yet to be determined.

6.4 OPE and anomalous dimensions

Let us now discuss the consistency of the expressions for the $G_{S,T,A}$ functions with the OPE and extract the anomalous dimensions of composite operators appearing in the intermediate channels as was done in the supersymmetric case in [11] (see (2.35)–(2.36) and Appendix B). Let us assume the following conformal-block expansion (cf. (2.11),(B.1))

$$G_c = \begin{cases} c_0 \chi^{h_0} F_{h_0} + c_2 \chi^{h_2} F_{h_2} + \dots, & c = S, T, \\ c_1 \chi^{h_1} F_{h_1} + c_3 \chi^{h_3} F_{h_3} + \dots, & c = A, \end{cases} \quad (6.65)$$

where

$$c_n = c_n^{(0)} + c_n^{(1)} \frac{1}{\sqrt{\lambda}} + c_n^{(2)} \frac{1}{(\sqrt{\lambda})^2} + \dots, \quad h_n = n + \gamma_n^{(1)} \frac{1}{\sqrt{\lambda}} + \gamma_n^{(2)} \frac{1}{(\sqrt{\lambda})^2} + \dots \quad (6.66)$$

Comparing (6.10),(6.11),(6.59) with (6.65) we find in the S-channel:

$$\begin{aligned}
h_{0,S} & = 0, & c_{0,S} & = 1 + \mathcal{O}\left(\frac{1}{(\sqrt{\lambda})^4}\right), \\
h_{2,S} & = 2 + \frac{3}{\sqrt{\lambda}} + \dots, & c_{2,S} & = \frac{10}{(\sqrt{\lambda})^2} + \left(\frac{205}{6} + 4d_2\right) \frac{1}{(\sqrt{\lambda})^3} + \dots, \\
h_{4,S} & = 4 - \frac{2}{\sqrt{\lambda}} + \dots, & c_{4,S} & = \frac{1}{6(\sqrt{\lambda})^2} + \left(\frac{24}{5} + \frac{1}{15}d_2\right) \frac{1}{(\sqrt{\lambda})^3} + \dots. \quad (6.67)
\end{aligned}$$

Here d_2 is the subleading coefficient in Δ in (4.2). $h_0 = 0$ should correspond to the identity operator ($Y_A Y_A = 1$), while h_2 to the $Y_A \partial_t^2 Y_A$ operator. Similarly, we get from (6.63)

$$\begin{aligned}
h_{0,T} & = \frac{12}{\sqrt{\lambda}} + \frac{12d_2}{5} \frac{1}{(\sqrt{\lambda})^2} + (-42 + \frac{12}{5}d_3) \frac{1}{(\sqrt{\lambda})^3} + \dots, & c_{0,T} & = \frac{3}{4} - 36[1 - 2\zeta_R(3)] \frac{1}{(\sqrt{\lambda})^3} + \dots, \\
h_{2,T} & = 2 + \frac{171}{17} \frac{1}{\sqrt{\lambda}} + \dots, & c_{2,T} & = \frac{51}{2} \frac{1}{(\sqrt{\lambda})^2} + \left(-\frac{2483}{8} + \frac{51}{5}d_2\right) \frac{1}{(\sqrt{\lambda})^3} + \dots, \\
h_{4,T} & = 4 + \frac{86}{17} \frac{1}{\sqrt{\lambda}} + \dots, & c_{4,T} & = \frac{17}{40} \frac{1}{(\sqrt{\lambda})^2} + \left(\frac{1893}{200} + \frac{17}{100}d_2\right) \frac{1}{(\sqrt{\lambda})^3} + \dots, \quad (6.68)
\end{aligned}$$

and from (6.64)

$$\begin{aligned}
h_{1,A} &= 1 + \frac{8}{\sqrt{\lambda}} + (8 + \frac{8}{5} d_2) \frac{1}{(\sqrt{\lambda})^2} + \dots, & c_{1,A} &= -\frac{6}{\sqrt{\lambda}} - \frac{6d_2}{5} \frac{1}{(\sqrt{\lambda})^2} + (93 - \frac{6}{5} d_3) \frac{1}{(\sqrt{\lambda})^3} + \dots, \\
h_{3,A} &= 3 + \frac{6}{\sqrt{\lambda}} + \dots, & c_{3,A} &= -\frac{8}{3} \frac{1}{(\sqrt{\lambda})^2} - (\frac{368}{9} + \frac{16}{15} d_2) \frac{1}{(\sqrt{\lambda})^3} + \dots, \\
h_{5,A} &= 5 - \frac{1}{\sqrt{\lambda}} + \dots, & c_{5,A} &= -\frac{12}{175} \frac{1}{(\sqrt{\lambda})^2} - (\frac{16997}{6125} + \frac{24}{875} d_2) \frac{1}{(\sqrt{\lambda})^3} + \dots.
\end{aligned} \tag{6.69}$$

We have found that the general form of the $\frac{1}{\sqrt{\lambda}}$ term in the anomalous dimensions in (6.67),(6.68),(6.69) is as in (6.66), i.e. $h_{n,c} = n + \gamma_{n,c}^{(1)} \frac{1}{\sqrt{\lambda}} + \dots$, with

$$\begin{aligned}
\gamma_{n,S}^{(1)} &= \begin{cases} 0, & n = 0, \\ 4 - \frac{1}{2} n (n - 1), & n = 2, 4, 6, \dots, \end{cases} & \gamma_{n,T}^{(1)} &= \begin{cases} 12, & n = 0, \\ \frac{188}{17} - \frac{1}{2} n (n - 1), & n = 2, 4, 6, \dots, \end{cases} \\
\gamma_{n,A}^{(1)} &= \begin{cases} 8, & n = 1, \\ 9 - \frac{1}{2} n (n - 1), & n = 3, 5, 7, \dots, \end{cases}
\end{aligned} \tag{6.70}$$

The dependence on n is the same in all three channels (apart from the ‘‘special’’ bottom states $n = 0$ for $c = S, T$ and $n = 1$ for $c = A$). This was also true in the supersymmetric case [11]. In fact, the large n behaviour of $\gamma_n^{(1)}$ is the same in the supersymmetric and the non-supersymmetric case

$$h_{n \gg 1} = n - \frac{n^2}{2\sqrt{\lambda}} + \dots \tag{6.71}$$

This universality (independence of boundary conditions on S^5 scalars) should be consistent with possible semiclassical explanation of this large n scaling (see also (5.22) and comments below it).

In the T-channel the OPE coefficients with $n > 0$ are subleading in $\frac{1}{\sqrt{\lambda}}$, because they come from 3-point functions like $\langle Y(t_1)Y(t_2)(Y^{\{A}\partial_t^n Y^{B\}})(t_3) \rangle$ which for $n > 0$ do not have an order-zero part. At order $\frac{1}{\sqrt{\lambda}}$ all the higher powers of χ in G_T in (6.12) agree with the OPE $c_n \chi^{\Delta_n} F_n$ containing only the $n = 0$ term (see also Appendix I). This means that the OPE coefficients with $n > 0$ start at $\frac{1}{(\sqrt{\lambda})^2}$. Indeed, we would get at least two ζ -propagators (each with $\frac{1}{\sqrt{\lambda}}$) in $\langle Y(t_1)Y(t_2)(Y\partial_t^n Y)(t_3) \rangle$ for $n \geq 2$. The anomalous dimension of $Y^{\{A}\partial_t^n Y^{B\}}$ should be $\frac{12}{\sqrt{\lambda}} + \dots$ as expected from the analysis of the two point function (cf. (4.6)). Note that the d_n corrections to the anomalous dimensions in the previous results are always encoded by a factor $1 + \frac{d_2}{5} \frac{1}{\sqrt{\lambda}} + \frac{d_3}{5} \frac{1}{(\sqrt{\lambda})^2} + \dots$ correcting the leading order. This is equal to the relative subleading corrections to Δ in (4.2). This follows from the universal ‘‘dressing’’ of the ζ -propagator (cf. also the expression for h_2 in (5.21)) at leading order in the coefficients d_n and is a feature that is not expected to hold at higher orders.

Similar comments apply to the S and A channels. The lowest-dimension operator appearing in the A channel is $Y^{[A}\partial_t Y^{B]}$ which, according to (6.69), has $h_{1,A} = 1 + \frac{8}{\sqrt{\lambda}} + \dots$ and $c_{1,A} = -\frac{6}{\sqrt{\lambda}} + \dots$.³²

Another consistency check is possible using the expressions (H.7),(H.8) for the ‘‘reducible’’ $\frac{1}{(\sqrt{\lambda})^3}$ contributions in the T and A channels. The lowest order the operator contributing to the OPE

³² The coefficient +8 in the anomalous dimension of $Y^{[A}\partial_t Y^{B]}$ may be understood using the same logic as leading to $J(J+4) = 12$ for $Y^{\{A}Y^{B\}}$ with $J = 2$ in the T channel, cf. also (4.6). In the latter case, one may consider perturbing the string action by the boundary interaction term $\int dt T(Y)$, $T(Y) = C_{A_1 \dots A_J} Y^{A_1} \dots Y^{A_J}$, and then its anomalous dimension operator (entering the condition of this being a marginal perturbation) is the scalar Laplacian on S^5 (see, e.g., [50, 3]). If instead one considers the perturbation by the operator $Y^{[A}\partial_t Y^{B]}$, i.e. $\int dt F_{AB} Y^A \partial_t Y^B \equiv \int dt V_A(Y) \partial_t Y^A$, where F_{AB} is antisymmetric then one gets a special case of the boundary vector perturbation for which the anomalous dimension operator is the Maxwell one or the vector Laplacian on S^5 (the above V_A is transverse). The eigenvalues of the latter on S^d are $\lambda_J = J(J+d-1) + d - 2$ giving +8 for $d = 5$ and $J = 1$.

expansion (6.65) in the T-channel has $h_{0,T} = \frac{12}{\sqrt{\lambda}} + \dots$. This means that we should find a peculiar contribution $\frac{216}{(\sqrt{\lambda})^3} \log^3 \chi$ coming from the expansion of $c_{0,T} \chi^{h_{0,T}} = \frac{3}{4} \chi^{\frac{12}{\sqrt{\lambda}} + \dots}$. There are no such $\log^3 \chi$ terms in the \overline{G}_c functions corresponding to the connected diagram contribution. In fact, this contribution is provided by the \tilde{G}_T function (H.7) that complements \overline{G}_T to the full G_T like in the S-channel in (6.43): it contains the required $\log^3 \chi$ term in its $\chi \rightarrow 0$ expansion in (6.63). Similarly, the A-channel expression (6.64),(H.8) contains the term $-\frac{192}{(\sqrt{\lambda})^3} \chi \log^2 \chi$ which is precisely the one appearing in the expansion of $c_{1,A} \chi^{h_{1,A}} = -\frac{6}{\sqrt{\lambda}} \chi^{1 + \frac{8}{\sqrt{\lambda}} + \dots}$, see (6.69).

Acknowledgments

We are grateful to S. Dubovsky, V. Gorbenko, S. Komatsu, J. Maldacena, R. Roiban and E. Vescovi for useful discussions on related topics. We also thank R. Roiban and E. Vescovi for comments on the draft. The work of SG is supported in part by the US NSF under Grant No. PHY-1620542. AAT was supported by the STFC grant ST/P000762/1.

A Four-point correlators of generalized free fields

Assuming that $\mathcal{O}_\Delta(t)$ is represented by a free field and normalized so that

$$\langle\langle \mathcal{O}_\Delta(t_1) \mathcal{O}_{\Delta'}(t_2) \rangle\rangle = \frac{\delta_{\Delta,\Delta'}}{(t_{12})^{2\Delta}}, \quad (\text{A.1})$$

and doing three separate contractions one finds for the correlator in (2.10)

$$\langle\langle \mathcal{O}_\Delta(t_1) \mathcal{O}_\Delta(t_2) \mathcal{O}_\Delta(t_3) \mathcal{O}_\Delta(t_4) \rangle\rangle = \frac{1}{(t_{12}t_{34})^{2\Delta}} G(\chi), \quad G = 1 + \chi^{2\Delta} + \frac{\chi^{2\Delta}}{(1-\chi)^{2\Delta}}. \quad (\text{A.2})$$

This can be checked against (2.11) by taking into account that the exchanged fields are the identity operator and the composites

$$[\mathcal{O}_\Delta \mathcal{O}_\Delta]_{2n} \sim \mathcal{O}_\Delta \partial_t^{2n} \mathcal{O}_\Delta, \quad h = 2\Delta + 2n, \quad n = 0, 1, \dots, \quad (\text{A.3})$$

with the OPE coefficients given by (see, e.g., [51, 52])

$$c_{\Delta,\Delta;2\Delta+2n} = \frac{2 [\Gamma(2n+2\Delta)]^2 \Gamma(2n+4\Delta-1)}{[\Gamma(2\Delta)]^2 \Gamma(2n+1) \Gamma(4n+4\Delta-1)}. \quad (\text{A.4})$$

One can show that the +1 in (A.2) comes from the identity, while the rest comes from the tower of operators in (A.3). Also, $1 + \frac{1}{(1-\chi)^{2\Delta}} = \sum_{n=0}^{\infty} c_{\Delta,\Delta;2\Delta+2n} \chi^{2n} {}_2F_1(2\Delta+2n, 2\Delta+2n, 4\Delta+4n, \chi)$. Similarly, in the case of two different dimensions (2.12) one gets

$$\langle\langle \mathcal{O}_{\Delta_1}(t_1) \mathcal{O}_{\Delta_2}(t_2) \mathcal{O}_{\Delta_1}(t_3) \mathcal{O}_{\Delta_2}(t_4) \rangle\rangle = \frac{1}{t_{13}^{2\Delta_1} t_{24}^{2\Delta_2}} = \frac{1}{(t_{12}t_{34})^{\Delta_1+\Delta_2}} \left| \frac{t_{24}}{t_{13}} \right|^{\Delta_{12}} G(\chi), \quad G = \chi^{\Delta_1+\Delta_2}. \quad (\text{A.5})$$

Here we assumed that $\Delta_1 \neq \Delta_2$ so that (A.2) is not a limit of (A.5). The form of $\mathcal{G} = \chi^{\Delta_1+\Delta_2}$ here can again be explained in terms of the fusion $\mathcal{O}_{\Delta_1} + \mathcal{O}_{\Delta_2} \xrightarrow{h} \mathcal{O}_{\Delta_1} + \mathcal{O}_{\Delta_2}$ leading to the composite operators

$$[\mathcal{O}_{\Delta_1} \mathcal{O}_{\Delta_2}]_n \sim \mathcal{O}_{\Delta_1} \partial_t^n \mathcal{O}_{\Delta_2}, \quad h = \Delta_1 + \Delta_2 + n, \quad n = 0, 1, \dots, \quad (\text{A.6})$$

with the OPE coefficients

$$c_{\Delta_1,\Delta_2;\Delta_1+\Delta_2+2n} = \frac{(-1)^n \Gamma(n+2\Delta_1) \Gamma(n+2\Delta_2) \Gamma(n+2\Delta_1+2\Delta_2-1)}{\Gamma(2\Delta_1) \Gamma(2\Delta_2) \Gamma(n+1) \Gamma(2n+2\Delta_1+2\Delta_2-1)}. \quad (\text{A.7})$$

B Anomalous dimensions from OPE in supersymmetric case

Here we recall how the anomalous dimensions may be extracted from the OPE expansion of the $G(\chi)$ function in (2.11) on the example of the symmetric traceless tensor part in the supersymmetric line case following [11]. The strong-coupling expansion of the 5-scalar four-point function (2.33) leads to (cf. (2.11))

$$G_T^{(0)}(\chi) + \frac{1}{\sqrt{\lambda}} G_T^{(1)}(\chi) + \dots = \sum_h c_h \chi^h F_h(\chi), \quad F_h(\chi) = {}_2F_1(h, h, 2h, \chi), \quad (\text{B.1})$$

$$h_n = 2 + 2n + \frac{1}{\sqrt{\lambda}} \gamma_{[\Phi\Phi]_{2n}^T}^{(1)} + \dots, \quad c_h = c_{\Phi\Phi[\Phi\Phi]_{2n}^T}^{(0)} + \frac{1}{\sqrt{\lambda}} c_{\Phi\Phi[\Phi\Phi]_{2n}^T}^{(1)} + \dots \quad (\text{B.2})$$

Comparing the leading order term with the free-field result (A.2),(A.4), we obtain

$$c_{\Phi\Phi[\Phi\Phi]_{2n}^T}^{(0)} = \frac{[\Gamma(2n+2)]^2 \Gamma(2n+3)}{\Gamma(2n+1)\Gamma(4n+3)}. \quad (\text{B.3})$$

To get the subleading order correction we use

$$\chi^h = \chi^{2+2n+\frac{1}{\sqrt{\lambda}}\gamma^{(1)}} = \chi^{2+2n} \left(1 + \frac{1}{\sqrt{\lambda}} \gamma^{(1)} \log \chi + \dots\right), \quad (\text{B.4})$$

and the general inversion formula

$$\sum_{n=0}^{\infty} c_n \chi^{2+2n} F_{2+2n}(\chi) = f(\chi) \quad \rightarrow \quad c_n = \oint \frac{d\chi}{2\pi i} \chi^{-3-2n} F_{-1-2n}(\chi) f(\chi). \quad (\text{B.5})$$

As a result,

$$\gamma_{[\Phi\Phi]_{2n}^T}^{(1)} = [c_{\Phi\Phi[\Phi\Phi]_{2n}^T}^{(0)}]^{-1} \oint \frac{d\chi}{2\pi i} \chi^{-3-2n} F_{-1-2n}(\chi) [G_T^{(1)}(\chi)]_{\log \chi} = -3n - 2n^2. \quad (\text{B.6})$$

One can compute in a similar way the correction to the OPE coefficients [11].

C AdS contact integrals

The building block for AdS_{d+1} diagrams with a 4-point contact term like in (2.33) is the D -function (see, e.g., [53–55])

$$D_{\Delta_1, \Delta_2, \Delta_3, \Delta_4}(x_1, x_2, x_3, x_4) = \int \frac{dz d^d x}{z^{d+1}} \prod_{n=1}^4 K_{\Delta_n}(z, x; x_n), \quad (\text{C.1})$$

where K_{Δ} was defined in (2.30). A useful identity is

$$\begin{aligned} & g^{\mu\nu} \partial_{\mu} K_{\Delta_1}(z, x; x_1) \partial_{\nu} K_{\Delta_2}(z, x; x_2) \\ &= \Delta_1 \Delta_2 \left[K_{\Delta_1}(z, x; x_1) K_{\Delta_2}(z, x; x_2) - 2x_{12}^2 K_{\Delta_1+1}(z, x; x_1) K_{\Delta_2+1}(z, x; x_2) \right], \end{aligned} \quad (\text{C.2})$$

where $\partial_{\mu} = (\partial_z, \partial_r)$ ($r = (0, i)$) and $g^{\mu\nu} = z^2 \delta^{\mu\nu}$. It is useful to replace D functions by \bar{D} functions that depend on the conformally invariant ratios $u = \frac{x_{12}x_{34}}{x_{13}x_{24}}$, $v = \frac{x_{14}x_{23}}{x_{13}x_{24}}$ ($\Sigma \equiv \frac{1}{2} \sum_n \Delta_n$)

$$D_{\Delta_1, \Delta_2, \Delta_3, \Delta_4} = \frac{\pi^{d/2} \Gamma(\Sigma - \frac{d}{2})}{2\Gamma(\Delta_1)\Gamma(\Delta_2)\Gamma(\Delta_3)\Gamma(\Delta_4)} \frac{x_{14}^{2(\Sigma-\Delta_1-\Delta_4)} x_{34}^{2(\Sigma-\Delta_3-\Delta_4)}}{x_{13}^{2(\Sigma-\Delta_4)} x_{24}^{2\Delta_2}} \bar{D}_{\Delta_1, \Delta_2, \Delta_3, \Delta_4}(u, v),$$

$$\bar{D}_{\Delta_1, \Delta_2, \Delta_3, \Delta_4}(u, v) = \int d^3\alpha \delta\left(\sum_{i=1}^3 \alpha_i - 1\right) \alpha_1^{\Delta_1-1} \alpha_2^{\Delta_2-1} \alpha_3^{\Delta_3-1} \frac{\Gamma(\Sigma - \Delta_4)\Gamma(\Delta_4)}{(\alpha_1\alpha_3 + \alpha_1\alpha_2 u + \alpha_2\alpha_3 v)^{\Sigma - \Delta_4}}. \quad (\text{C.3})$$

Specializing to AdS₂ or $d = 1$ where $u = \chi^2$, $v = (1 - \chi)^2$, one can prove that

$$\begin{aligned} \bar{D}_{\Delta_1, \Delta_2, \Delta_3, \Delta_4} &= \frac{\Gamma(\Delta_1)\Gamma(\Delta_4)\Gamma\left(\frac{\Delta_1+\Delta_2+\Delta_3-\Delta_4}{2}\right)\Gamma\left(\frac{-\Delta_1+\Delta_2+\Delta_3+\Delta_4}{2}\right)}{\Gamma\left(\frac{\Delta_1+\Delta_2+\Delta_3+\Delta_4}{2}\right)} \chi^{-\frac{\Delta_1+\Delta_2-\Delta_3-\Delta_4}{2}} (1-\chi)^{-\Delta_1-\Delta_2-\Delta_3+\Delta_4} \\ &\times \int_{-\infty}^{\infty} d\tau e^{-\tau} \frac{\Delta_1-\Delta_2+\Delta_3-\Delta_4}{2} (e^\tau + \chi)^{\Delta_1-\Delta_4} {}_2F_1\left(\Delta_1, \frac{\Delta_1+\Delta_2+\Delta_3-\Delta_4}{2}, \frac{\Delta_1+\Delta_2+\Delta_3+\Delta_4}{2}, -\frac{4\chi}{(1-\chi)^2} \cosh^2 \frac{\tau}{2}\right). \end{aligned} \quad (\text{C.4})$$

In particular, we get (assuming $0 < \chi < 1$)

$$\begin{aligned} \bar{D}_{1,1,1,1} &= -\frac{2 \log \chi}{1-\chi} - \frac{2 \log(1-\chi)}{\chi}, & \bar{D}_{1,1,2,2} &= \frac{\chi^2 \log(\chi)}{3(\chi-1)^2} - \frac{1}{3(\chi-1)} - \frac{(\chi+2) \log(1-\chi)}{3\chi}, \\ \bar{D}_{1,2,2,1} &= \frac{\log(1-\chi)}{3\chi^2} + \frac{1}{3(\chi-1)^2\chi} - \frac{(\chi-3) \log(\chi)}{3(\chi-1)^3}, & \bar{D}_{2,2,1,1} &= -\frac{(\chi+2) \log(1-\chi)}{3\chi^3} - \frac{1}{3(\chi-1)\chi^2} + \frac{\log(\chi)}{3(\chi-1)^2}, \\ \bar{D}_{1,2,1,2} &= -\frac{(2\chi+1) \log(1-\chi)}{3\chi^2} + \frac{1}{3(\chi-1)\chi} + \frac{(2\chi-3) \log(\chi)}{3(\chi-1)^2}, \\ \bar{D}_{2,1,2,1} &= -\frac{(2\chi+1) \log(1-\chi)}{3\chi^2} + \frac{1}{3(\chi-1)\chi} + \frac{(2\chi-3) \log(\chi)}{3(\chi-1)^2}, \\ \bar{D}_{2,1,1,2} &= \frac{(\chi-1)^2 \log(1-\chi)}{3\chi^2} + \frac{1}{3\chi} - \frac{(\chi-3) \log(\chi)}{3(\chi-1)}, \\ \bar{D}_{2,2,2,2} &= -\frac{2(\chi^2-\chi+1)}{15(\chi-1)^2\chi^2} + \frac{(2\chi^2-5\chi+5) \log(\chi)}{15(\chi-1)^3} - \frac{(2\chi^2+\chi+2) \log(1-\chi)}{15\chi^3}. \end{aligned} \quad (\text{C.5})$$

D Green's functions for 2d massless scalar

In this Appendix we discuss the form of 2d massless scalar propagator with Neumann boundary conditions on a space with half-plane or disc topology (with AdS₂ being a special case).

It is useful first to recall the case of compact 2d surface with no boundary (i.e. sphere topology). The Laplace-Beltrami operator $-D^2 = -\frac{1}{\sqrt{g}} \partial_\mu (\sqrt{g} g^{\mu\nu} \partial_\nu)$ has eigenvectors $-D^2 u_n = \lambda_n^2 u_n$ with $\int d^2\sigma \sqrt{g} u_n u_m = \delta_{nm}$ and $\sum_n u_n(\sigma) u_n(\sigma') = \frac{1}{\sqrt{g}} \delta^{(2)}(\sigma - \sigma')$. Separating the constant zero mode $u_0(\sigma) = \frac{1}{\sqrt{V}}$ we get for the Green's function (see, e.g., [56])

$$\text{G}(\sigma, \sigma') = \sum_{n>0} \frac{1}{\lambda_n^2} u_n(\sigma) u_n(\sigma'), \quad -D^2 \text{G}(\sigma, \sigma') = \sum_{n>0} u_n(\sigma) u_n(\sigma') = \delta^{(2)}(\sigma, \sigma') - \frac{1}{V}, \quad (\text{D.1})$$

where $\delta^{(2)}(\sigma, \sigma') = \frac{1}{\sqrt{g}} \delta^{(2)}(\sigma - \sigma')$.

In conformally flat coordinates $ds^2 = e^{2\rho} dw d\bar{w}$ the Green's function formally should not depend on the conformal factor; assuming plane topology it may still enter via a (covariant) UV cutoff $\varepsilon \equiv \varepsilon_{\text{UV}}$ introduced as

$$\text{G}(w, w') = -\frac{1}{4\pi} \log(|w - w'|^2 + \varepsilon^2 e^{-\rho(w) - \rho(w')}). \quad (\text{D.2})$$

For a sphere topology a natural counterpart of this expression is

$$\text{G}(w, w') = -\frac{1}{4\pi} \log[s^2(w, w') + \varepsilon^2], \quad s^2(w, w') = e^{\rho(w) + \rho(w')} |w - w'|^2. \quad (\text{D.3})$$

In critical string theory in Polyakov approach [57] the dependence on conformal factor should completely cancel out in the expressions for on-shell scattering amplitudes (see, e.g., [58]).³³

³³ It survives in general in sigma model partition function [59].

Similarly, for the critical string on a world sheet with a boundary (with, e.g., half-plane topology) the standard massless propagator can be found using the method of images

$$G_{D,N}(w, w') = -\frac{1}{4\pi} \left[\log |w - w'|^2 \mp \log |w - \bar{w}'|^2 \right], \quad (\text{D.4})$$

where the \mp signs correspond to the Dirichlet (D) and Neumann (N) boundary conditions. Introducing a covariant UV cutoff like in (D.2) gives (see also [60])

$$G_{D,N}(w, w') = -\frac{1}{4\pi} \left[\log (|w - w'|^2 + \varepsilon^2 e^{-\rho(w) - \rho(w')}) \mp \log |w - \bar{w}'|^2 \right]. \quad (\text{D.5})$$

This is true on a half-plane with any conformal factor. In the special case of AdS₂

$$ds^2 = \frac{1}{z^2} (dt^2 + dz^2) = \frac{dw d\bar{w}}{(\text{Im } w)^2}, \quad w = t + iz, \quad (\text{D.6})$$

we get from (D.5) (cf. (3.12))

$$\text{AdS}_2: \quad G_{D,N}(t, z; t', z') = -\frac{1}{4\pi} \left[\log [(t-t')^2 + (z-z')^2 + \varepsilon^2 z z'] \mp \log [(t-t')^2 + (z+z')^2] \right]. \quad (\text{D.7})$$

The bulk-to-boundary propagators are obtained by taking $z = \varepsilon \rightarrow 0$ ($\varepsilon = \varepsilon_{\text{IR}}$ is an IR cutoff):

$$G_D(t, z; t', \varepsilon) = \varepsilon K(t, z; t') + \mathcal{O}(\varepsilon^2), \quad K(t, z; t') = \frac{1}{\pi} \frac{z}{(t-t')^2 + z^2}, \quad (\text{D.8})$$

$$G_N(t, z; t', \varepsilon) = -\frac{1}{2\pi} \log [(t-t')^2 + z^2] + \mathcal{O}(\varepsilon). \quad (\text{D.9})$$

In the Dirichlet case we obtain the standard bulk-to-boundary propagator (2.30) in AdS₂; the extra ε factor may be absorbed into a rescaling of boundary fields. In the Neumann case the rescaling is not needed (consistently with the free boundary fields being dimensionless) and we recover (5.4).

If the Weyl invariance of the theory is not manifest (like in the expansion of the Nambu action) we may use instead a covariant approach specific to a particular 2-space. For a homogeneous space like a half-sphere or AdS₂ it is natural to represent the propagator in terms of the geodesic distance $s(\sigma, \sigma')$. Then in conformally flat coordinates for a half-plane topology ($ds^2 = e^{2\rho} dw d\bar{w}'$) we get

$$G_{D,N}(w, w') = -\frac{1}{4\pi} \left[\log s^2(w, w') \mp \log s^2(w, \bar{w}') \right], \quad (\text{D.10})$$

where the covariant bulk UV cutoff may be introduced as in (D.3) by $s^2(w, w') \rightarrow s^2(w, w') + \varepsilon^2$. In the AdS₂ case we then get explicitly for the Neumann case³⁴

$$G_N(t, z; t', z') = -\frac{1}{4\pi} \left[\log \frac{(t-t')^2 + (z-z')^2}{2zz'} + \log \frac{(t-t')^2 + (z+z')^2}{2zz'} \right]. \quad (\text{D.11})$$

Note that the normal derivative of G_N is constant at $z = 0$, instead of being zero as for the naive Neumann boundary conditions. In fact, the natural Neumann boundary condition on a massless scalar here is $\partial_n \varphi \Big|_{z=0} = h = \text{constant}$: near the boundary $\varphi(z \rightarrow 0) = h \log z + \dots$ which is consistent with

³⁴Notice that here for the separated points (when the delta-function is zero) we get $-D^2 G_N = -z^2 \partial_a \partial_a G_N = \frac{1}{2\pi}$. This may be interpreted as in (D.1) as a consequence of projecting out the constant zero-mode contribution present for the Neumann boundary conditions: indeed, this expression is in agreement with (D.1) after taking into account that the regularized volume of AdS₂ with the S^1 boundary is $V = -2\pi$.

$\varphi \sim az^\Delta + \dots$ when $\Delta \rightarrow 0$. A closely related discussion of the Neumann function for AdS₂ may be found in [61].³⁵

In bosonic model where power divergences do not automatically cancel out results for correlators involving derivatives of the Green's function at coinciding points in general depend on regularization scheme. In the case of string sigma model that scheme should be fixed so that to preserve underlying (target-space) symmetries of the theory. For example, the second derivative at coinciding points $g^{\mu\nu} D_\mu D'_\nu G(\sigma, \sigma')|_{\sigma=\sigma'}$, depends on the choice of UV regularization as discussed, e.g., in [56, 62]. Using spectral or heat kernel regularization $G(\sigma, \sigma'; \varepsilon) = \sum_{n>0} \frac{1}{\lambda_n^2} u_n(\sigma) u_n(\sigma') e^{-\varepsilon \lambda_n^2}$, one finds in conformally-flat coordinates (in the absence of the boundary)

$$\partial_\mu G(\sigma, \sigma'; \varepsilon)|_{\sigma=\sigma'} = \frac{1}{4\pi} \partial_\mu \rho(\sigma), \quad (\text{D.12})$$

$$\partial_\mu \partial'_\mu G(\sigma, \sigma'; \varepsilon)|_{\sigma=\sigma'} = \frac{e^{2\rho(\sigma)}}{4\pi \varepsilon} + \frac{a}{4\pi} \partial^2 \rho(\sigma) - e^{2\rho(\sigma)} u_0^2, \quad (\text{D.13})$$

where $u_0^2 = \frac{1}{V}$ and $a = \frac{2}{3}$. The coefficient a of the $\partial^2 \rho$ in $\partial_a \partial'_a G$ is regularization dependent: it becomes $a = 1$ in dimensional regularization and is $a = 0$ if one uses the covariant Green's function on S^2 (see [56]). It is a particular (dimensional regularization or equivalent) scheme that leads to results consistent with string theory symmetries in the 2-sphere case (see, e.g., [63, 64]).

Similar expressions are found in the presence of the boundary. Using that for AdS₂ $\rho = -\log z$, $z^2 \partial_\mu \partial_\mu \rho = 1$ (and ignoring the first and the last term in (D.13)) the coefficient $a = 1$ of $\partial^2 \rho$ term in (D.13) corresponds to $k = 1$ choice in (4.11).³⁶ At the same time, as discussed in [64], in the boundary case a more natural option is to keep only the last term in the analog of (D.13). Then (with $V_{\text{AdS}_2} = -2\pi$) we get

$$e^{-2\rho} \partial_\mu \partial'_\mu G_{\text{N}}(\sigma, \sigma'; \varepsilon)|_{\sigma=\sigma'} = \frac{1}{2\pi}, \quad (\text{D.14})$$

which corresponds to $k = 2$ choice in (4.11) that we used in (4.19).

E Equivalence of different parametrizations of S^5

The quartic Lagrangian (2.9) used in the supersymmetric line case [11] corresponds to the parametrization of S^5 defined in (1.8). At the same time, in the discussion of the non-supersymmetric case in section 3 we used a different parametrization (3.8) with the corresponding Lagrangian in (3.10). Choosing there $n^a = 0, n^6 = 1 (a = 1, \dots, 5)$ and renaming $\zeta^a \rightarrow y^a$ the two Lagrangians become special cases of the following family

$$L_4 = r_1 y^b y^b (\partial y^a \cdot \partial y^a) + r_2 y^a y^b (\partial y^a \cdot \partial y^b) + \mathcal{O}((\partial y)^4) \quad (\text{E.1})$$

where (2.9) corresponds to $r_1 = -\frac{1}{4}, r_2 = 0$ and (3.10) – to $r_1 = 0, r_2 = \frac{1}{2}$. That the two cases are related by a field redefinition is reflected in the fact that if we integrate by parts and ignore the term proportional to the y^a equations of motion ($\square y^a = 0$) then the quartic Lagrangian becomes the same – depending on the combination $r_1 - \frac{1}{2} r_2$ which is equal to $-\frac{1}{4}$ in both cases:

$$L_{4y} = (r_1 - \frac{1}{2} r_2) y^b y^b (\partial y^a \cdot \partial y^a) + \mathcal{O}((\partial y)^4). \quad (\text{E.2})$$

³⁵In [61] one finds equivalent expressions: in global AdS₂ coordinates $ds^2 = dr^2 + \sinh^2 r d\phi^2$ the geodesic distance $s(r, \phi; r', \phi')$ satisfies $\cosh s = \cosh r \cosh r' - \sinh r \sinh r' \cos(\phi - \phi')$ and then $G_{\text{D}} = -\frac{1}{4\pi} \log \frac{u}{u+1}$ and $G_{\text{N}} = -\frac{1}{4\pi} \log[u(u+1)]$ where $u = \sinh^2 \frac{s}{2}$, $u+1 = \cosh^2 \frac{s}{2}$, etc. Here again $\partial_n G_{\text{N}}$ tends to a constant at the boundary, see Eq.(5.21) of [61].

³⁶This follows also directly from (D.7) as well as (D.11) supplemented with the ε -regularization term.

Explicitly, $y^a y^b (\partial y^a \cdot \partial y^b) = \frac{1}{4} \partial(y^2) \cdot \partial(y^2) \rightarrow -\frac{1}{4} y^2 \square(y^2) = -\frac{1}{2} (y^2) (\partial y \cdot \partial y) + \mathcal{O}(\square y)$. One can check that field redefinitions leave boundary (“on-shell”) AdS correlators invariant: the correlator (2.33) computed starting directly with (E.1) depends only on $r_1 - \frac{1}{2} r_2$, i.e. is the same as the one corresponding to (E.2).

F Neumann/Dirichlet relations for bulk integrals

Let us provide some details of the proof of the relations leading to (6.23),(6.24).

To show (6.23) let us note that the contribution of the contact vertex in (2.8) to the mixed correlator involves the following integral (here contractions are with flat metric in (t, z) space and $\int \equiv \int_0^\infty dz \int_{-\infty}^\infty dt$)

$$I_N = \frac{1}{4} I_N^{(1)} - \frac{1}{2} I_N^{(2)}, \quad (F.1)$$

$$I_N^{(1)} = \int \partial_\mu K_2(t_1) \partial_\mu K_2(t_2) \partial_\nu N'(t_3) \partial_\nu N'(t_4), \quad I_N^{(2)} = \int \partial_\mu K_2(t_1) \partial_\nu K_2(t_2) \partial_\mu N'(t_3) \partial_\nu N'(t_4).$$

Denoting by $I_D^{(k)}$ similar integrals with $N' \rightarrow K_1$, we using the identity in (6.18)

$$I_N^{(1)} = 4 I_D^{(1)}, \quad I_N^{(2)} = 4 \int \partial_\mu K_2(t_1) \partial_\nu K_2(t_2) \varepsilon_{\mu\rho} \varepsilon_{\nu\lambda} \partial_\rho K_1(t_3) \partial_\lambda K_1(t_4) = 4 (I_D^{(1)} - I_D^{(2)}). \quad (F.2)$$

As a result, (F.1) becomes

$$I_N = -I_D^{(1)} + 2 I_D^{(2)} = -4 I_D. \quad (F.3)$$

This gives the relation in (6.23) after dividing by the ratio of the factors in the propagators $\mathcal{C}_1/\mathcal{C}_N = -2$ (cf. (2.32),(5.4)).

The contribution of the $(\partial\zeta)^4$ vertex in (3.10) to $\langle YYY Y \rangle$ in the Neumann case involves the integral

$$J_N = \int N'(t_1) N'(t_2) \partial_\mu N'(t_3) \partial_\mu N'(t_4) = 4 \int N'(t_1) N'(t_2) \partial_\mu K_1(t_3) \partial_\mu K_1(t_4), \quad (F.4)$$

where the second equality follows again from (6.19). Now using that $\square N' = 0$ and $\square K_1 = 0$ ($\square = \partial_\mu \partial_\mu$) and formally integrating by parts one finds that

$$\begin{aligned} J_N &= 2 \int N'(t_1) N'(t_2) \square [K_1(t_3) K_1(t_4)] \rightarrow 2 \int \square [N'(t_1) N'(t_2)] K_1(t_3) K_1(t_4) \\ &= 4 \int \partial_\mu N'(t_1) \partial_\mu N'(t_2) K_1(t_3) K_1(t_4) = 16 \int \partial_\mu K_1(t_1) \partial_\mu K_1(t_2) K_1(t_3) K_1(t_4) \\ &\rightarrow 16 \int K_1(t_1) K_1(t_2) \partial_\mu K_1(t_3) \partial_\mu K_1(t_4). \end{aligned} \quad (F.5)$$

It turns out that, in fact, the $z = 0$ boundary term is non-zero and is given by Ω in (6.22). Namely, using AdS₂ covariant form of the integrands we have for the difference of (F.4) and (F.5)

$$\Omega = \int_0^\infty \frac{dz}{z^2} \int_{-\infty}^\infty dt \left[N'(t_1) N'(t_2) \partial^\mu N'(t_3) \partial_\mu N'(t_4) - 16 K_1(t_1) K_1(t_2) \partial^\mu K_1(t_3) \partial_\mu K_1(t_4) \right]. \quad (F.6)$$

The integrand here is a rational function of z, t . The integral over t can be done by computing the residues at $t = t_a + i z$ ($a = 1, 2, 3, 4$). The result is a rational function of z (and t_a) that can be

integrated over z explicitly. Finally, we get³⁷

$$\Omega(t_1, t_2, t_3, t_4) = -8\pi \frac{t_{13} t_{23} + t_{14} t_{24}}{t_{13} t_{23} t_{14} t_{24} t_{34}^2}. \quad (\text{F.7})$$

G “Reducible” contributions to G_S at order $\frac{1}{(\sqrt{\lambda})^3}$

Here we shall consider the $\frac{1}{(\sqrt{\lambda})^3}$ correction to $G_S \equiv G_{N,S}$ in (6.3),(6.14) coming from the “reducible” diagrams (tree level plus loop corrections to the ζ -propagators, cf. Fig. 9 and Fig. 10). This is part of the total $G_S^{(3)}$ in (6.14) which is the direct analog of the $\frac{1}{(\sqrt{\lambda})^2}$ term in (6.11).

According to the definition in (6.3),(6.4)

$$G_S = |t_{12}t_{34}|^{2\Delta} \langle Y^A(t_1)Y^A(t_2)Y^B(t_3)Y^B(t_4) \rangle = 1 + \sum_{n=1}^{\infty} \frac{1}{(\sqrt{\lambda})^n} G_S^{(n)}, \quad (\text{G.1})$$

$$\langle Y^A(t_1)Y^A(t_2)Y^B(t_3)Y^B(t_4) \rangle = 1 + \sum_{n=1}^{\infty} \frac{1}{(\sqrt{\lambda})^n} Q^{(n)}. \quad (\text{G.2})$$

At order $\frac{1}{(\sqrt{\lambda})^2}$, the contributions to $\langle Y^A Y^A Y^B Y^B \rangle$ are given by the sum of the expressions in (6.4),(6.6),(6.8), (6.9) and after the extracting the contribution of the prefactor $|t_{12}t_{34}|^{-2\Delta}$ we have found $G_S^{(2)}$ in (6.11).

In general, the total expression $G_S^{(3)}$ will be given by the sum on the “reducible” and “connected” (bulk contact, see Fig. 11) diagram contributions

$$G_S^{(3)} = G_{S,\text{red}}^{(3)} + G_{S,\text{conn}}^{(3)}, \quad G_{S,\text{red}}^{(3)} = G_{S,\log^2}^{(3)} + G_{S,\log^3}^{(3)}, \quad (\text{G.3})$$

with the “reducible” contribution being the sum of the terms $G_{S,\log^2}^{(3)}$ and $G_{S,\log^3}^{(3)}$ containing products of two and three $\log t_{ij}$ factors respectively. It is the total expression $G_S^{(3)}$ that should be conformally invariant. Our aim below will be to compute $G_{S,\text{red}}^{(3)}$.

The $\frac{1}{(\sqrt{\lambda})^3}$ contributions to (G.2) will come from: (i) tree diagrams (given by products of three ζ -propagators as in Fig. 10), and (ii) diagrams with loops corresponding to the ζ -propagator “self-energy” corrections (cf. Fig. 3).³⁸ The tree diagrams will give $\frac{1}{(\sqrt{\lambda})^3} \log^3$ terms while the ones with loop corrections will give also $\frac{1}{(\sqrt{\lambda})^3} \log^2$ terms.

To find $G_S^{(3)}$ will then need to multiply the resulting expression for (G.2) by (see (4.2))

$$\begin{aligned} |t_{12}t_{34}|^{2\Delta} &= 1 + \left[\frac{5}{\sqrt{\lambda}} + \frac{d_2}{(\sqrt{\lambda})^2} + \frac{d_3}{(\sqrt{\lambda})^3} + \dots \right] (N_{12} + N_{34}) + \left[\frac{25}{2(\sqrt{\lambda})^2} + \frac{5d_2}{(\sqrt{\lambda})^3} + \dots \right] (N_{12} + N_{34})^2 \\ &\quad + \left[\frac{125}{6(\sqrt{\lambda})^3} + \dots \right] (N_{12} + N_{34})^3 + \dots, \quad N_{ij} \equiv \log(t_{ij}^2), \end{aligned} \quad (\text{G.4})$$

³⁷For example, choosing $t_1 = 0, t_2 = 1, t_3 = -1, t_4 = 2$, one finds

$$\begin{aligned} \Omega &= \int_0^\infty dz \int_{-\infty}^\infty dt \frac{16(t^2 - t - z^2)[t^4 - 2t^3 + t^2(2z^2 - 3) - 2t(z^2 - 2) + z^4 - 13z^2 + 4]}{(t^2 + z^2)(t^2 - 4t + z^2 + 4)^2(t^2 - 2t + z^2 + 1)(t^2 + 2t + z^2 + 1)^2} \\ &= -16\pi \int_0^\infty dz \frac{z(256z^8 - 2624z^6 - 4192z^4 + 812z^2 + 999)}{(z^2 + 1)^2(4z^2 + 1)^2(4z^2 + 9)^3} = -\frac{8\pi}{9}. \end{aligned}$$

³⁸One can see that a diagram with a bulk fermionic loop and three ζ -propagators attached to it gives zero contribution as one of the legs will be contracted with n_A .

and extract the order $\frac{1}{(\sqrt{\lambda})^3}$ term. Multiplying $1 + \frac{1}{\sqrt{\lambda}} Q^{(1)} + \frac{1}{(\sqrt{\lambda})^2} Q^{(2)} + \frac{1}{(\sqrt{\lambda})^3} Q^{(3)} + \dots$ by (G.4) and using the expressions in (6.5),(6.9) gives

$$G_S^{(3)} = d_2(N_{12} + N_{34})Q^{(1)} + 5d_2(N_{12} + N_{34})^2 + \frac{125}{6}(N_{12} + N_{34})^3 + \frac{25}{2}(N_{12} + N_{34})^2 Q^{(1)} + 5(N_{12} + N_{34})Q^{(2)} + Q^{(3)} \quad (\text{G.5})$$

$$= -5d_2(N_{12} + N_{34})^2 + \frac{125}{6}(N_{12} + N_{34})^3 + 5(N_{12} + N_{34})\bar{Q}^{(2)} + Q^{(3)}, \quad (\text{G.6})$$

where we used that $Q^{(1)} = -5(N_{12} + N_{34})$ in (6.5) and $Q^{(2)} = Q_{\log}^{(2)} + \frac{25}{2}(N_{12} + N_{34})^2 + \bar{Q}^{(2)}$ where $Q_{\log}^{(2)} = -d_2(N_{12} + N_{34})$, see (6.7), (6.9). Note that the d_2 -dependent terms in the first line of (G.5) cancelled out. Also, some terms in $Q^{(3)}$ which come from disconnected diagrams involving ‘‘dressed’’ 12 and 34 propagators will cancel in (G.6) (like that happened in $G_S^{(2)}$ in (6.9),(6.11)).

As was mentioned at the beginning of section 6.2, the log contribution to $Q^{(3)}$ from the 2-loop propagator correction should cancel against the $\frac{d_3}{(\sqrt{\lambda})^3}$ term in (G.4) so let us consider the \log^2 contributions to $Q^{(3)}$. These may come from the tree diagrams with two propagators in Fig. 8 where one of the propagators replaced by the 1-loop corrected one corresponding to the $d_2 \log$ term in (4.1). The \log^2 terms may thus be obtained by the replacement

$$N_{ij} \rightarrow \left(1 + \frac{d_2}{5\sqrt{\lambda}}\right)N_{ij} \quad (\text{G.7})$$

in the expression for $Q_0^{(2)}$ in (6.6). At the same time, no additional contributions should come from diagrams in Fig. 9 as they are already accounted for in the Δ -dependent terms. As a result, we get the following \log^2 contribution to $Q^{(3)}$

$$Q_{\log^2}^{(3)} = d_2 \left[5(N_{12}^2 + N_{34}^2) + 10N_{12}N_{34} + (N_{13} + N_{24} - N_{14} - N_{23})^2 \right]. \quad (\text{G.8})$$

Substituting this into (G.6) we end up with the \log^2 term in $G_S^{(3)}$

$$G_{S,\log^2}^{(3)} = d_2 \left[-4(N_{12}^2 + N_{34}^2) + (N_{13} + N_{24} - N_{14} - N_{23})^2 \right] = d_2 \left[-4(N_{12}^2 + N_{34}^2) + 4\log^2(1 - \chi) \right]. \quad (\text{G.9})$$

While the first term here depending separately on 12 and 34 pairs of points is not conformally invariant, the second is – it is, in fact, the same as in (6.9),(6.11). While the non-invariant part of (G.9) should cancel in the total combination in (G.3), this invariant part will simply combine with $G_S^{(2)}$ in (6.11) as

$$\frac{1}{(\sqrt{\lambda})^2} G_S^{(2)} + \frac{1}{(\sqrt{\lambda})^3} G_{S,\log^2}^{(3)} \rightarrow \left[\frac{10}{(\sqrt{\lambda})^2} + \frac{4d_2}{(\sqrt{\lambda})^3} \right] \log^2(1 - \chi). \quad (\text{G.10})$$

Note also that under the four derivatives over t_i only the second term in (G.9) contributes, i.e.

$$t_{12}^2 t_{34}^2 \partial_{t_1} \partial_{t_2} \partial_{t_3} \partial_{t_4} G_{S,\log^2}^{(3)} = 8d_2 \left(\frac{t_{12}^2 t_{34}^2}{t_{13}^2 t_{24}^2} + \frac{t_{12}^2 t_{34}^2}{t_{23}^2 t_{14}^2} \right) = 8d_2 \left[\chi^2 + \frac{\chi^2}{(1 - \chi)^2} \right] \quad (\text{G.11})$$

is conformally invariant.

Let us now turn to the more non-trivial \log^3 contribution to (G.2) at order $\frac{1}{(\sqrt{\lambda})^3}$. One finds from the tree diagrams in Fig. 12 (cf. (6.4)–(6.6))

$$Q_1^{(3)} = -\frac{25}{2}(N_{12}^2 N_{34} + N_{12} N_{34}^2) + 5[N_{12}(N_{13} N_{23} + N_{14} N_{24}) + N_{34}(N_{13} N_{14} + N_{23} N_{24})] - 5(N_{12} N_{14} N_{23} + N_{34} N_{13} N_{24}) - 5(N_{12} N_{13} N_{24} + N_{34} N_{14} N_{23}). \quad (\text{G.12})$$

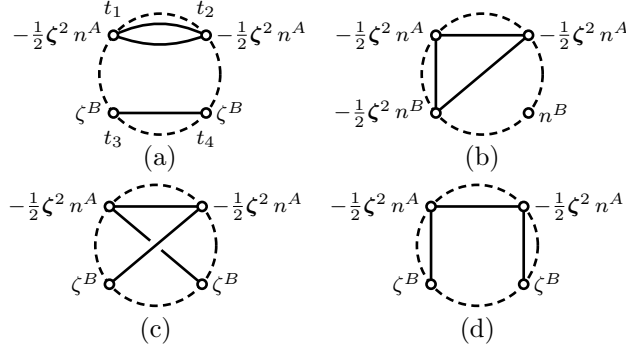


Figure 12. Tree-level diagrams (and similar ones obtained by permutations) contributing to (G.12).

The first bracket comes from (a) in Fig. 12 and its analog; the second bracket comes from 4 diagrams of type (b) (which is same as Fig. 10); the third bracket comes from (c) and its analog; the fourth comes from (d) and its analog.

To (G.12) we should add also the contributions of loop diagrams, i.e. the terms coming from the same diagrams as the lower order terms in (6.4) where the ζ -propagators are replaced by the ones containing “self-energy” corrections (see Fig. 3, Fig. 4, Fig. 9). The 2-loop corrections to the propagator in Fig. 4 should produce the analog of the $\gamma_3^{(2)}$ term in (4.7),(4.26)

$$Q_2^{(3)} = -\frac{65}{6}(N_{12}^3 + N_{34}^3) . \quad (\text{G.13})$$

Other $\frac{1}{(\sqrt{\lambda})^3}$ terms coming from 1-loop corrections to propagators in the order $\frac{1}{(\sqrt{\lambda})^2}$ tree diagrams in Fig. 8 can be generated from $Q^{(2)}$ in (6.6) by the substitution (4.25) or $N_{ij} \rightarrow N_{ij} - \frac{2}{\sqrt{\lambda}}N_{ij}^2$:

$$\begin{aligned} Q_3^{(3)} = & -10(N_{12}^3 + N_{34}^3) - 50(N_{12}^2 N_{34} + N_{12} N_{34}^2) - 10(N_{13}^3 + N_{14}^3 + N_{23}^3 + N_{24}^3) \\ & + 10(N_{13}^2 N_{14} + N_{13} N_{14}^2 + N_{23}^2 N_{24} + N_{23} N_{24}^2 + N_{13}^2 N_{23} + N_{13} N_{23}^2 + N_{14}^2 N_{24} + N_{14} N_{24}^2) \\ & - 10(N_{13}^2 N_{24} + N_{13} N_{24}^2 + N_{14}^2 N_{23} + N_{14} N_{23}^2) . \end{aligned} \quad (\text{G.14})$$

The total $\frac{1}{(\sqrt{\lambda})^3}$ term in (G.2) is then given by the sum of (G.12),(G.13) and (G.14)

$$Q_{\log^3}^{(3)} = Q_1^{(3)} + Q_2^{(3)} + Q_3^{(3)} = -\frac{125}{6}(N_{12} + N_{34})^3 + \bar{Q}^{(3)} , \quad (\text{G.15})$$

$$\begin{aligned} \bar{Q}^{(3)} = & 5[N_{12}(N_{13} - N_{14})(N_{23} - N_{24}) + N_{34}(N_{13} - N_{23})(N_{14} - N_{24})] \\ & - 10[(N_{13} - N_{14})(N_{13} + N_{14}) + (N_{24} - N_{23})(N_{24} + N_{23})](N_{13} - N_{14} + N_{24} - N_{23}) . \end{aligned} \quad (\text{G.16})$$

To compute the corresponding \log^3 term in $G_S^{(3)}$ we need to substitute this into (G.6). As a result (using (6.5),(6.9))

$$G_{S,\log^3}^{(3)} = 5(N_{12} + N_{34})\bar{Q}^{(2)} + \bar{Q}^{(3)} = \frac{25}{2}(N_{12} + N_{34})(N_{13} + N_{24} - N_{14} - N_{23})^2 + \bar{Q}^{(3)} . \quad (\text{G.17})$$

Thus most of the terms with N_{12} and N_{34} cancelled out (as expected as they correspond to “factorized” contributions of dressed propagators connecting points 12 and 34) but in contrast to their complete cancellation at order $\frac{1}{(\sqrt{\lambda})^2}$ in (6.11) here the terms linear in N_{12} and N_{34} survive. This is not surprising as $\bar{Q}^{(3)}$ contains them in the “irreducible” contributions of diagrams like (b),(c),(d) in Fig. 12 and as

they may appear also in the product of the linear term ($N_{12} + N_{34}$) in the expansion of the prefactor and the “irreducible” $\bar{Q}^{(2)}$ part of $\frac{1}{(\sqrt{\lambda})^2}$ term corresponding to the diagrams (c),(d),(e) in Fig. 8.

Like $G_{S,\log^2}^{(3)}$ in (G.9) the expression for $G_{S,\log^3}^{(3)}$ in (G.17) is not conformally invariant by itself.³⁹ The conformal invariance should be restored in the total expression (G.3), i.e. after adding the contribution $G_{S,\text{cont}}^{(3)}$ of the contact bulk contribution discussed in sections 6.2 and 6.3. An indication that this is indeed what happens is that the operator $t_{12}^2 t_{34}^2 \partial_{t_1} \partial_{t_2} \partial_{t_3} \partial_{t_4}$ applied to $G_{S,\text{cont}}^{(3)} + G_{S,\log^3}^{(3)}$ gives indeed a conformally invariant expression depending only on χ . To demonstrate this (see section 6.2) we will need the following expression that follows directly from (G.16),(G.17) (cf. (G.11))

$$\begin{aligned}
t_{12}^2 t_{34}^2 \partial_{t_1} \partial_{t_2} \partial_{t_3} \partial_{t_4} G_{S,\log^3}^{(3)} = & 40 t_{12}^2 t_{34}^2 \left(\frac{4}{t_{12}^2 t_{14} t_{23}} + \frac{4}{t_{12} t_{14}^2 t_{23}} - \frac{5}{t_{12}^2 t_{23} t_{24}} + \frac{5}{t_{12} t_{23}^2 t_{24}} + \frac{4}{t_{14}^2 t_{23} t_{34}} \right. \\
& - \frac{5}{t_{14}^2 t_{24} t_{34}} - \frac{4}{t_{14} t_{23}^2 t_{34}} - \frac{5}{t_{14} t_{24}^2 t_{34}} - \frac{4}{t_{12} t_{14} t_{23}^2} + \frac{8}{t_{14}^2 t_{23}^2} + \frac{5}{t_{12} t_{23} t_{24}^2} + \frac{4}{t_{14} t_{23} t_{34}^2} \\
& - \frac{5}{t_{14} t_{24} t_{34}^2} - \frac{5}{t_{12}^2 t_{14} t_{13}} + \frac{4}{t_{12}^2 t_{24} t_{13}} + \frac{5}{t_{23}^2 t_{34} t_{13}} + \frac{4}{t_{24}^2 t_{34} t_{13}} - \frac{5}{t_{12} t_{14}^2 t_{13}} - \frac{4}{t_{12} t_{24}^2 t_{13}} \\
& \left. - \frac{5}{t_{23} t_{34}^2 t_{13}} + \frac{4}{t_{24} t_{34}^2 t_{13}} - \frac{5}{t_{12} t_{14} t_{13}^2} + \frac{4}{t_{12} t_{24} t_{13}^2} + \frac{5}{t_{23} t_{34} t_{13}^2} - \frac{4}{t_{24} t_{34} t_{13}^2} \right) \\
& + 160 \left[\chi^2 (1 + \log \chi) + \frac{\chi^2}{(1-\chi)^2} \log \frac{\chi}{1-\chi} \right]. \tag{G.18}
\end{aligned}$$

The terms in the last line are conformally invariant while other non-invariant parts of other terms will cancel against non-invariant terms coming from $G_{S,\text{cont}}^{(3)}$.

H Direct computation of G_T and G_A functions at order $\frac{1}{(\sqrt{\lambda})^3}$

In section 6.3 we computed the function $G_S^{(3)}$ by a direct diagram computation combined with integration of the relation (6.38) or (6.55) and obtained the final result (6.59). The expressions for $G_T^{(3)}$ and $G_A^{(3)}$ in (6.2) we found using the crossing symmetry relations (6.36),(6.37) and led to (6.61), (6.62). In this Appendix, we will discuss a direct computation of $G_T^{(3)}$ and $G_A^{(3)}$ based on the same approach as used for $G_S^{(3)}$. This will provide a useful check of (6.61), (6.62) and is also of technical interest.

To find the \widehat{G}_T function (related to G_T as in (6.29)) we start from the corresponding combination of contractions of \widehat{G}_N^{ABCD} (see (2.17))

$$\widehat{G}_T = \frac{1}{56} \left(\widehat{G}_N^{ABAB} + \widehat{G}_N^{ABBA} - \frac{2}{5} \widehat{G}_N^{AABB} \right). \tag{H.1}$$

We have checked that as in the case of G_S in section 6.3 the expression for the square of the conformal Casimir operator \mathcal{D}^2 applied to the total (contact diagram plus “reducible”) contribution to \widehat{G}_T or \widehat{G}_A is conformally invariant, i.e. non-invariant parts of boundary terms from integrating by parts in bulk integrals cancel against the non-invariant parts of “reducible” diagram contributions.

A straightforward computation of $\partial_{t_1} \partial_{t_2} \widehat{G}_T$ gives (adding bar as in (6.54),(6.55) to indicate that we have used formal integration by parts)⁴⁰

$$t_{12}^2 \partial_{t_1} \partial_{t_2} \widehat{G}_T = -\mathcal{D} \widehat{G}_T = \frac{\chi^2}{1-\chi} - \chi(\chi+2) \log(1-\chi) + \frac{\chi^4}{(1-\chi)^2} \log \chi. \tag{H.2}$$

³⁹For example, it is easy to see the absence of scale invariance: under $N_{ij} \rightarrow N_{ij} + \ell$ the second line in (G.16) is invariant while the first changes by $5\ell[(N_{13} - N_{14})(N_{23} - N_{24}) + (N_{13} - N_{23})(N_{14} - N_{24})]$; the second by $-20\ell(N_{13} + N_{24} - N_{14} - N_{23})^2$; the variation of the term with $\bar{Q}^{(2)}$ in (G.17) is $25\ell(N_{13} + N_{24} - N_{14} - N_{23})^2$ and in total $\delta G_{S,\log^3}^{(3)} = 5\ell[(N_{13} - N_{14})(N_{23} - N_{24}) + (N_{13} - N_{23})(N_{14} - N_{24}) + (N_{13} + N_{24} - N_{14} - N_{23})^2]$.

⁴⁰Note that the expression for $\mathcal{D} \widehat{G}_T$ is correctly invariant under $3 \leftrightarrow 4$ exchange ($\chi \rightarrow \frac{\chi}{\chi-1}$) upon the assumed replacement $\log(1-\chi) \rightarrow \log|1-\chi|$, $\log \chi \rightarrow \log|\chi|$.

Integrating, we obtain

$$\begin{aligned}\widehat{G}_T &= c_{1T} + c_{2T} \log(1 - \chi) + 6 \operatorname{Li}_3(\chi) + 6 \operatorname{Li}_3\left(\frac{\chi}{\chi-1}\right) - 2 \operatorname{Li}_2(\chi) \log(1 - \chi) \\ &\quad - \log^3(1 - \chi) + \log \chi \log^2(1 - \chi) - \frac{\chi^2}{1-\chi} \log \chi - \chi \log(1 - \chi).\end{aligned}\quad (\text{H.3})$$

Here the first two terms are the possible 0-mode contribution as, e.g., in (6.34). A non-trivial consistency check is that the analog of (6.43) (cf. (6.27), (6.38)) is satisfied, i.e. $\mathcal{D}^2 \widehat{G}_T(\chi) = 4 G_{D,T}(\chi)$ where $G_{D,T}(\chi)$ is given by (2.34).

In the case of $\mathcal{D} \widehat{G}_A$ it turns out that we cannot express the structure V_3 in (6.53) in terms of the Dirichlet K_n functions only so we go back to solving the analog of (6.27),(6.38), i.e. $\mathcal{D}^2 \widehat{G}_{N,A} = 4 G_{D,A}$ with $G_{D,A}$ from (2.34). From the explicit expression for the operator \mathcal{D} in (6.30), one can check that the solution f of the equation $\mathcal{D}f = g$ obeys

$$f'(\chi) = \frac{c_2}{1 - \chi} + \frac{1}{1 - \chi} \int_0^\chi \frac{d\chi'}{\chi'^2} g(\chi'). \quad (\text{H.4})$$

Integrating (H.4) for $f = \mathcal{D} \widehat{G}_N$ with $g = 4 G_{D,A}$ or $4 G_A^{(1)}(\chi)$ from (2.34) and including the zero-mode terms we get⁴¹

$$\begin{aligned}\mathcal{D} \widehat{G}_A &= 8 \operatorname{Li}_2(\chi) - \frac{(x-2)(x^2-2x+2)\chi}{(x-1)^2} \log \chi + [3 + (1 - \chi)^2 + 4 \log \chi] \log(1 - \chi) + \frac{(x-2)\chi}{x-1} \\ &\quad + c_{1A} + c_{2A} \log(1 - \chi).\end{aligned}\quad (\text{H.5})$$

We can impose the last relation in (2.20) to show that $c_{1A} = 0$ (the operator \mathcal{D} commutes with the crossing transformation $\chi \rightarrow \frac{\chi}{\chi-1}$). Instead of directly integrating (H.5) we may find \widehat{G}_A order by order in small χ expansion (and again applying also (2.20)). This gives the following expression depending on the two free zero-mode parameters c_{2A}, c_{3A}

$$\begin{aligned}\widehat{G}_A &= \chi [(6 - c_{2A}) \log \chi + c_{3A}] + \chi^2 \left[(3 - \frac{c_{2A}}{2}) \log \chi - \frac{c_{2A}}{2} + \frac{c_{3A}}{2} + 3 \right] \\ &\quad + \chi^3 \left[\left(\frac{22}{9} - \frac{c_{2A}}{3} \right) \log \chi - \frac{4c_{2A}}{9} + \frac{c_{3A}}{3} + \frac{37}{18} \right] + \chi^4 \left[\left(\frac{13}{6} - \frac{c_{2A}}{4} \right) \log \chi - \frac{3c_{2A}}{8} + \frac{c_{3A}}{4} + \frac{14}{9} \right] + \dots\end{aligned}\quad (\text{H.6})$$

The total expressions for the $\frac{1}{(\sqrt{\lambda})^3}$ terms in the functions G_T and G_A are given by the sums of the ‘‘connected’’ \overline{G} -expressions computed using (6.29) added to the analogs of \widetilde{G}_S in (6.43),(6.44). The explicit expressions for the $\frac{1}{(\sqrt{\lambda})^3}$ terms in the latter are found to be

$$\begin{aligned}\widetilde{G}_T &= 96 [2 \operatorname{Li}_3(1 - \chi) + \operatorname{Li}_2(\chi) \log(1 - \chi)] - 83 \log^3(1 - \chi) + 216 \log^3 \chi \\ &\quad + 354 \log \chi \log^2(1 - \chi) - 324 \log^2 \chi \log(1 - \chi)\end{aligned}\quad (\text{H.7})$$

$$= 216 \log^3 \chi + 192 \zeta_R(3) + (324 \log^2 \chi - 32 \pi^2) \chi + (162 \log^2 \chi + 258 \log \chi + 48 - 16 \pi^2) \chi^2 + \dots,$$

$$\begin{aligned}\widetilde{G}_A &= 96 [2 \operatorname{Li}_3(1 - \chi) + 4 \operatorname{Li}_3(\chi) - 2 \operatorname{Li}_2(\chi) \log \chi + \operatorname{Li}_2(\chi) \log(1 - \chi)] \\ &\quad + 84 \log^3(1 - \chi) - 144 \log \chi \log^2(1 - \chi) + 192 \log^2 \chi \log(1 - \chi) \\ &= 192 \zeta_R(3) + (-192 \log^2 \chi - 192 \log \chi + 384 - 32 \pi^2) \chi + \dots,\end{aligned}\quad (\text{H.8})$$

⁴¹The application of (H.4) in the case of $g = 4 G_{D,S}$ or $g = 4 G_{D,T}$ requires only elementary integrations and the result is precisely (6.55) and (H.2).

where we omitted for simplicity the d_2 and d_3 dependent contributions coming from the loop corrections to the propagators in the “reducible” contributions.⁴²

The final expressions for $G_T^{(3)}$ and $G_A^{(3)}$ can be shown to be equivalent to (6.61) and (6.62) up to the zero mode contributions. In particular, the latter account for the fact that the small χ expansions in (6.63),(6.64) do not start at order $\mathcal{O}(\chi^2)$, consistently with the OPE analysis in section 6.4.

I 3-point function $\langle Y Y [Y Y] \rangle$

In considering the OPE decomposition of 4-point Y -scalar correlator in (6.65) in the T-channel (6.68) one finds the contribution of the traceless symmetric operator $Y^{\{A} \partial_t^n Y^{B\}}$ (cf. also Appendix B). For $n = 0$ its dimension is $\Delta_0 = \frac{12}{\sqrt{\lambda}} + \dots$ and the OPE coefficients should be proportional to the square of the coefficients in the 3-point function $\langle Y^A(t_1) Y^B(t_2) [Y^{\{C} Y^{D\}}](t_3) \rangle$. Introducing a complex null 6-vector u^A ($u^2 = 0$) we have $(u \cdot Y)^2 = Y^{\{A} Y^{B\}} u_A u_B$ so that we may consider the equivalent correlator

$$\langle Y^A(t_1) Y^B(t_2) [u \cdot Y(t_3)]^2 \rangle = T(t_1, t_2, t_3) u^A u^B, \quad T(t_1, t_2, t_3) = \frac{c_{112}}{|t_{12}|^{2\Delta - \Delta_0} |t_{23}|^{\Delta_0} |t_{13}|^{\Delta_0}}, \quad (\text{I.1})$$

$$\Delta = \frac{5}{\sqrt{\lambda}} + \dots, \quad \Delta_0 = \frac{12}{\sqrt{\lambda}} + \dots, \quad c_{112} = c_{112}^{(0)} + \frac{1}{\sqrt{\lambda}} c_{112}^{(1)} + \dots \quad (\text{I.2})$$

Its form is fixed by the $SO(6)$ and conformal invariance. To order $\frac{1}{(\sqrt{\lambda})^2}$ we find from tree-level contributions with one or two boundary-to-boundary propagators $N_{12} = \log(t_{12})^2$ (cf. (5.4))

$$T_{\text{tree}} = \frac{1}{24} \left[1 + \frac{1}{\sqrt{\lambda}} (N_{12} - 6N_{13} - 6N_{23}) + \frac{1}{(\sqrt{\lambda})^2} \left(\frac{5}{2} N_{12}^2 - 6N_{13}N_{12} - 6N_{23}N_{12} + 6N_{13}^2 + 6N_{23}^2 + 36N_{13}N_{23} \right) + \dots \right]. \quad (\text{I.3})$$

1-loop “self-energy” corrections (as in Fig. 3) to the ζ -propagator are taken into account (to the leading log order) by the replacement (4.25). This gives

$$T_{\text{tree+loop}} = \frac{1}{24} \left[1 + \frac{1}{\sqrt{\lambda}} (N_{12} - 6N_{13} - 6N_{23}) + \frac{1}{(\sqrt{\lambda})^2} \left(\frac{1}{2} N_{12}^2 - 6N_{13}N_{12} - 6N_{23}N_{12} + 18N_{13}^2 + 18N_{23}^2 + 36N_{13}N_{23} \right) + \dots \right]. \quad (\text{I.4})$$

Using that

$$|t_{12}|^{2\Delta - \Delta_0} |t_{23}|^{\Delta_0} |t_{13}|^{\Delta_0} = 1 + \frac{1}{\sqrt{\lambda}} (-N_{12} + 6N_{13} + 6N_{23}) + \frac{1}{(\sqrt{\lambda})^2} \left(\frac{N_{12}^2}{2} - 6N_{13}N_{12} - 6N_{23}N_{12} + 18N_{13}^2 + 18N_{23}^2 + 36N_{13}N_{23} \right) + \dots, \quad (\text{I.5})$$

we find that c_{112} does not receive $\frac{1}{\sqrt{\lambda}}$ and $\frac{1}{(\sqrt{\lambda})^2}$ corrections

$$c_{112} = \frac{1}{24} + \mathcal{O}\left(\frac{1}{(\sqrt{\lambda})^3}\right). \quad (\text{I.6})$$

Notice that (I.4) differs from (I.5) just in the sign of the $\frac{1}{\sqrt{\lambda}}$ correction, i.e. it is the inverse of the exponential expansion in (I.5).

⁴²Note that in contrast to $G_S^{(3)}$ the functions $G_T^{(3)}$ and $G_A^{(3)}$ can receive (in agreement with (6.61),(6.62)) the contributions proportional to the coefficient d_3 of the 2-loop correction (cf. Fig.4(b)) in the 2-point function or Δ in (4.2): these come from diagrams like in Fig. 9 where the two points carry indices other than A and B , i.e. from contractions like $\langle \zeta^A n^B \zeta^C n^D \rangle$, etc., that do not contribute to the prefactor in (6.1).

References

- [1] L. F. Alday and J. Maldacena, *Comments on gluon scattering amplitudes via AdS/CFT*, *JHEP* **11** (2007) 068, [[0710.1060](#)].
- [2] J. Polchinski and J. Sully, *Wilson Loop Renormalization Group Flows*, *JHEP* **10** (2011) 059, [[1104.5077](#)].
- [3] M. Beccaria, S. Giombi and A. Tseytlin, *Non-supersymmetric Wilson loop in $N=4$ SYM and defect 1d CFT*, [1712.06874](#).
- [4] A. M. Polyakov and V. S. Rychkov, *Gauge field strings duality and the loop equation*, *Nucl. Phys.* **B581** (2000) 116–134, [[hep-th/0002106](#)].
- [5] N. Drukker and S. Kawamoto, *Small deformations of supersymmetric Wilson loops and open spin-chains*, *JHEP* **07** (2006) 024, [[hep-th/0604124](#)].
- [6] M. Sakaguchi and K. Yoshida, *Holography of Non-relativistic String on $AdS(5) \times S^5$* , *JHEP* **02** (2008) 092, [[0712.4112](#)].
- [7] N. Drukker and V. Forini, *Generalized quark-antiquark potential at weak and strong coupling*, *JHEP* **06** (2011) 131, [[1105.5144](#)].
- [8] D. Correa, J. Henn, J. Maldacena and A. Sever, *An exact formula for the radiation of a moving quark in $N=4$ super Yang Mills*, *JHEP* **06** (2012) 048, [[1202.4455](#)].
- [9] M. Cooke, A. Dekel and N. Drukker, *The Wilson loop CFT: Insertion dimensions and structure constants from wavy lines*, *J. Phys.* **A50** (2017) 335401, [[1703.03812](#)].
- [10] M. Billo, V. Goncalves, E. Lauria and M. Meineri, *Defects in conformal field theory*, *JHEP* **04** (2016) 091, [[1601.02883](#)].
- [11] S. Giombi, R. Roiban and A. A. Tseytlin, *Half-BPS Wilson loop and AdS_2/CFT_1* , *Nucl. Phys.* **B922** (2017) 499–527, [[1706.00756](#)].
- [12] M. Kim, N. Kiryu, S. Komatsu and T. Nishimura, *Structure Constants of Defect Changing Operators on the $1/2$ BPS Wilson Loop*, [1710.07325](#).
- [13] S. Giombi and S. Komatsu, *Exact Correlators on the Wilson Loop in $\mathcal{N} = 4$ SYM: Localization, Defect CFT, and Integrability*, [1802.05201](#).
- [14] M. Kim and N. Kiryu, *Structure constants of operators on the Wilson loop from integrability*, *JHEP* **11** (2017) 116, [[1706.02989](#)].
- [15] N. Drukker, I. Shamir and C. Vergu, *Defect multiplets of $\mathcal{N} = 1$ supersymmetry in $4d$* , *JHEP* **01** (2018) 034, [[1711.03455](#)].
- [16] D. Correa, M. Leoni and S. Luque, *Spin chain integrability in non-supersymmetric Wilson loops*, *JHEP* **12** (2018) 050, [[1810.04643](#)].
- [17] P. Liendo, C. Meneghelli and V. Mitev, *Bootstrapping the half-BPS line defect*, [1806.01862](#).
- [18] M. Beccaria and A. A. Tseytlin, *On non-supersymmetric generalizations of the Wilson-Maldacena loops in $N = 4$ SYM*, *Nucl. Phys.* **B934** (2018) 466–497, [[1804.02179](#)].
- [19] L. Bianchi, M. Lemos and M. Meineri, *Line Defects and Radiation in $\mathcal{N} = 2$ Conformal Theories*, *Phys. Rev. Lett.* **121** (2018) 141601, [[1805.04111](#)].
- [20] S. Giombi and S. Komatsu, *More Exact Results in the Wilson Loop Defect CFT: Bulk-Defect OPE, Nonplanar Corrections and Quantum Spectral Curve*, [1811.02369](#).

- [21] N. Kiryu and S. Komatsu, *Correlation Functions on the Half-BPS Wilson Loop: Perturbation and Hexagonalization*, [1812.04593](#).
- [22] D. Mazac and M. F. Paulos, *The Analytic Functional Bootstrap I: 1D CFTs and 2D S-Matrices*, [1803.10233](#).
- [23] A. Cavaglia, N. Gromov and F. Levkovich-Maslyuk, *Quantum spectral curve and structure constants in $\mathcal{N} = 4$ SYM: cusps in the ladder limit*, *JHEP* **10** (2018) 060, [[1802.04237](#)].
- [24] S. Samuel, *Color zitterbewegung*, *Nucl. Phys.* **B149** (1979) 517–524.
- [25] J. Ishida and A. Hosoya, *Path Integral for a Color Spin and Path Ordered Phase Factor*, *Prog. Theor. Phys.* **62** (1979) 544.
- [26] I. Ya. Arefeva, *Quantum contour field equations*, *Phys. Lett.* **93B** (1980) 347–353.
- [27] J.-L. Gervais and A. Neveu, *The Slope of the Leading Regge Trajectory in Quantum Chromodynamics*, *Nucl. Phys.* **B163** (1980) 189–216.
- [28] J. Gomis and F. Passerini, *Holographic Wilson Loops*, *JHEP* **08** (2006) 074, [[hep-th/0604007](#)].
- [29] C. Hoyos, *A defect action for Wilson loops*, *JHEP* **07** (2018) 045, [[1803.09809](#)].
- [30] N. Drukker, D. J. Gross and A. A. Tseytlin, *Green-Schwarz string in $AdS(5) \times S^5$: Semiclassical partition function*, *JHEP* **04** (2000) 021, [[hep-th/0001204](#)].
- [31] A. Faraggi and L. A. Pando Zayas, *The Spectrum of Excitations of Holographic Wilson Loops*, *JHEP* **05** (2011) 018, [[1101.5145](#)].
- [32] B. Fiol, B. Garolera and G. Torrents, *Exact momentum fluctuations of an accelerated quark in $N=4$ super Yang-Mills*, *JHEP* **06** (2013) 011, [[1302.6991](#)].
- [33] D. Carmi, L. Di Pietro and S. Komatsu, *A Study of Quantum Field Theories in AdS at Finite Coupling*, [1810.04185](#).
- [34] I. R. Klebanov and E. Witten, *AdS / CFT correspondence and symmetry breaking*, *Nucl. Phys.* **B556** (1999) 89–114, [[hep-th/9905104](#)].
- [35] J. K. Erickson, G. W. Semenoff and K. Zarembo, *Wilson loops in $N=4$ supersymmetric Yang-Mills theory*, *Nucl. Phys.* **B582** (2000) 155–175, [[hep-th/0003055](#)].
- [36] D. Medina-Rincon, A. A. Tseytlin and K. Zarembo, *Precision matching of circular Wilson loops and strings in $AdS_5 \times S^5$* , *JHEP* **05** (2018) 199, [[1804.08925](#)].
- [37] S. Elitzur, *The Applicability of Perturbation Expansion to Two-dimensional Goldstone Systems*, *Nucl. Phys.* **B212** (1983) 501–518.
- [38] F. David, *Cancellations of Infrared Divergences in the Two-dimensional Nonlinear Sigma Models*, *Commun. Math. Phys.* **81** (1981) 149.
- [39] J. L. Miramontes and J. M. Sanchez de Santos, *Are there infrared problems in the 2-d nonlinear sigma models?*, *Phys. Lett.* **B246** (1990) 399–404.
- [40] J. Maldacena, S. H. Shenker and D. Stanford, *A bound on chaos*, *JHEP* **08** (2016) 106, [[1503.01409](#)].
- [41] A. Dekel, *Wilson Loops and Minimal Surfaces Beyond the Wavy Approximation*, *JHEP* **03** (2015) 085, [[1501.04202](#)].
- [42] R. Ishizeki, M. Kruczenski and S. Ziama, *Notes on Euclidean Wilson loops and Riemann Theta functions*, *Phys. Rev.* **D85** (2012) 106004, [[1104.3567](#)].
- [43] F. A. Dolan and H. Osborn, *Conformal Partial Waves: Further Mathematical Results*, [1108.6194](#).

- [44] J. Maldacena and D. Stanford, *Remarks on the Sachdev-Ye-Kitaev model*, *Phys. Rev.* **D94** (2016) 106002, [[1604.07818](#)].
- [45] J. Maldacena, D. Stanford and Z. Yang, *Diving into traversable wormholes*, *Fortsch. Phys.* **65** (2017) 1700034, [[1704.05333](#)].
- [46] J. de Boer, E. Llabres, J. F. Pedraza and D. Vegh, *Chaotic strings in AdS/CFT*, *Phys. Rev. Lett.* **120** (2018) 201604, [[1709.01052](#)].
- [47] S. Dubovsky, R. Flauger and V. Gorbenko, *Solving the Simplest Theory of Quantum Gravity*, *JHEP* **09** (2012) 133, [[1205.6805](#)].
- [48] E. D'Hoker and D. Z. Freedman, *Supersymmetric gauge theories and the AdS/CFT correspondence*, in *Strings, Branes and Extra Dimensions: TASI 2001: Proceedings*, pp. 3–158, 2002. [hep-th/0201253](#).
- [49] M. Hogervorst and B. C. van Rees, *Crossing symmetry in alpha space*, *JHEP* **11** (2017) 193, [[1702.08471](#)].
- [50] A. A. Tseytlin, *On semiclassical approximation and spinning string vertex operators in $AdS_5 \times S^5$* , *Nucl. Phys.* **B664** (2003) 247–275, [[hep-th/0304139](#)].
- [51] I. Heemskerck, J. Penedones, J. Polchinski and J. Sully, *Holography from Conformal Field Theory*, *JHEP* **10** (2009) 079, [[0907.0151](#)].
- [52] A. L. Fitzpatrick and J. Kaplan, *Unitarity and the Holographic S-Matrix*, *JHEP* **10** (2012) 032, [[1112.4845](#)].
- [53] E. D'Hoker, D. Z. Freedman, S. D. Mathur, A. Matusis and L. Rastelli, *Graviton exchange and complete four point functions in the AdS/CFT correspondence*, *Nucl. Phys.* **B562** (1999) 353–394, [[hep-th/9903196](#)].
- [54] F. A. Dolan and H. Osborn, *Conformal four point functions and the operator product expansion*, *Nucl. Phys.* **B599** (2001) 459–496, [[hep-th/0011040](#)].
- [55] G. Arutyunov, F. A. Dolan, H. Osborn and E. Sokatchev, *Correlation functions and massive Kaluza-Klein modes in the AdS/CFT correspondence*, *Nucl. Phys.* **B665** (2003) 273–324, [[hep-th/0212116](#)].
- [56] S. Randjbar-Daemi, A. Salam and J. A. Strathdee, *σ Models and String Theories*, *Int. J. Mod. Phys.* **A2** (1987) 667.
- [57] A. M. Polyakov, *Quantum Geometry of Bosonic Strings*, *Phys.Lett.* **B103** (1981) 207–210.
- [58] R. I. Nepomechie, *Duality of the Polyakov N Point Amplitude*, *Phys. Rev.* **D25** (1982) 2706.
- [59] E. S. Fradkin and A. A. Tseytlin, *Quantum String Theory Effective Action*, *Nucl. Phys.* **B261** (1985) 1–27.
- [60] B. Durhuus, H. B. Nielsen, P. Olesen and J. L. Petersen, *Dual Models as Saddle Point Approximations to Polyakov's Quantized String*, *Nucl. Phys.* **B196** (1982) 498–508.
- [61] S. N. Solodukhin, *Correlation functions of boundary field theory from bulk Green's functions and phases in the boundary theory*, *Nucl. Phys.* **B539** (1999) 403–437, [[hep-th/9806004](#)].
- [62] A. A. Tseytlin, *Graviton Amplitudes, Effective Action and String Generating Functional on the Disk*, *Int. J. Mod. Phys.* **A4** (1989) 3269.
- [63] S. P. de Alwis, *The Dilaton Vertex in the Path Integral Formulation of Strings*, *Phys. Lett.* **168B** (1986) 59–62.
- [64] A. A. Tseytlin, *Renormalization of String Loop Corrections on the Disk and the Annulus*, *Phys. Lett.* **B208** (1988) 228–238.